ORNL/SPR-2018/912

MERCURY REMEDIATION TECHNOLOGY DEVELOPMENT

for Lower East Fork Poplar Creek—FY 2018 Update

OAK RIDGE National Laboratory

ORNL/SPR-2018/912

Mercury Remediation Technology Development

for Lower East Fork Poplar Creek—FY 2018 Update

Mark J. Peterson
Scott C. Brooks
Teresa J. Mathews
Melanie A. Mayes
Alexander Johs
Ryan McManamay
David B. Watson
Katherine Muller
Leroy Goñez-Rodríguez
Chris Derolph
Sujith Nair

December 2018

Prepared by
OAK RIDGE NATIONAL LABORATORY
Oak Ridge, Tennessee 37831-6283 managed by
UT-BATTELLE, LLC
for the
US DEPARTMENT OF ENERGY
under contract DE-AC05-00OR22725

Acknowledgments

We would like to thank Janice Hensley and Jimmy Massey of URS | CH2M Oak Ridge LLC (UCOR) and Elizabeth Phillips and Brian Henry of the US Department of Energy's Oak Ridge Office of Environmental Management for their support of mercury technology development in Oak Ridge and their project oversight and support for this document. Additional contributors to various research and technology development activities that provided a basis of the report's evaluations and recommendations include Carrie Miller (Troy University), Johnbull Dickson (now at Savannah River National Laboratory), Jesse Morris (RSI), Jennifer Earles (Xcel Engineering), José L. Martínez-Collado (University of Puerto Rico), and ORNL's Michael Jones, Tonia Mehlhorn, and Kenneth Lowe. Charlie Horak and Kathy Jones of ORNL were responsible for editing and graphic design work, and their contributions are sincerely appreciated.

Contents

Introduction

Mercury (Hg) remediation is a high priority for the US Department of Energy (DOE) Oak Ridge Office of Environmental Management (OREM). Mercury contamination in the environment can be found at all three DOE facilities in Oak Ridge, but probably the greatest environmental risk concern relative to Hg on the Oak Ridge Reservation is associated with historical Hg losses at and near the Y-12 National Security Complex (Y-12). Water and fish from East Fork Poplar Creek (EFPC) downstream of Y-12 exceed regulatory thresholds. Because of the complexities of Hg transport and fate in the aquatic environment, conventional remedial options for EFPC are highly uncertain.

DOE is using a phased, adaptive management approach to Hg remediation at Y-12, with a focus in the next few years on construction of the Mercury Treatment Facility (MTF) to treat the most contaminated Y-12 outfall entering EFPC (DOE 2017a; DOE 2017b). Once operational, the MTF will provide additional protection against inadvertent releases of Hg into the stream from decontamination and decommissioning of Y-12 Hg-use buildings. Although it is anticipated that the MTF will substantially decrease Hg water concentrations and flux in the upper part of EFPC, research and technology development is needed to develop appropriate and longer-term remedial solutions for the downstream environment. Since late 2014, OREM and UCOR/RSI (URS | CH2M Oak Ridge LLC/Restoration Services, Inc.) have supported Oak Ridge National Laboratory (ORNL) Environmental Sciences Division staff in conducting field and laboratory studies to develop Hg remedial technology solutions for lower EFPC (LEFPC).

A technology development strategy for lower EFPC was developed in 2014 that was consistent with the adaptive management paradigm and DOE's Technology Readiness Level (TRL) guidelines (Peterson et al. 2015). Initially, a thorough review of the literature and site-specific information was conducted to develop a broad number of potential technologies that might be applied in lower EFPC. An adaptive management approach was then used to focus on technologies that might have the most promise and potential remediation benefit. Field and laboratory studies conducted during 2014–2018 have (1) identified the major drivers of Hg flux and bioaccumulation in EFPC and (2) narrowed the list of high-merit technologies that might be of use in remediating the downstream environment.

Whereas previous annual reporting updates for *Mercury Remediation Technology Development for Lower East Fork Poplar Creek* have focused on presenting detailed results from the previous fiscal year, this FY 2018 update takes a comprehensive, higher-level approach to the research and technology development activities conducted since 2014. The report is organized consistent with the three tasks defined in the LEFPC strategic plan (Peterson et al. 2015) as follows:

- Task 1, Soil and Groundwater Source Control, focuses on addressing downstream Hg sources to the creek (especially floodplain and bank soils) and groundwater.
- Task 2, Surface Water and Sediment Manipulation, centers on potential manipulation of instream processes, including the many water and sediment chemistry factors that affect Hg methylation.
- Task 3, Ecological Manipulation, investigates methods to manipulate the food chain at both lower and higher levels of organization to decrease Hg concentrations in fish.

Together, the three study tasks focus on manipulating the key factors that affect Hg concentrations in fish: the amount of inorganic Hg available to the ecosystem, conversion of inorganic Hg to methylmercury (MeHg), and bioaccumulation of MeHg through the food web (Figure 1). A major focus of the project has been on understanding Hg transport and fate processes in the EFPC system so that targeted, site-specific technologies can be developed. Field study data is being used to define conceptual and quantitative models for EFPC to inform future remedial decision-making (see *"Watershed Modeling"*). Bench-scale technology development activities are also presented for each task.

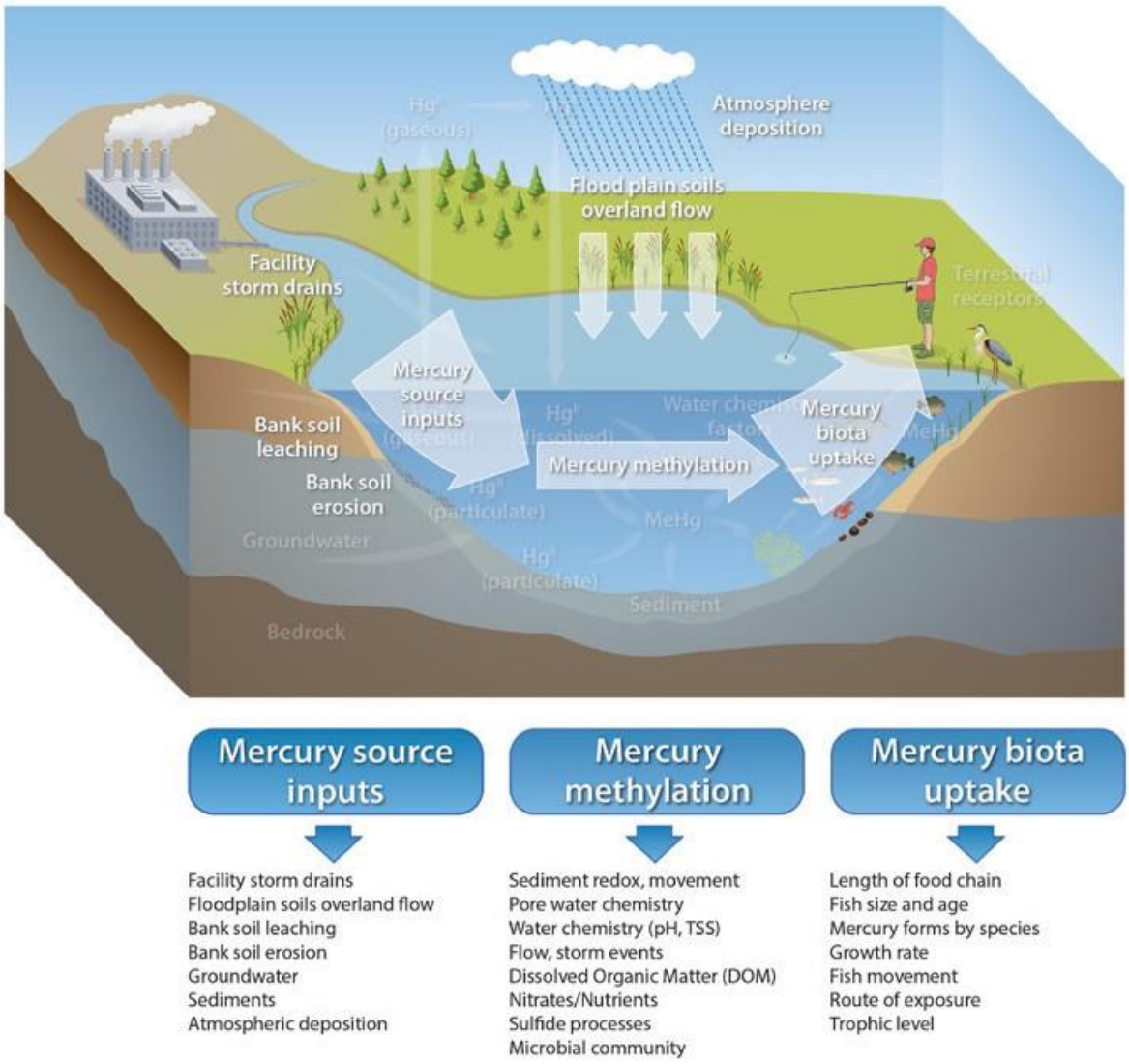

Figure 1. Research and technology development tasks have been defined for this project to address the three major factors affecting Hg concentrations in fish (image courtesy of Peterson et al. 2015).

Research and Technology Development Results

The results from the LEFPC Mercury Remediation Technology Development Project in FY 2018, as well as the key findings from previous years, are provided in the following subsections: (1) Soil and Groundwater Source Control, (2) Surface Water and Sediment Manipulation, (3) Ecological Manipulation, and (4) Watershed Modeling.

Soil and Groundwater Source Control

Importance of Bank and Floodplain Soil Inputs

Knowledge of the extent of contamination of the stream bank soils with Hg and MeHg in EFPC has been greatly improved. During the last 4 years, two longitudinal surveys of the stream banks were performed involving a repeated cyclic sampling strategy at every kilometer beginning just outside of Y-12 and extending to 5 km above the mouth of EFPC. Bulk soil samples and core samples were collected at 15%, 50%, and 85% of the height of the creek bank above the water level and were characterized for Hg, MeHg, soil type, particle size, total carbon and nitrogen, pH, and stability to erosion. During the course of the investigation, more details emerged about the dark-colored layer of higher Hg contamination near the National Oceanic and Atmospheric Administration (NOAA) facility and near the former Bruner's market. Previous studies had identified the layer (Southworth et al. 2013), but we learned the spatial extent is much greater than previously believed. Several high-resolution sampling activities involving the vertical (profile) distribution of Hg and its longitudinal extent were conducted. Now dubbed the "Historical Release Deposit (HRD)," the layer extends through approximately 1.5 km—although it may not be continuous—of the creek in the vicinity of the former Bruner's market. It is also found in the vicinity of the NOAA facility. The HRD was also identified through augering into the floodplain near Bruner's market in about 20 different places, but these surveys cannot be considered exhaustive.

These activities, together with some previously published analyses, resulted in nearly 800 analyses of Hg and 250 analyses of MeHg from the stream banks. The 25th and 75th percentile of Hg concentrations in soils from the longitudinal surveys was 7.08 and 23.7 mg/kg dry weight (dw), respectively, with a mean and median of 26.4 and 15.3 mg/kg dw, respectively (p = 0.401; n = 143 for 2014; n = 138 for 2015) (Dickson et al. In review). The 15%, 50%, and 85% creek bank heights used in the longitudinal surveys missed most of the HRD because it is usually between the 50% and 85% creek bank height. The 25th and 75th percentile of Hg concentrations in the HRD soils was much higher than the longitudinal surveys—184 and 1053 mg/kg dw (n = 83), respectively—with a mean and a median of 707 and 429 mg/kg dw, respectively. These findings strongly suggest the most significant concentrations of Hg in the stream banks are associated with the HRD outcrops. The effect of the HRD is apparent when the watershed is split into reaches based on catchments. The HRD is found only in the upper two reaches, and its thickness ranges from 5 to 45 cm. The concentrations of Hg in the upper two reaches, including all soil and HRD soil samples, averaged 206 mg/kg dw (n = 457), while it was only 13 mg/kg dw in the lower two reaches (n = 321). Therefore, a clear pattern has emerged; there are two major areas of high contamination associated with the HRD layers in the upper part of the watershed: one near NOAA and one near the former Bruner's market.

The creek bank Hg concentrations were compared with those of the sediments (Brooks et al. 2017) to consider the role of the soils as a source of Hg to the stream and to determine changes as a function of creek bank distance. The 25th and 75th percentile of Hg in the streambed sediments was 12.6 and 19.8 mg/kg dw (n = 19), respectively, with a mean and median of 16.1 and 14.1 mg/kg dw, respectively (Dickson et al. In review). Concentrations of Hg are therefore considerably higher in the HRD layer compared with the surrounding soil or the streambed sediments. There are peaks of slightly higher Hg concentrations in the streambed sediments in the vicinity of both NOAA and the former Bruner's market, suggesting that soils have eroded from the HRD and deposited into the streambed sediments. A simple ratio of the log of Hg concentrations in the stream bank soils compared with that of the streambed sediments highlights the potential source areas, where the ratio exceeds zero (Figure 2).

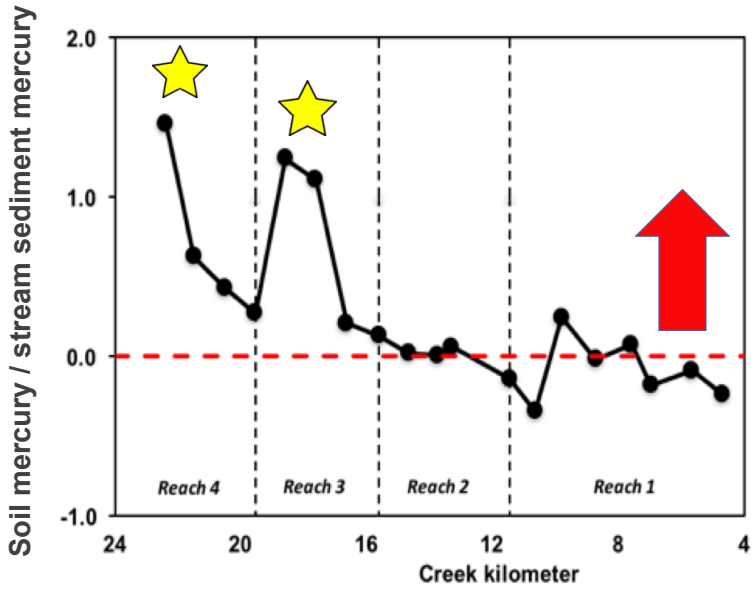

Figure 2. The ratio of the log of Hg concentrations in the stream bank soils compared with that of the streambed sediments, encompassing the entire dataset. The dotted red line notes where the soil and streambed sediment Hg concentrations are equivalent, and the arrow highlights that soils could be a source to the stream when the ratio of their logged concentrations exceeds zero. The two stars denote approximate locations of HRD outcrops.(Source: Dickson et al. In review)

Stream bank soils are also an important source of MeHg to the EFPC system. The 25th and 75th percentile of MeHg in stream bank soils from the 2014 and 2015 longitudinal surveys (n = 163) was 1.25 and 4.43 µg/kg dw, respectively, with a mean of 3.76 and a median of 2.75 µg/kg dw, respectively (Dickson et al. In review). The HRD also had higher MeHg concentrations compared with the creek bank soils analyzed in the longitudinal surveys. The 25th and 75th percentile of MeHg from the HRD areas (n = 21) was 11.4 and 30.1 µg/kg dw with a mean of 23.5 and a median of 17.8 µg/kg dw, respectively. Consistent with these observations, soil MeHg concentrations in Reaches 3 and 4 were significantly different (ANOVA, p = 2.64e-8) and approximately three times higher (8.3 ± 11 µg/kg dw, n = 124) than in Reaches 2 and 1 (2.6 ± 3.2 µg/kg dw, n = 131). The differences between the upper and lower reaches likely, again, reflects the contributions of the HRD layers.

KEY CONCEPTS

- Creek bank soils account for a substantial proportion of Hg export to the EFPC watershed
- The historical release deposit (HRD) is a key contributor to Hg and MeHg concentrations from creek bank soils
- Reducing Hg fluxes from soils into EFPC should decrease Hg available for methylation

Consequently, understanding the role of erosive forces in delivering Hg to the streambed is of primary importance (Figure 3). There are now 4 years of monitoring a set of erosion pins installed throughout the length of EFPC (Figure 4). The method consists of driving a narrow diameter metal rod into the stream bank until it is flush with the surface. To quantify erosion, the length of exposed part of the pin is measured over time. Deposition is measured similarly after carefully exposing the tip of the pin. Mean bank erosion rates are calculated and are combined with measurements of reach length and bank height to estimate volume and mass of erosion (Watson et al. 2016, Watson et al. 2017). Connecting the erosion measurements and the erosion potential as determined from the previous kayak studies to the small-scale stream bank morphology (i.e., meander bends and stream bank height) and to the HRD outcrop locations is still needed. Additional and targeted deployment of erosion pins would help increase our understanding of the erosive potential, particularly in the areas of the HRD outcrops.

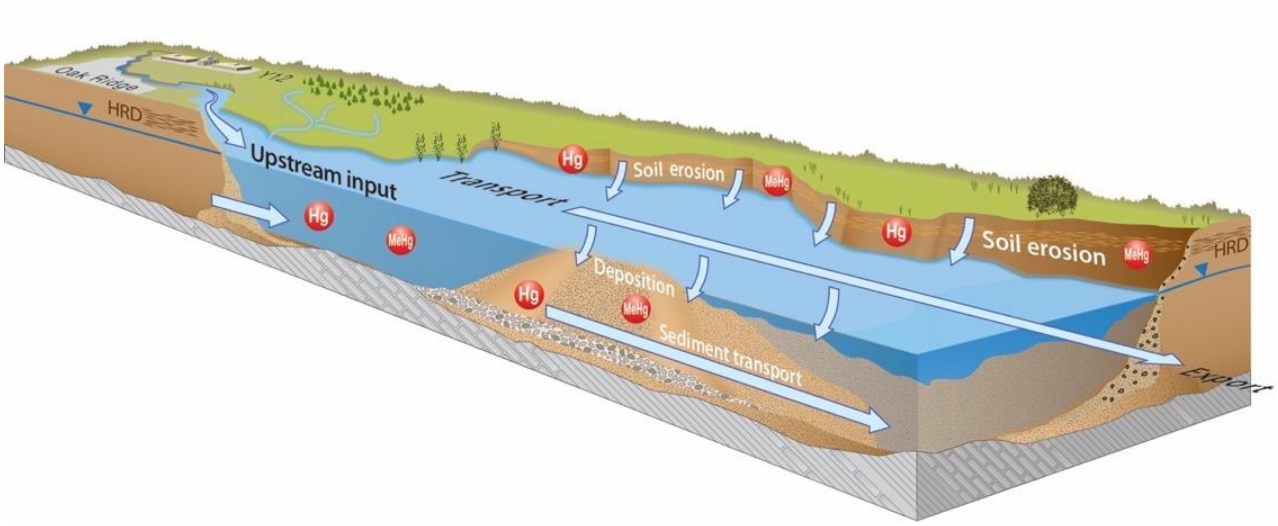

Figure 3. Concept diagram of Hg and MeHg release from stream bank soils, and incorporation into stream water and streambed sediments. The HRD is shown as a distinct layer above the water table. (Source: Dickson et al. In review)

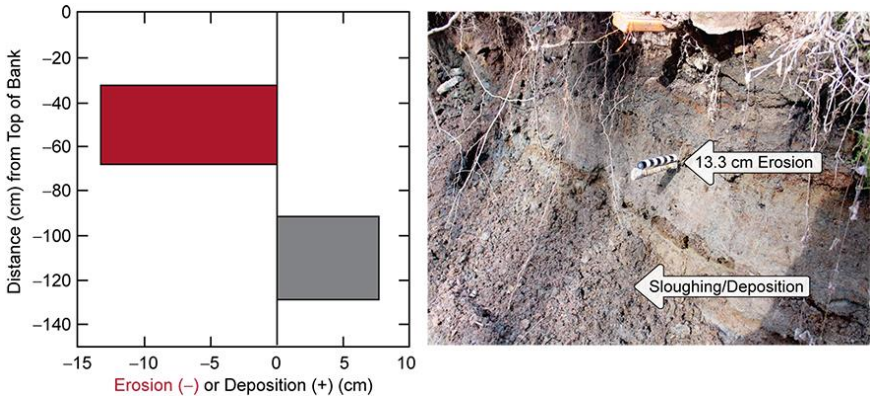

Figure 4. An erosion pin survey at East Fork Poplar Creek kilometer (EFK) 22 showing pins highlighted with arrows (right) and the erosion and deposition in the graph (left). The images reveal erosion in the upper pins and sloughing and deposition at the lower pins. (Source: Peterson et al. 2014)

Further, the fate of the eroded soil particles remains unclear. The particle size of the streambed sediments is on average much greater than that of the soils, potentially reflecting inadequate sampling of the streambed sediments and/or export of the eroded soil particles out of EFPC (as opposed to deposition). A true understanding of where and under what conditions soils are eroded, as well as the fate of those particles, still remains to be elucidated. Finally, the lability of Hg in association with soil particles is much less than the lability of Hg associated with streambed sediments (Dickson et al. In review), as assessed by a widely used sequential extraction method (Bloom et al. 2003). The extent to which these differences are due to chemical interactions with EFPC waters versus biological processing associated with heterotrophic and/or periphyton communities remains unclear. This kind of information will be essential in the development of a complete conceptual model.

Soil Technologies

There is now much greater understanding of where to target remedial efforts in EFPC—the HRD outcrop areas (Figure 5). Investigations planned for the coming year will bring improved understanding of the most pertinent locations regarding erosive forces. Meanwhile, testing of technologies that might be effective for minimizing the flux of Hg and MeHg from the stream bank soils (engineered sorbents) continues as described in the subsequent section. Here, we revisit technologies initially proposed in our first remedial technology development document (Peterson et al. 2015) in light of our findings.

Optimal technology development could involve some combination of bank stabilization strategies in key locations (e.g., the HRD) while seeking to both preserve and enhance the existing environment. For example, bank stabilization with armoring, decreasing the slope of creek banks, removing unstable trees, and stabilizing the slope with native plants or other materials could effectively reduce erosion. In the coming year, the team will incorporate site-specific information to help compare and narrow the potential soil remediation technologies that could be directly tested in EFPC (Table 1; Peterson et al. 2015).

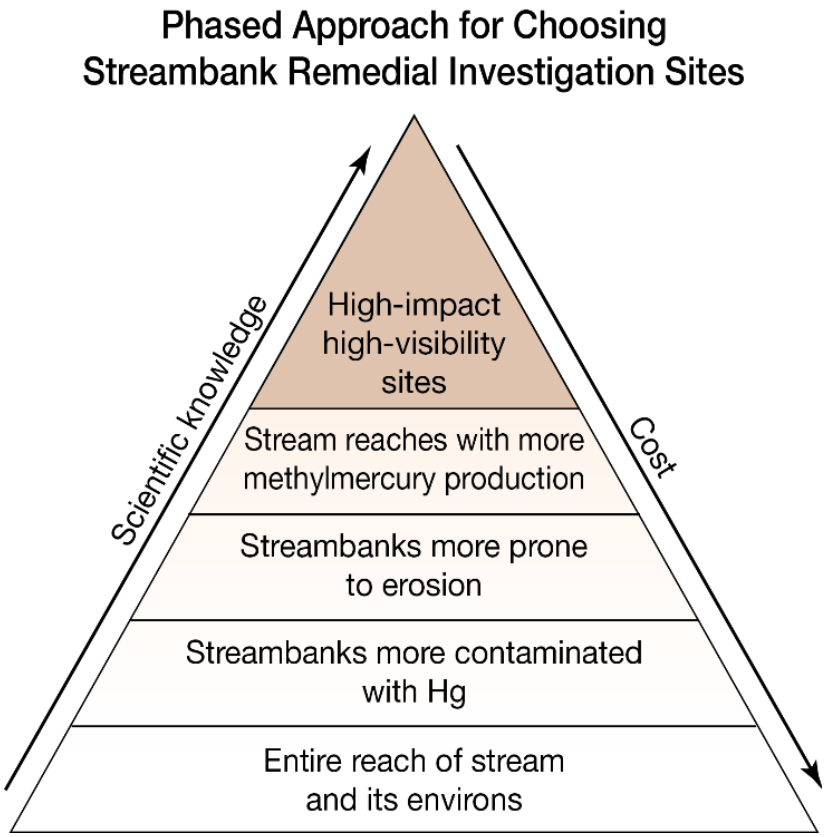

Figure 5. Phased approach for choosing stream bank remedial investigation sites and to determine target areas for remediation. (Source: Peterson et al. 2015)

One technology that has been investigated in considerable detail thus far is the use of engineered sorbents (see the next section, "Evaluation of Sorbent Technologies"). Engineered sorbents are designed for uptake of Hg or MeHg, and they could be applied in concert with other stabilization measures or designed to function as a stand-alone stabilization technology. The South River in western Virginia provides an example of bank stabilization and sorbent deployment to reduce Hg contamination in a stream environment similar to EFPC (Rhodes et al. 2009, DuPont 2013, Stahl et al. 2014). At South River, two different generations of pilot-scale projects have been completed involving a combination of soil removal, geosorbent deployment, slope reduction, and native plantings to promote slope stabilization. ORNL staff are on the South River Science Team are closely following progress.

As described in Peterson et al. (2015), soil remedial options range from "no action" to "removal and reburial," but there is not a scientific consensus that these options will meet the needs for site cleanup (Looney et al. 2008). Remedial actions focused only on Y-12 are unlikely to fully address Hg contamination in the downstream environment, especially at the lower end of the creek where methylation rates are high, as well as at the upper end where stream bank soils are highly contaminated. Cleanup technologies involving removal and reburial will be disruptive to local communities and the environment and could be prohibitively expensive when deployed over significant reaches of the creek. This would be particularly true if the HRD contamination extends significantly into the floodplains, as our initial findings suggest that it does. The goal of soil technology development in this project is, therefore, to find alternative approaches that reduce Hg fluxes while avoiding large-scale soil removal.

Table 1. Potential soil remedial technologies and approaches for LEFPC (Peterson et al. 2015).

Technology	Description	Objective	Positives	Negatives	Technical Maturity	Research Needs	Overall Evaluation
Bank or floodplain soil removal	Removal of soils with significant bioavailable mercury	Minimize releases of bioavailable mercury to creek	Permanent source removal	Environmentally disruptive. High public visibility. Volume of low contamination is large. High potential cost	Common remedial approach with history of use in EFPC watershed	Lack of understanding of what constitutes bioavailable mercury in bank soils	Viable but not preferred unless hot spots of bioavailable mercury are identified
Bank stabilization through physical armoring	Armoring of bank soils susceptible to erosion with riprap, geotextiles, etc.	Minimize erosive release of particle-associated mercury into EFPC	Straightforward to implement	Environmentally disruptive. Continued maintenance and monitoring is required. Delivery of sunlight may enhance methylation in the water column	Common remedial approach with history of use at EFPC	Identification of "high-risk" locations with high mercury and erosion potential. Demonstrate that reducing erosion reduces mercury concentrations in fish	Viable if bank soils contribute to mercury accumulation in fish
Reduction of slope angles of bank soils	Reducing bank slope angles to minimize erosion	Minimize erosive release of particle-associated mercury into EFPC	Straightforward to implement	Environmentally disruptive. Continued maintenance and monitoring is required.	Common remedial approach to prevent bank erosion	Identification of "high-risk" locations with high mercury and erosion potential. Mercury by depth into bank not well known	Viable if bank soils contribute to mercury accumulation in fish. Less certain to provide significant decrease in erosion
Removal of unstable vegetation	Remove trees and vegetation that are at risk of falling and destabilizing bank channels	Prevent treefalls that destabilize bank soils	Straightforward to implement. Can be coupled with armoring, bank slope angle reduction, and/or new plantings	Environmentally disruptive. Continued maintenance and monitoring is required. Effect of changes in sunlight on bioaccumulation not well understood	Common remedial approach for erosive creek banks	Identification of "high-risk" locations with high mercury and erosion potential. Demonstrate that reducing erosion reduces mercury concentrations in fish	Viable if benefits to mercury loading to stream and fish can be demonstrated
Stabilize creek bank and floodplain soils with native plants	Plant rhizomous native plants along creek banks and in floodplain soils	Reduce or minimize erosion of floodplain and bank soils	High potential to enhance existing environment. High potential to reduce erosion. Can be coupled with vegetative removal, reduction of bank slope angles, and armoring	Uncertain target locations for deployment. Continued maintenance and monitoring is required	Stream riparian restoration commonly deployed on Oak Ridge Reservation	Identification of high-risk mercury sources that are also susceptible to erosion. Requires demonstration that reducing erosion also reduces mercury concentrations in fish	Viable if benefits to mercury loading to stream and fish can be demonstrated
Sorbents to capture mercury and MeHg	Sorbents are applied to bank soils to accumulate mercury and prevent release to EFPC	Prevent mercury and MeHg from being released from bank soils	High potential for sequestration of mercury and MeHg. Can be coupled with vegetative removal, reduction of bank slope angles, and armoring	Method for stabilizing added sorbents is required. Potential high cost of sorbents. Uncertain target locations for deployment. Continued maintenance and monitoring is required	Field demonstrations are few. Deployment will require skill and experience	Requires testing to identify appropriate sorbents. Sorbents must have long-term chemical and physical stability and retention capacity	Viable, but more research is needed
Relocate creek channel	Identify locations for diversion of existing creek and reroute creek to flow through areas with lower mercury loading	Reduce or eliminate reaches where mercury is being released through erosion or where methylation is significant	Permanent solution to problem areas. Contaminated soils are left in abandoned channel	Much of surrounding land is privately owned. Extremely costly	Strategy has been deployed on smaller scale on the Oak Ridge Reservation	Identification of role of bank soils. Demonstrate that reducing erosion reduces mercury concentrations in fish	Viable but not preferred in most *locations* because of land ownership

Comparison of Sorbent Effectiveness

Remediation of Hg-contaminated ecosystems constitutes a significant long-term challenge because even low-level Hg contamination can result in transformation to toxic MeHg and biomagnification up trophic levels. Periodic flooding and erosion events can mobilize inorganic Hg and MeHg from sediments, bank soils and floodplains. The application of bank stabilization strategies coupled with amendments of sorbents aims to capture Hg species within a high affinity sorbent matrix. This approach is expected to limit migration of Hg species, production of MeHg, and transfer of MeHg into food webs. Strong binding of Hg species to the sorbent material results in a reduction in the pore water concentrations (Gilmour et al. 2013). However, the effectiveness of sorbent materials is sensitive to a variety of water characteristics, such as co-contaminants, competing metals, and ligands. Many environmental parameters, such as pH, redox conditions, and inorganic and organic ligands, influence the chemical speciation of Hg and its mobility. Dissolved organic matter (DOM) and suspended solids exert significant influence on the speciation, distribution, transport, and bioavailability of Hg in freshwater ecosystems (Aiken et al. 2011; Dong et al. 2010). Partitioning of Hg and MeHg species between various biogeochemical compartments controls net MeHg production and bioaccumulation of MeHg (Figure 6). Biogeochemically active regions are particularly important, because microbial activity drives the transformation of inorganic Hg to MeHg. Thus, the primary goal of sorbent amendments is to effectively lower the fraction of Hg and MeHg species available for methylation and bioaccumulation, respectively.

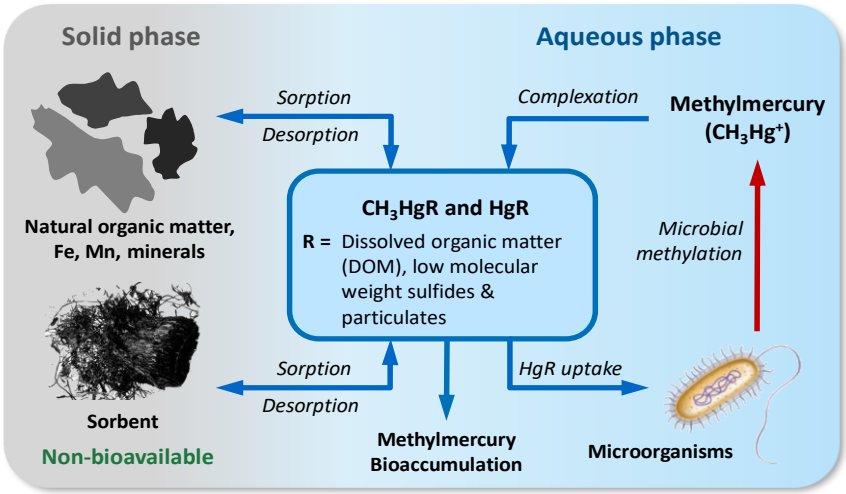

Figure 6. Partitioning of Hg species between aqueous and solid phase (natural organic matter, DOM, particulates, microorganisms, minerals, and sorbent amendments).

We evaluated sorbents in a series of small-scale laboratory studies and investigated the effectiveness of sorbent materials in the presence of Hg-DOM complexes, which are the predominant Hg species in freshwater ecosystems such as EFPC. The sorbent materials evaluated comprise several classes of materials and are listed in Table 2.

Table 2. Commercial and noncommercial sorbent materials under consideration

Class of material	Sorbent	Abbreviation	Description	Source
Functionalized mesoporous silica	Thiol-SAMMS THSL-62 (granular)	TS	Thiol-functionalized, self-assembled monolayer on mesoporous silica support	Steward Advanced Materials, LLC
Organoclays	Organoclay MRM	MRM	Functionalized bentonite-based clay (sulfur impregnated)	CETCO
	Organoclay PM199	PM199	Functionalized bentonite-based clay	CETCO
Carbon based	SediMite	SM	Activated charcoal, bentonite, and sand as a weighing agent	Sediment Solutions, LLC
	Biochar	BC	Natural charcoal from Colorado Pine converted by slow pyrolysis	Biochar Now
	Carbonized lignin	CL A	Lignin carbon foam carbonized at 1,000 ºC	University of Tennessee, Knoxville
	Carbonized lignin	CL B	Lignin carbon foam carbonized at 2,000 ºC	University of Tennessee, Knoxville
Brass	Brass wire mesh	BS	Cu/Zn alloy, immobilizes Hg(II) by reductive amalgamation	Alfa Aesar

At low-to-intermediate Hg concentrations (~2 µg/g), DOM severely limited the sorption capacities of all sorbent materials evaluated in this study at environmentally relevant Hg:DOM ratios (Figure 7). Thiol-SAMMS, SediMite, and biochar were most effective and have the potential to reach high removal efficiencies. Consequently, the effectiveness of sorbent treatments is anticipated to be highest in low dissolved organic carbon (DOC) environments and in systems with high Hg concentrations (high Hg:DOM ratios). Therefore, site-specific evaluations and pilot studies need to be conducted before sorbent deployment to assess impacts of the local biogeochemistry and the long-term effectiveness and stability of sorbents under site-relevant conditions (see the next section, "Testing of Sorbent Materials").

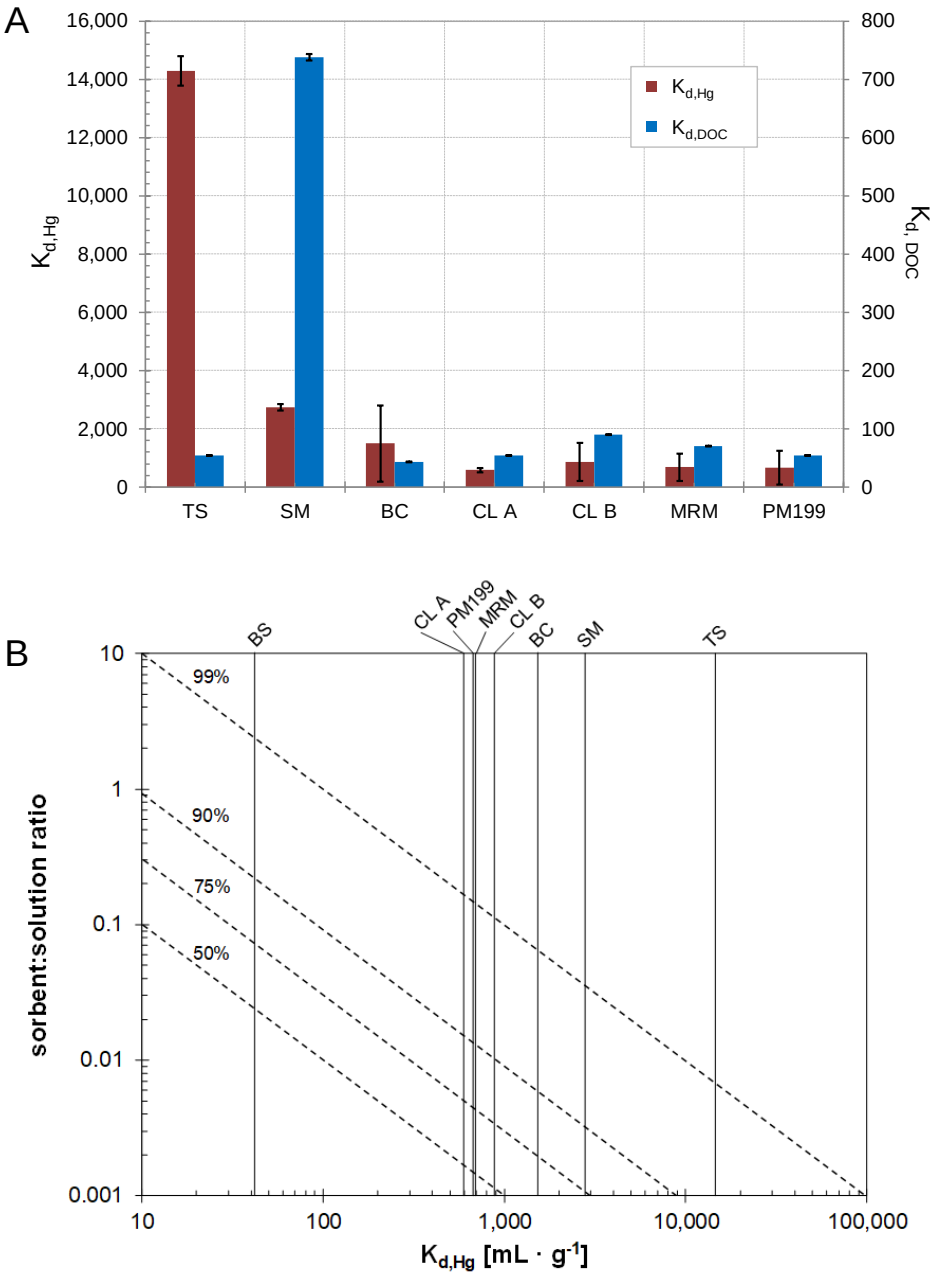

Figure 7. A. Hg(II) partition coefficients ($K_{d,Hg}$, red) between solution and sorbent materials in the presence of DOM. DOC partition coefficients ($K_{d,DOC}$, blue) provide insights into the distribution of DOM between solution and sorbent materials. Hg(II) was preequilibrated with DOM at a molar Hg:DOC ratio of $2.4 \cdot 10^{-6}$ (2 µg/L Hg(II), 60 mg/L DOC). B. Sorption nomograph correlating $K_{d,Hg}$ to sorbent:solution ratios. Isopleths (dashed lines) correspond to percent Hg removed from solution, vertical lines indicate the respective $K_{d,Hg}$ values. See Table 2 for definitions of acronyms.

Testing of Sorbent Materials on the HRD

A series of column studies have been performed for direct testing of the efficacy of sorbents. Large columns were packed with HRD soils to constitute a significant source of Hg (Figure 8). An artificial creek water recipe is used to leach Hg from the soil columns. Much smaller columns loaded with sorbent materials are connected to the outlet end of the soil columns. The concentration of Hg going into the sorbent columns is compared with the concentration of Hg coming out of the sorbent columns to determine the efficacy of the sorbent. Two columns each of sand (control), Thiol-SAMMS, biochar, SediMite, and organoclay PM199 were tested (Table 2). The rate of Hg elution from the columns was determined by comparison of the initial breakthrough of sorbents with that of a nonreactive tracer bromide. The extent of Hg elution from the columns was determined by comparison of the mass eluted from the soil column compared with the mass eluted from the sorbent column.

Figure 8. Column setup for testing the efficacy of engineered sorbents. A pump delivers artificial EPFC water to the soil column. Mercury and other ions are leached from the soil column, which also serves as the inlet for the sorbent column. The efficacy of the sorbents is determined by the difference of the concentration of mercury entering and exiting the sorbent column.

In no case were any sorbents 100% effective in retaining Hg. For example, Figure 9 shows that the timing of the breakthrough of Hg and bromide were identical in both SediMite columns. This implies that the sorbents will not slow the rate of transport of Hg. Modeling of bromide with the convective-dispersive equation (Figure 9a) demonstrates that flow along the walls of the columns or other preferential flow phenomena was not significant; thus, no experimental artefacts contribute to the rapid observed breakthrough of Hg. The initial breakthrough of Thiol-SAMMS, in contrast, showed significant retardation of Hg breakthrough, indicating that Thiol-SAMMS is much more effective at slowing the rate of transport of Hg (Figure 9b). Figure 9 is designed to show only the initial breakthrough of Hg through the sorbent columns to understand the rates of transport.

Over the entire experiment, the total proportion of Hg eluted was calculated using mass balance. In total, the experiments leached a total of more than 12 L through each sorbent column. Figure 10 shows an example, where the soil curve represents the Hg that came out of the soil (and went into the sorbent column) and the Thiol-SAMMS curve represents the Hg that transported through the sorbent. The shaded area in the middle is what was retained by the sorbent. By calculating the area under both curves, the amount of Hg retained by the sorbent can be calculated by the difference. Table 3 shows that Thio-SAMMS was the most effective sorbent, removing 85 and 89% of Hg added in the respective duplicate columns. Organoclay PM199 and biochar also retained considerable Hg, while SediMite retained only 62% of Hg added. The differences in the two biochar columns is due to the variability of the soil source. Interestingly, the sorbent column that retained more Hg also experienced much higher Hg concentrations coming from the soil.

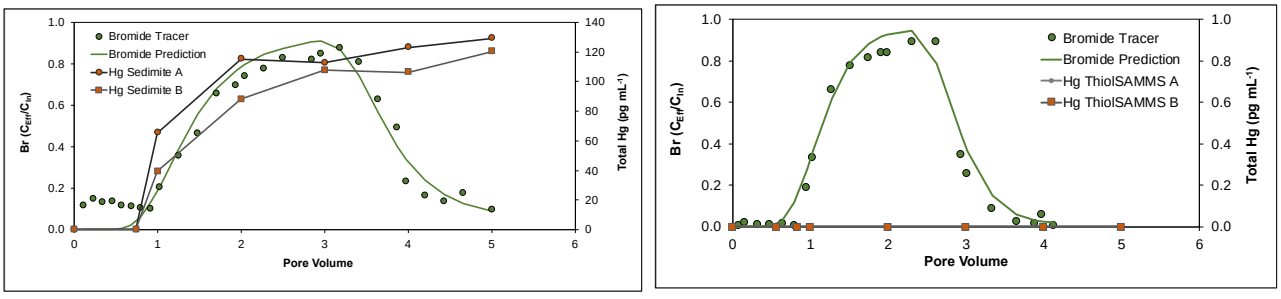

Figure 9. Breakthrough curves of nonreactive tracer bromide (Br) as relative concentration (effluent/influent) and Hg as pg Hg/mL as a function of pore volume. Observed (points) and modeled (lines) through (a) SediMite (left) and (b) Thiol-SAMMS (right).

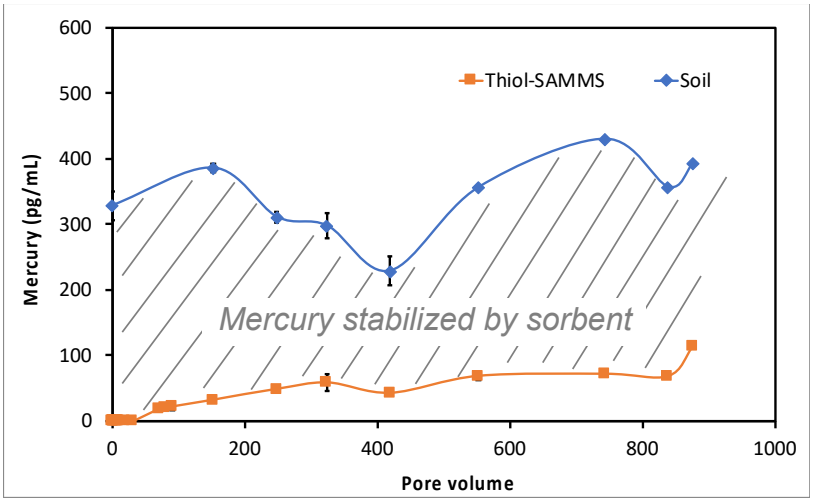

Figure 10. Example of determining the concentration of Hg exiting the soil column (blue curve) and entering the sorbent column (orange curve), the concentration of Hg exiting the sorbent column, and the gray area representing the mass of Hg retained by the sorbent column.

Table 3. Extent of Hg retained by engineered sorbent column experiments

Material	Mercury retained (pg)	Mercury retained (%)
Sand (control)	498	**15.4**
Sand (control)	337	**7.5**
Thiol-SAMMS	3,494	**84.7**
Thiol-SAMMS	3,072	**88.8**
SediMite	3,927	**61.6**
SediMite	4,417	**62.0**
Organoclay PM199	5,385	**70.7**
Organoclay PM199	7,366	**81.3**
Biochar	12,101	**84.9**
Biochar	3,920	**52.1**

These experiments demonstrate that Hg retention by sorbents is overall quite significant. The concentration of Hg added by the soil was large and occurred over a period of several months. The extent of uptake was not consistent with the previous batch experiments, which showed much greater efficacy of Thio-SAMMS compared with the other sorbents. Here, the efficacy of Thiol-SAMMS was only somewhat greater than that of the other sorbents. However, the rate data show that some Hg can readily and quickly escape all of the sorbents with the exception of Thiol-SAMMS. In other words, the initial breakthrough of Hg was rapid for all sorbents except for Thiol-SAMMS. Consequently, Thiol-SAMMS remains the most effective at capturing Hg. Overall, these findings are sufficiently encouraging to continue investigations with sorbents because of the significant quantity of Hg retention. The second phase of these experiments, in which both Hg and MeHg are being monitored, is ongoing.

One of the drawbacks of these experiments is that the leached Hg from the soil columns might not be fully representative of field conditions. For example, because concentrations leaching from the soils are high, the leached Hg might not be effectively associated with DOC, which is the predominant form of Hg in EFPC (as discussed previously), which seriously reduces the sorption potential. The high concentrations of Hg leaching from the HRD could also impart unrealistic sorption rates or extents. Consequently, similar experiments are planned using sorbent columns and real EFPC water in the upgraded Aquatic Ecology Laboratory at ORNL.

Based on these encouraging laboratory results, the sorbents were deployed in a field-scale pilot test. Biochar sorbent "coupons" were placed in the stream at NOAA and the former Bruner's market and in the creek bank soils at Bruner's. Initial tests in the lab were completed to ensure that the coupons were durable and that the sorbents did not leak out. The sorbents were encased in fine mesh and then placed into protective open plastic mesh cylinders. The soils were cored out and then the mesh cylinders were emplaced in the holes left in the creek bank (Figure 11). The soil cores were analyzed to determine the initial concentration of soil Hg. When deployed in the creek, the cylinders were affixed to metal T-shaped rods that were driven into the creek bottoms (Figure 11). Six replicates were emplaced near the bottom of the streambed at each location, and six replicates each were emplaced above, within, and below the HRD in the creek bank at Bruner's.

Figure 11. Sorbent coupon deployment in the creek bank at the former Bruner's market showing the mesh enclosing the sorbents, emplacement into mesh plastic cylinders, and attachment to rods for securing within EFPC.

Figure 12: Recovery of sorbent coupons after 3 weeks.

The coupons were recovered after residing in the field for about 3 weeks, and only a few were lost (Figure 12). All deployed coupons contained Hg, and the concentrations observed were consistent with expectations; for example, the creek NOAA samples had higher Hg compared with the Bruner's creek samples, which is consistent with higher EFPC Hg concentrations higher in the watershed (Table 4). Further, the coupons deployed in the HRD layer had higher Hg concentrations than the soils above or below the HRD layer, which is consistent with the higher Hg concentrations in the HRD compared with the surrounding soils. Consequently, we consider the study a complete success, and a much more detailed, long-term study is being planned (more sites, more sorbent types, longer overall time frames, more sampling time frames, and analyses for both Hg and MeHg). Beyond that, pilot-scale field studies may involve some form of creek bank modification coupled with deployment of sorbents, assuming continued acceptable performance of the technology.

Table 4. Recovery of Hg from creek bank soils above, within, and below the HRD and from the creek bed at NOAA and the former Bruner's market

Location	Mercury (µg Hg/g sorbent dw)
Above HRD	2.41 ± 0.65
HRD	5.21 ± 1.22
Below HRD	2.45 ± 0.78
NOAA creek bed	6.73 ± 1.37
Bruner's creek bed	3.73 ± 1.89

Groundwater Inputs

There were two major reasons for the groundwater investigation—to understand the extent to which Hg in groundwater is contributing to EFPC waters and to determine whether methylation in groundwater is contributing to observed MeHg in EFPC waters. Groundwater was monitored for more than 2 years at three locations (NOAA, the former Bruner's market, and the Horizon Center) in the EFPC watershed (Figure 13). At each location, the wells were configured to allow the calculation of a potentiometric gradient (i.e., the water table). One inland well, one upstream well, and one downstream well were emplaced at depths less than 12 ft deep, as described in previous reports. An additional stilling well was emplaced in the stream at each location. Each well contains a sonde that measures water elevation, temperature, and electrical conductivity at high frequency. Every 2 to 3 months, the wells were purged then manually sampled for Hg, MeHg, DOC, pH, redox potential, electrical conductivity, dissolved oxygen, reduced and total iron, sulfide and sulfate redox couples, anions, and select cations.

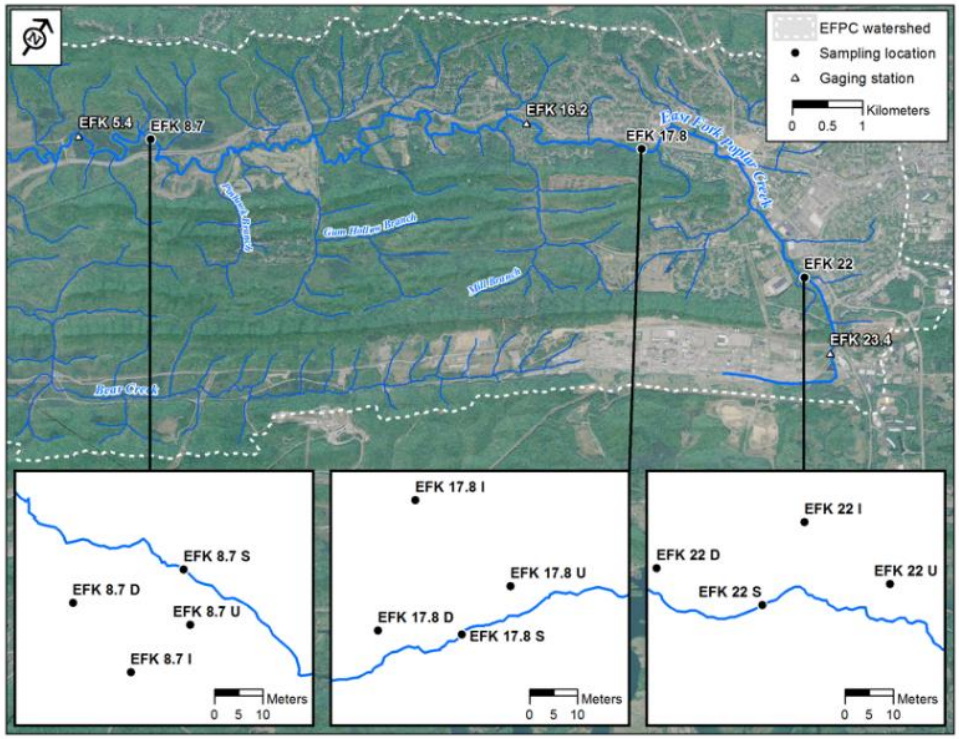

Figure 13. Groundwater sampling locations at the National Oceanic and Atmospheric Administration (EFK 22), Bruner's market (EFK 17.8), and the Horizon Center (EFK 8.7) along EFPC. (Notes: U = upstream; D = downstream; S = stream; I = inland). (Source: Peterson et al. 2018)

The water table elevations were averaged over each month for each site. When averaged over a month, all water head gradients were found to be consistently towards the creek, even in dry summer periods (e.g., Figure 14). Initially, it was thought that there may be seasonal reversals of the gradient, such that the stream might directly recharge the groundwater. Instead, water flow was consistently towards rather than away from the creek, suggesting that observed Hg in groundwater is more likely to be a result of leaching from contaminated soils in the floodplain than from interactions with the creek. However, it is possible that individual flooding events in the creek recharge the groundwater. Closer examination of the head data during events is being used to determine the role of individual events, but results are not yet available.

Mercury concentrations in the surface water were highest at NOAA (East Fork Poplar Creek kilometer [EFK] 22), followed by the former Bruner's market (EFK 17.8), and finally the Horizon Center (EFK 8.7) (see Surface Water and Sediment Manipulation section for more details). Groundwater, on the other hand, had much higher concentrations in EFK 17.8, whereas Hg in the groundwater at EFK 22 and EFK 8.7 were similar to each other (Figure 15). It is likely that the much higher concentrations at EFK 17.8 represent the effects of leaching through the HRD in the floodplain at this location.

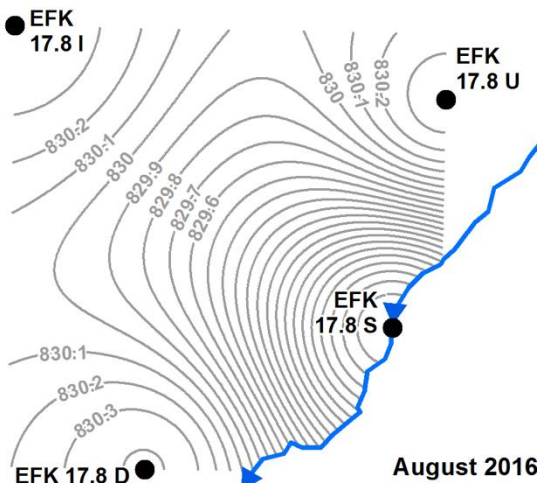

Figure 14. Example of potentimetric head (water table elevation) at the former Bruner's market at EFK 17.8 from August 2016. Flowlines (gray) are estimated from the water table elevations at the three groundwater wells EFK 17.8 I (inland), EFK 17.8 U (upstream), and EFK 17.8 D (downstream) and the surface water stilling well EFK 17.8 S. Flow can be inferred to move from high water table elevations at EFK 17.8 I to low water table elevations at EFK 17.8 S .

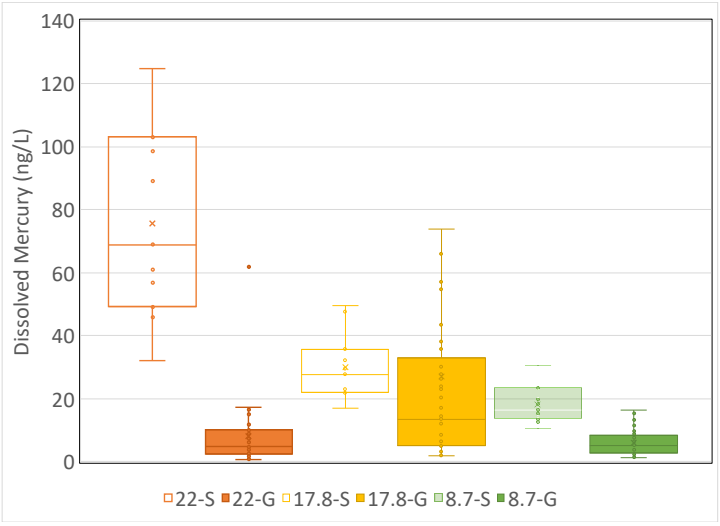

Figure 15. Concentrations of dissolved Hg in the surface water (S) and groundwater (G) at EFK 22, 17.8, and 8.7. Plots shown are box and whisker plots showing all data as points. The box represents the interquartile range (25% to75% percentile), the median is denoted by the central line, the mean is denoted by an "x," and the minimum and maximums are denoted by the brackets. Outliers are points outside of the minimum and maximum brackets.

Figure 16. Pit in the vadose zone at the former Bruner's market, with the dark-colored HRD layer visibly apparent, and the emplacement of a soil moisture sensor in the HRD layer. After the sensor was emplaced, the pit was backfilled.

The vadose zone in the former Bruner's market was monitored for soil moisture and oxygen content, where sensors were emplaced above, within, and below the HRD layer (Figure 16) and then subsequently backfilled. Results show that the HRD layer is often wetter than the soil above and below the layer (Figure 17). Consequently, there might be a greater opportunity for Hg to leach from the HRD layer and into groundwater. The results from the groundwater investigation were incorporated into a mercury source flux model to calculate the amount of groundwater recharging EFPC (Watson et al. 2016, Watson et al. 2017). The study compared the potential contributions of groundwater, soils, Y-12, and sediments to Hg in EFPC and determined that the role of groundwater was relatively minor.

Methylmercury concentrations in surface water were highest at EFK 8.7, followed by EFK 17.8, and then EFK 22 (Figure 18), consistent with many years of monitoring under the Water and Sediment Manipulation task. Mean and median groundwater MeHg concentrations, however, were much higher at EFK 17.8 compared with EFK 22 and 8.7. Much greater variability was observed at EFK 17.8 (Figure 18). The much higher MeHg values in groundwater versus surface water clearly suggests the production of MeHg in groundwater. These observations also support the idea that the stream recharge to groundwater is minor. The proportion of dissolved MeHg to Hg is also much greater in groundwater versus surface water, further suggesting the production of MeHg in groundwater.

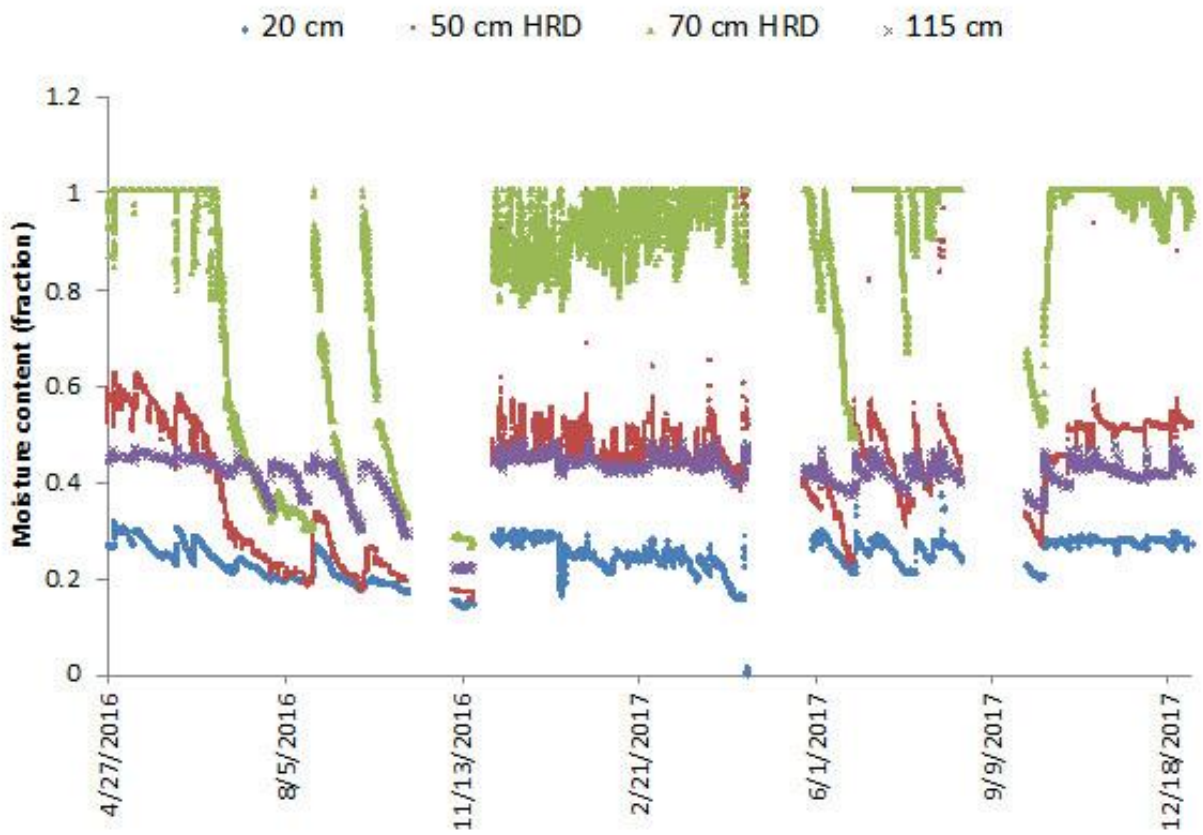

Figure 17. Soil moisture content in the creek bank at EFK 17.8. Sensors were emplaced at four depths above, within, and below the HRD.

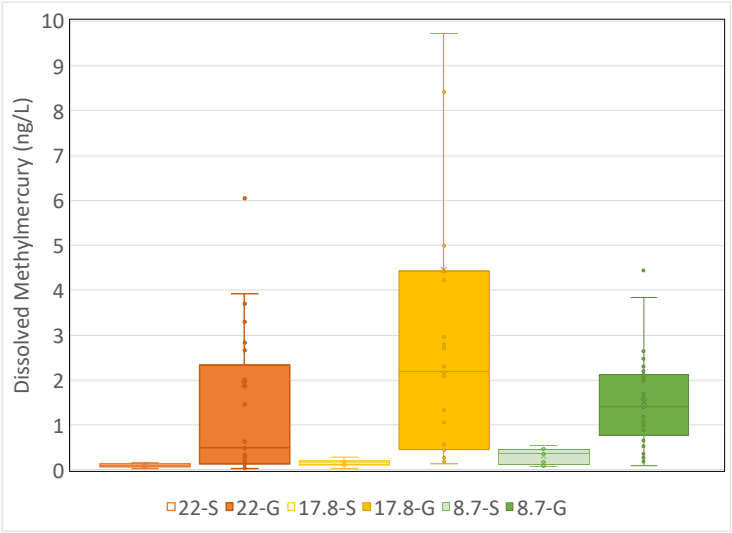

Figure 18. Concentrations of dissolved MeHg in the surface water (S) and groundwater (G) at EFK 22, 17.8, and 8.7. Plots shown are box and whisker plots showing all data as points. The box represents the interquartile range (25% to 75% percentile), the median is denoted by the central line, the mean is denoted by an "x," and the minimum and maximums are denoted by the brackets. Outliers are points outside the minimum and maximum brackets. Two outliers are not shown for EFK 22, and four outliers are not shown for EFK 17.8.

The ratios also tend to increase with downstream distance (Figure 19), which is consistent with observations in stream waters. In fact, most indicators of reducing conditions tend to increase in the downstream distance.

There are many indicators that groundwater conditions can be conducive for the production of MeHg since it is produced by anaerobic archaea and bacteria including methanogens, sulfate reducers, and iron reducers. Observations of low dissolved oxygen, reduced iron, reduced sulfur, and negative oxidation-reduction potential values are common in many of the wells throughout our observation period (Figure 20). Dissolved oxygen remains very low in all groundwater wells compared with surface water samples (Figure 20a). Reduced (ferrous) iron is common in groundwater wells and is not observed in surface water samples (Figure 20b). Thus, conditions conducive to the methylation of Hg are more common in groundwater samples compared with surface water samples, again suggesting that production of MeHg occurs in EFPC groundwaters. Similar to the HgT flux, Watson et al. 2017 used the groundwater data to model MeHg groundwater contributions to EFPC and MeHg flux was estimated to be much smaller than the potential production of MeHg in periphyton in the creek bed sediments.

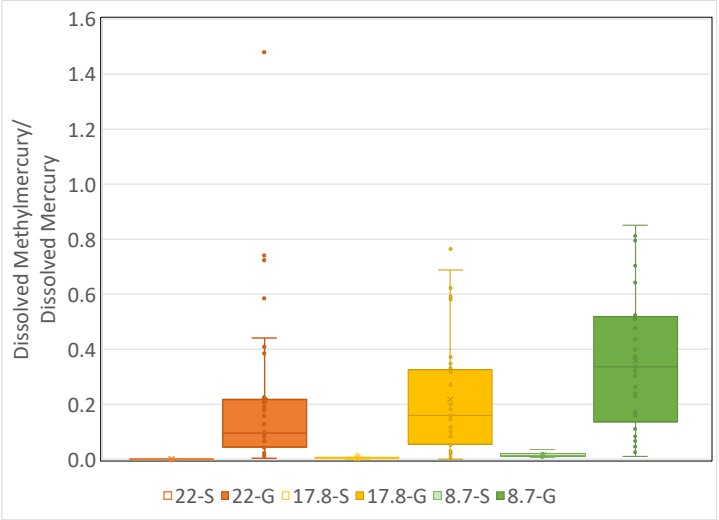

Figure 19. Ratio of the concentrations of dissolved MeHg to dissolved Hg in the surface water (S) and groundwater (G) at EFK 22, 17.8, and 8.7. Plots shown are box and whisker plots showing all data as points. The box represents the interquartile range (25% to 75% percentile), the median is denoted by the central line, the mean is denoted by an "x," and the minimum and maximums are denoted by the brackets. Outliers are points outside the minimum and maximum brackets. Two outliers are not shown for EFK 22, and four outliers are not shown for EFK 17.8.

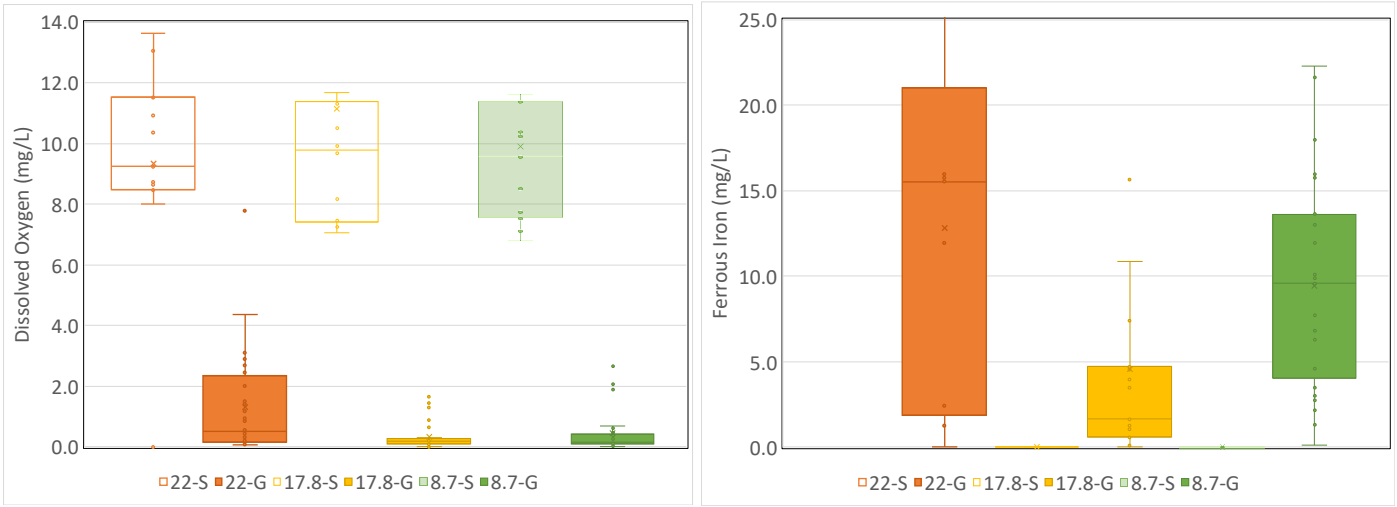

(a) *(b)*

Figure 20. Concentrations of (a) dissolved oxygen and (b) ferrous (reduced) iron in the surface water (S) and groundwater (G) at EFK 22, 17.8, and 8.7. Plots shown are box and whisker plots showing all data as points. The box represents the interquartile range (25% to 75% percentile), the median is denoted by the central line, the mean is denoted by an "x," and the minimum and maximums are denoted by brackets. Outliers are points outside the minimum and maximum brackets.

The current accumulation of evidence suggests that groundwater is a relatively small contributor of Hg or MeHg in the EFPC system. Routine well monitoring for the Mercury TD project was discontinued in FY2018. Through a university partnership not funded by the project, the wells will remain open to collect data useful to a watershed scale assessment of different sources of mercury using stable isotopes. This innovative project has the potential to advance our understanding of mechanisms of Hg cycling that might be of use in future remedial decision-making.

Soil and Groundwater Future Needs

Science-based solutions are being developed to address creek bank soil contamination in EFPC. Watershed-based sampling of the creek bank soils resulted in a clear prioritization of the locations at which contamination is the greatest concern. Continued effort is needed to connect Hg concentrations with erosive processes in the field, which will be the primary focus of the coming year. Thorough analyses of the erosion pin data and better connection with the erosion potential as inferred by the kayak study will be coupled with a detailed stream geomorphology investigation and new, targeted deployment of high-resolution erosion pins. The Aquatic Ecology Laboratory (AEL) will also be used to better understand how the form and lability of Hg in stream bank soils is affected by long-term chemical and microbiological reactions.

Lab-scale tests have conclusively shown that sorbents can be quite effective in accumulating Hg, but that none of them are 100% effective. Some questions remain regarding the suitability of the tests thus far employed, and resolving these questions will require the new capabilities afforded by the new AEL. Additionally, association of MeHg with sorbents has not yet been measured. New experiments in the field in the coming year and in the AEL when available will help to resolve these remaining concerns. Additional coupon studies in the coming year will provide better information on field-based efficacy of sorbents. Subsequently, some effort will need to be devoted to understanding exactly how sorbents might be deployed in the field in a remediation scenario. It is likely that sorbents will be applied in concert with other bank rehabilitation methods, such as vegetation removal, reducing creek bank slopes, creek bank stabilization through physical armoring, and vegetative replantings to stabilize creek banks.

Using groundwater total mercury concentrations in a watershed scale source model, the role of groundwater in contributing Hg into the EFPC system is dwarfed by more important sources, including erosion of stream bank soils and direct releases from Y-12. Task studies have determined that groundwater contains seasonally high MeHg, but concentrations appear to be much smaller than MeHg production by periphyton located in the hyporheic zone. Consequently, based on the current information we conclude that further investigation into groundwater technology development is not warranted at this time. This study's end provides a good example of how hypothesis-based research can help in prioritizing technology development efforts.

Consistent with the adaptive management approach, promising ideas from field and laboratory soil studies and sorbent testing are moving forward and up the technology readiness ladder. This task is on target for providing valid, science-based technologies for decreasing the flux of Hg from EFPC stream banks.

Surface Water and Sediment Manipulation

Importance of Surface Water Chemistry

The goal of water chemistry manipulation technologies is to disrupt Hg transport and loading, aqueous partitioning, methylation, and exposure/bioaccumulation mechanisms. By decreasing total and MeHg concentrations in surface water, the expectation is decreased flux of these constituents and their concentration in fish tissue. New water chemistry manipulation strategies and technologies are sought to effectively decrease Hg bioavailability and bioaccumulation, while limiting impacts to the environment or costly soil removals.

MeHg is generally assumed to be the form of Hg that is assimilated and bioaccumulated. Although this is true in many nonpolluted sites, it is worth considering that in an industrially contaminated setting with very high Hg concentrations, such as EFPC, inorganic Hg could also contribute to Hg body burden (Hines et al. 2000, Horvat et al. 2003). If this is the case, then decreasing waterborne Hg concentration should lead to rapid decreases in fish Hg because inorganic Hg is eliminated from tissues more rapidly than MeHg (Trudel and Rasmussen 1997). Therefore, actions targeted at lowering inorganic Hg concentration might directly lower Hg accumulation in EFPC biota in addition to lowering the supply of Hg for methylation by bacteria.

Total Hg concentration in LEFPC surface water exceeds the state of Tennessee's ambient water quality criterion, with the largest percentage of surface water Hg concentrations composed of inorganic Hg bound to particles. Point source discharges of Hg from Y-12 and redistribution and transport of legacy Hg within the watershed (e.g., bank soils, sediments) were believed to be the largest source of Hg in LEFPC. Nevertheless, the role of current releases of Hg from Y-12 versus downstream legacy sources outside of Y-12 was not well understood and was, therefore, an area of investigation.

Key questions concerning the role of surface water chemistry previously identified (Peterson et al. 2015) included quantifying Hg and MeHg flux along EFPC. Flux measurements serve several purposes for site management and technology development including (1) supporting conceptual model development and site characterization, (2) assessing exposure and risk evaluation, (3) informing site prioritization, (4) remediation selection and design, and (5) providing baseline information for performance, compliance, and long-term monitoring and evaluation. The prevailing conceptual model at the start of this project held that OF200 discharge was the dominant source of baseflow Hg loading to EFPC (Peterson et al. 2015). That might have been the case in the past, but changes in operations (e.g., cessation of the flow management program in mid-2014) and ongoing improvements in water quality in upper EFPC might have altered the components of the mass balance.

To address these needs and fill knowledge gaps, a new water monitoring station was established at the Wiltshire Drive overpass (EFK 16.2) to supplement our existing stations at EFK 5.4 and EFK 23.4 (Station 17). Using stream discharge and concentration data obtained under baseflow conditions at each of the three stations, instantaneous material fluxes have been calculated.

Mercury Flux

Our results to date indicate that diffuse legacy sources, outside of Y-12, make substantial contributions to the Hg flux along EFPC. For example, since October 2014 base flow instantaneous flux of total Hg (Hg_T), dissolved Hg (Hg_D), and particulate Hg (Hg_P) at EFK 16.2 has averaged 165%, 23%, and 338%, respectively, greater than the corresponding flux at EFK 23.4. Similarly, the flux of Hg_T, Hg_D, and Hg_P at EFK 5.4 has averaged 35%, 23%, and 38%, respectively, greater than the corresponding flux at EFK 16.2 (Figure 21). Mercury flux was generally lower in autumn, corresponding to annual lows in creek discharge and similar fluxes among the other seasons of the year at each location. More than 70% of the total Hg flux at EFK 5.4 derived from sources outside of Y-12. The lower reach of LEFPC, that section from EFK 16.2 to EFK 5.4, contributed about half as much Hg as the upper reach (EFK 23.4 to EFK 16.2). This was expected given that the upper reach encompasses the known areas of the HRD and might be expected to contribute more Hg than the lower reach. Discharge from the Oak Ridge Wastewater Treatment Facility makes a minor (<1%) contribution to the

overall Hg flux. Previous work (Brooks et al. 2018) suggests that Mill Branch, which makes its confluence with EPFC downstream of EFK 16.2, also makes minor contributions to the overall Hg budget.

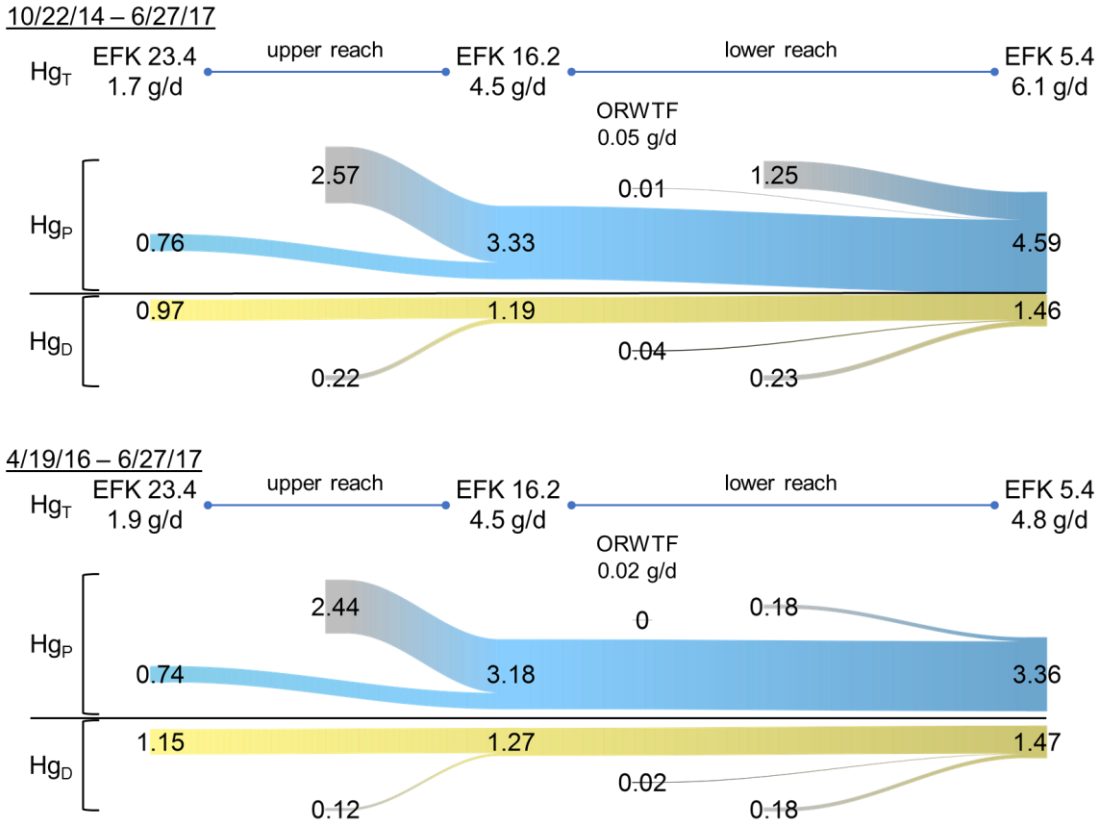

Figure 21. Average daily baseflow flux of different components of the Hg budget from EFK 23.4 to EFK 5.4 for the whole data record (upper) and the last 14 months of the record (lower). Numbers on the figure indicate flux in grams per day. The flux of all three components increases along the length of the creek suggesting that diffuse legacy sources outside of Y-12 contribute substantial amounts to the flux as measured at EFK 5.4. ORWTF = Oak Ridge Wastewater Treatment Facility outfall.

The mean Hg flux estimates at EFK 5.4 are dominated by a few high values measured during the earlier part of the record. In the last 14 months, our data record indicates changes in these patterns in which additions of Hg_P from the lower reach decreased by 85%. In comparison, there was little change to the Hg flux at EFK 23.4 or in Hg additions along the upper reach (Figure 21). Consequently, total Hg flux measured is unchanged at EFK 16.2 and has been lower at EFK 5.4. Note that our data record begins almost 6 months after flow augmentation was stopped, so this does not appear to be responsible for the change in flux in the latter part of the record. Nevertheless, this suggests that unidentified sources of legacy Hg in the lower reach of LEFPC periodically increase the Hg load in EFPC. The location of these sources and the mechanisms that activate or deactivate their loading of Hg to EFPC are unknown.

These flux calculations indicate sustained additions of Hg, predominantly as Hg_P, to EFPC in the upper study reach, which is known to encompass the HRD layer. Previous assessments suggest that HRD bank soils erode into EFPC and are a probable source of the increased Hg flux between EFK 23.4 and EFK 16.2 (Brooks et al. 2017, Brooks et al. 2018, Dickson et al. In review). Additions of Hg_D along this reach are much smaller in comparison. Actions that minimize or stop erosion of contaminated bank soils, with emphasis on the HRD layer, likely will decrease Hg flux throughout much of EFPC.

In the lower reach, no feature like the HRD has been identified, leaving the source of the additional Hg unknown and, therefore, warranting further study and investigation. Our measurements have eliminated Mill Branch and the Oak Ridge Wastewater Treatment Facility (ORWTF) outfall as sources of the increased Hg flux.

In addition to these average flux data, over the latter portion of our record, total Hg flux has been increasing over time at all three stations (Figure 22). The mean daily increase in Hg_T flux at EFK 16.2 and EFK 5.4 was 7.1 µg and 5.1 µg, respectively. Both trends were significant at the 95% confidence level. The mean daily increase at EFK 23.4 (2.9 µg) was not significant at the 95% confidence level, but there are fewer observations at that station. The increased total Hg flux was due to relatively equal increases in the flux of both Hg_D and Hg_P.

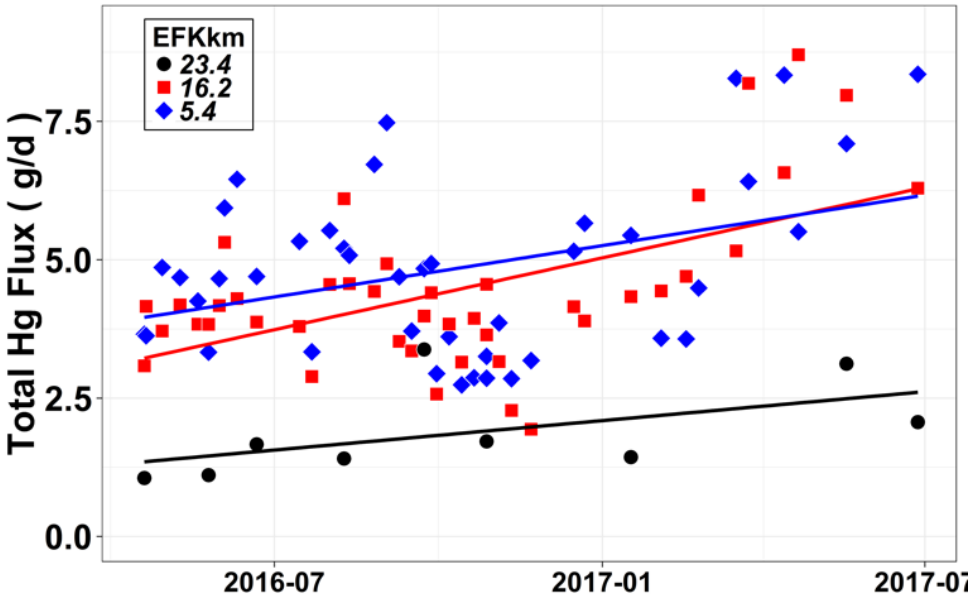

Figure 22. Total Hg flux at EFK 23.4, EFK 16.2, and EFK 5.4 over time from 4/19/16 to 6/27/17. Linear regression slopes are significantly different from zero for EFK 16.2 (p = 1.16e-4) and EFK 5.4 (p = 0.0144).

Methylmercury Flux

Methylmercury is not a direct contaminant to EFPC; rather, it is formed via an anaerobic microbial process. MeHg concentration increases with distance downstream in EFPC, but data on MeHg flux were largely lacking before the start of this project. Our data show MeHg flux increases downstream with most of that flux derived from watershed processes outside of Y-12 (Figure 23). Prior research indicates that in-stream processes control net MeHg concentration as opposed to out of stream processes (Riscassi et al. 2016).

Because Hg methylation is a biotically mediated process and, in EFPC, is generated partially in periphyton biofilms, temperature and light regimes influence MeHg concentration in the creek (Olsen et al. 2016, Olsen et al. 2018). MeHg concentration tends to be higher in spring and summer and lower in winter. Creek discharge also varies seasonally, and the interplay between these patterns results in higher MeHg flux in spring and lower MeHg flux in autumn (Figure 23); but the relative contributions of MeHg loading from different areas remain similar throughout the year. Neither Mill Branch nor the ORWTF are important sources of MeHg to EFPC.

In addition to the average seasonal MeHg flux results shown in Figure 23, total MeHg ($MeHg_T$) flux increased over time at both EFK 16.2 and EFK 5.4 (Figure 24). The mean daily increase in $MeHg_T$ flux at EFK 16.2 and EFK 5.4 was 5.5 ng and 14 ng, respectively. Both trends were significant at the 95% confidence level. The increased $MeHg_T$ flux was due to the increased flux of $MeHg_D$ as $MeHg_P$ flux did not change over our period of observation.

Intraday Patterns

Coupled with the longer-term patterns summarized previously, we conducted a diel sampling campaign at three locations (EFK 23.4, EFK 16.2, EFK 5.4), during which samples were collected every 2 hours over a 30-hour period. Full details of the study are described in Brooks et al. (2018). During this study we observed intraday concentration patterns in which Hg_P and $MeHg_P$ increased overnight due to increased bioturbation (Figure 25). These increases coincided with overnight maxima in total suspended solids and turbidity. Daytime maxima in dissolved MeHg were consistent with previous studies linking MeHg production in EFPC to actively photosynthesizing periphyton biofilms (Olsen et al. 2016).

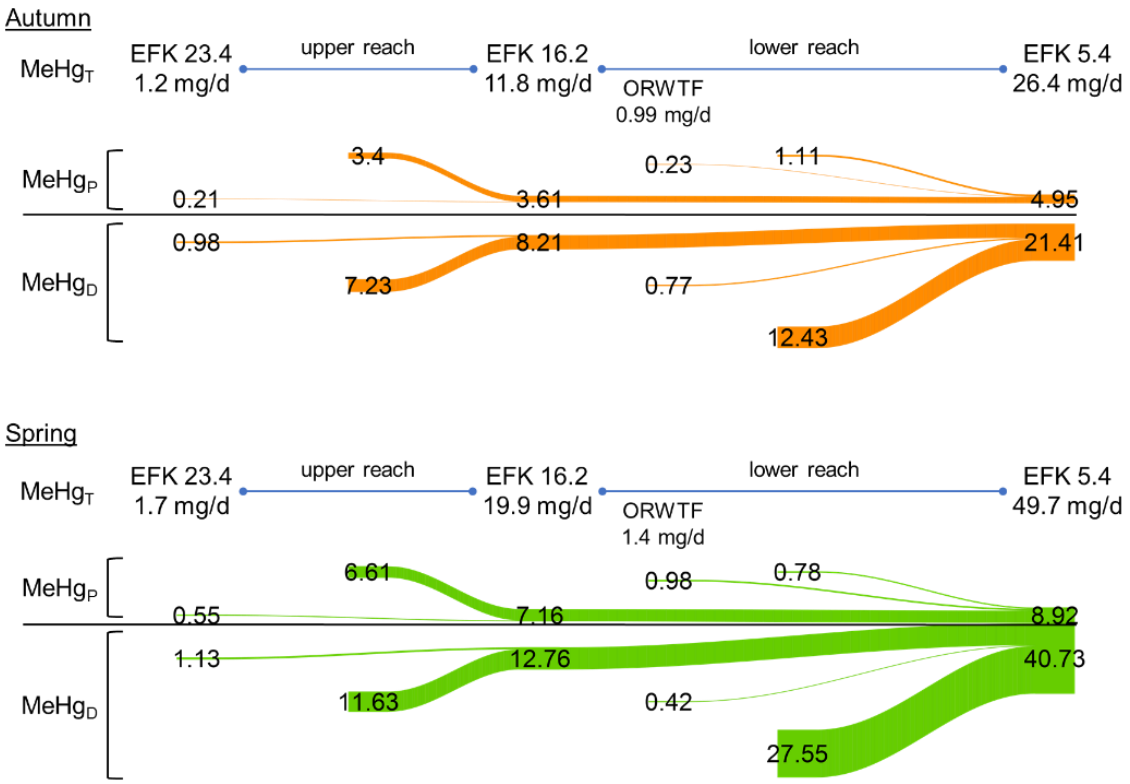

Figure 23. Average daily base flow flux of different components of the MeHg budget from EFK 23.4 to EFK 5.4 in Autumn (upper, orange) and Spring (lower, green). Numbers on the figure indicate flux in milligrams per day. ORWTF = Oak Ridge Wastewater Treatment Facility outfall.

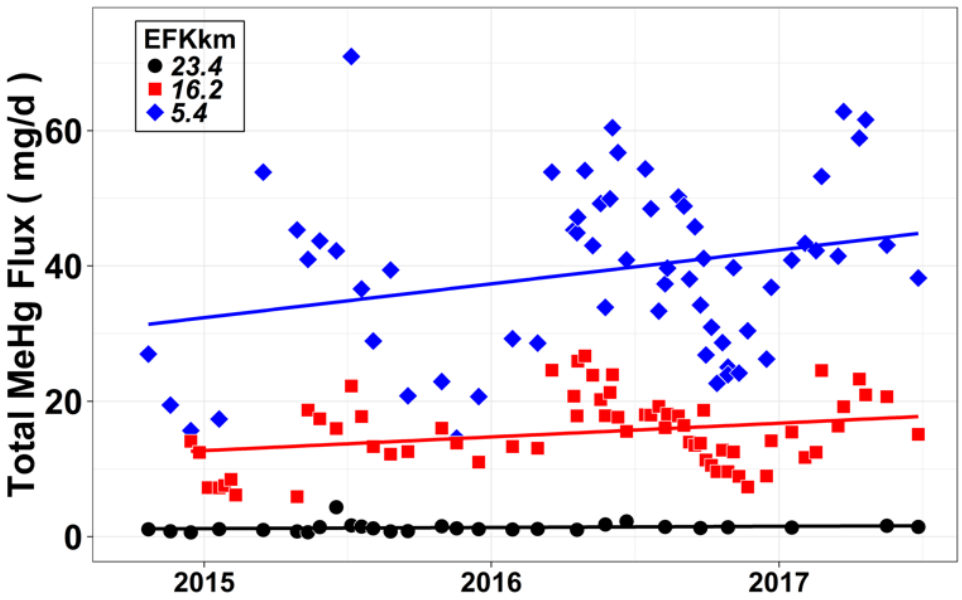

Figure 24. Total MeHg flux at EFK 23.4, EFK 16.2, and EFK 5.4 over time from 10/22/14 to 6/27/17. *Linear regression slopes are significantly different from zero at EFK 16.2 ($p = 0.0292$) and EFK 5.4 ($p = 0.0362$).*

Consistent with the flux estimates described previously, loading of total and dissolved Hg and MeHg increased downstream. The greatest increase in Hg_T, Hg_D, and Hg_P occurred over the reach from EFK 23.4 to EFK 16.2, implicating the HRD as a source of the added Hg. The HRD might contribute some $MeHg_P$ load to EFPC, but the majority of $MeHg_T$, $MeHg_D$, and $MeHg_P$ originates from in-stream production.

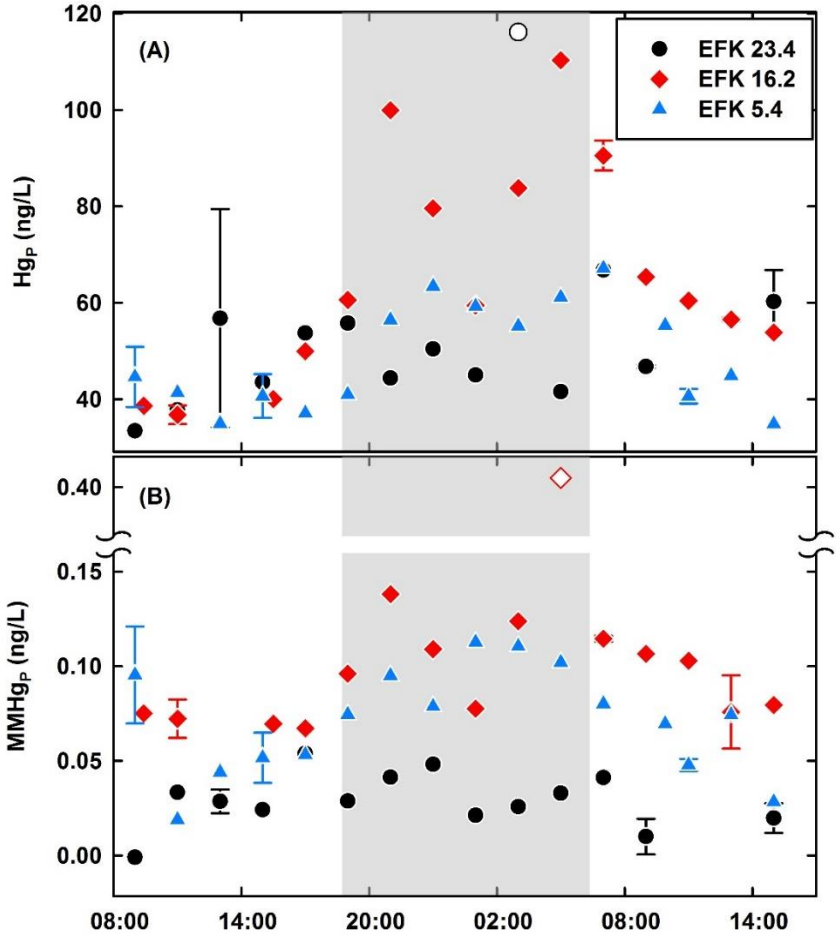

Figure 25. Particulate Hg (A) and MMHg (B) over the diel sampling period September 17–18, 2015. Error bars indicate the range of values for field duplicates. Strong potential outliers are indicated by the open symbols. The shaded area indicates the period from sunset to sunrise. MMHg = monomethylmercury

Studies of Alternative Treatment Chemicals at Y-12

Extensive spills of liquid Hg(0) in buildings, soils, and storm drains are the source of Hg_D in water exiting outfall 200 (OF200) and other outfalls along upper EFPC (UEFPC). Residual contamination in the stream channel itself contributes smaller amounts of Hg. The Hg(0) in Y-12 storm drain pipes is exposed to anthropogenic chemicals (e.g., chlorine, chloramines, excess dechlorination reagents) that can alter the water chemistry, thereby increasing Hg_D concentrations and fluxes to UEFPC.

For example, residual chlorine in process water can oxidize both liquid and dissolved Hg(0) into the much more soluble Hg(II) (Figure 26). Additionally, the Hg(II) that is generated is more readily methylated contributing to Hg bioaccumulation in the fish of EFPC. Our laboratory tests have shown that tap water with less than 3 mg/L of residual chlorine yields Hg(II) concentrations about 70 times greater than chlorine-free distilled water. Commonly used dechlorination reagents such as ammonium bisulfite (NH_4HSO_3) form strong aqueous complexes with Hg, increasing its solubility and concentration in solution. Further, our tests have also shown that these residual chemicals can release Hg

from creek sediments. Results like this suggest that exposure of Hg(0) to residual chlorine in the storm drain system increases Hg flux substantially relative to a situation in which residual chlorine is removed before contacting the Hg.

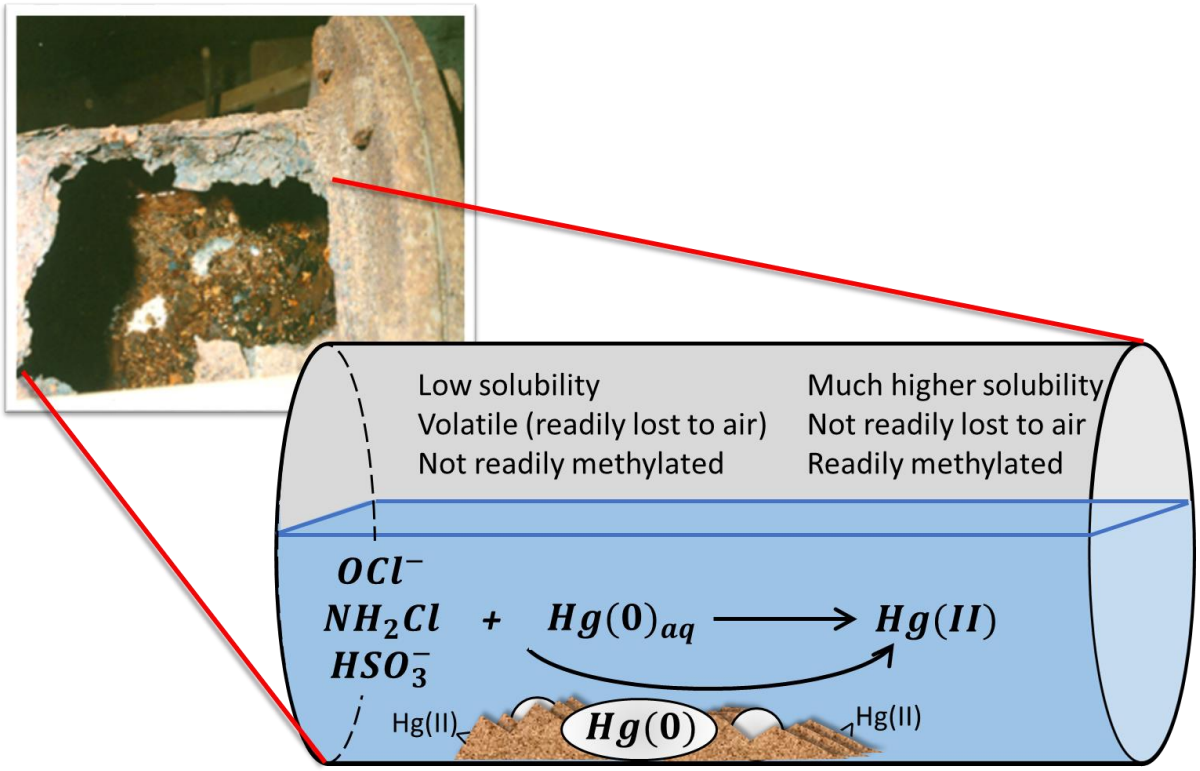

Figure 26. Oxidants such as chlorine and monochloramine present in the storm drain water can oxidize Hg(0) to Hg(II), increasing Hg concentrations and fluxes from the underground drain system to upper EFPC. Unreacted dechlorinating agents such as bisulfite can form strong complexes with Hg(II), promoting its release from sediments and other surfaces in the storm drain system and bed sediments in UEFPC and leading to higher Hg(II) concentrations in water.

At the same time, the combination of control (e.g., flow confined to the underground storm drain system), access and infrastructure at Y-12, and the relatively simpler chemistry in these storm drains relative to the open channel of LEFPC created a unique opportunity to directly manipulate water chemistry to reduce Hg flux at the headwaters of EFPC. Eliminating or reducing chlorine concentrations in the storm drain system could significantly reduce the amount of soluble Hg(II) produced as chlorinated water comes in contact with liquid and dissolved Hg(0) and could reduce the Hg_D discharged to LEFPC under base flow conditions.

We tested the effect of different dechlorinating agents on Hg solubility using beads of liquid Hg(0). An example of the results is provided in Figure 27. A 50 µL bead of liquid Hg(0) was added to either untreated water from invert E3125 (inside Y-12, located between Alpha-4 and Alpha-5), with total and free chlorine concentrations of 0.9 mg/L, E3125 water dechlorinated with sodium sulfite, or water dechlorinated with ascorbic acid (vitamin C). Mercury concentration rose rapidly to more than 1,600 µg/L in the untreated water. In water dechlorinated with sodium sulfite, Hg concentration rose rapidly but reached a final concentration of about 300 µg/L; and following dechlorination with ascorbic acid Hg, concentrations rose more slowly and reached a final value of about 200 µg/L. Dechlorinating the water has demonstrable benefits with respect to decreasing Hg concentration, but the choice of which dechlorinating agent to use is also important to the goal of lowering Hg concentrations. Although sodium sulfite released similar albeit greater amounts of Hg than did ascorbic acid, the use of sodium sulfite carries with it the risk of creating hypoxic to anoxic conditions in the water if it is not carefully applied. This would lead to the undesirable death of fish in parts of UEFPC. Overapplication of ascorbic acid does not lead to hypoxic/anoxic conditions in the water. Other environmental benefits of using ascorbic acid instead of sulfur-based dechlorinating agents have been detailed elsewhere (Ryon et al. 2002).

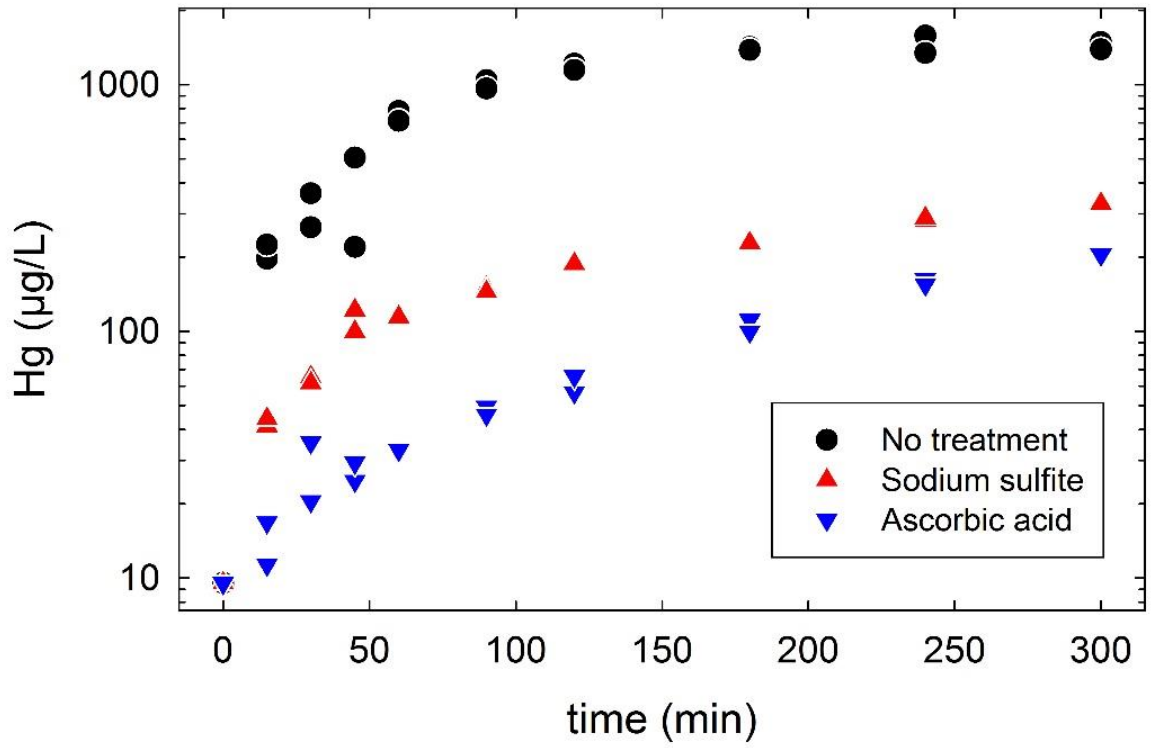

Figure 27. Mercury concentration in water over time using water from E3125, which had initial free and total chlorine and Hg concentrations of 0.9 mg/L and 9.6 µg/L. A single 50 µL drop of liquid Hg(0) was added to the water, and Hg concentration was measured over time. The water was used without dechlorination treatment (black circles) or after dechlorinating with either sodium sulfite (Na_2SO_3, upward red triangles) or ascorbic acid (i.e., vitamin C, downward blue triangles).

Following these laboratory studies, we tested the efficacy of dechlorinating water in Hg-contaminated storm drain systems just downstream of discharge points to the storm drain, especially in areas where Hg(0) contamination is known to exist, for the purpose of decreasing Hg concentration and flux. Two short-term field tests were conducted, one at ORNL and the second at Y-12, using ascorbic acid (i.e., vitamin C) as the dechlorinating agent. In the test at Y-12, ascorbic acid (AA) tablets were placed at several outfalls in the West End Mercury Use Area and Hg concentrations, as well as other water chemistry parameters (dissolved oxygen, pH, conductivity), were monitored at 200A6. AA addition locations were several hundred meters upstream of the sampling point.

Results of this test showed that shortly after AA additions chlorine was completely removed from the water and did not return until after AA additions were stopped. Both Hg_T and Hg_D concentrations decreased over the duration of the 4-hour test by approximately 20-25% and were slower to recover than chlorine concentrations after the AA additions stopped (Figure 28). Encouragingly, there were no adverse effects observed for other water quality parameters.

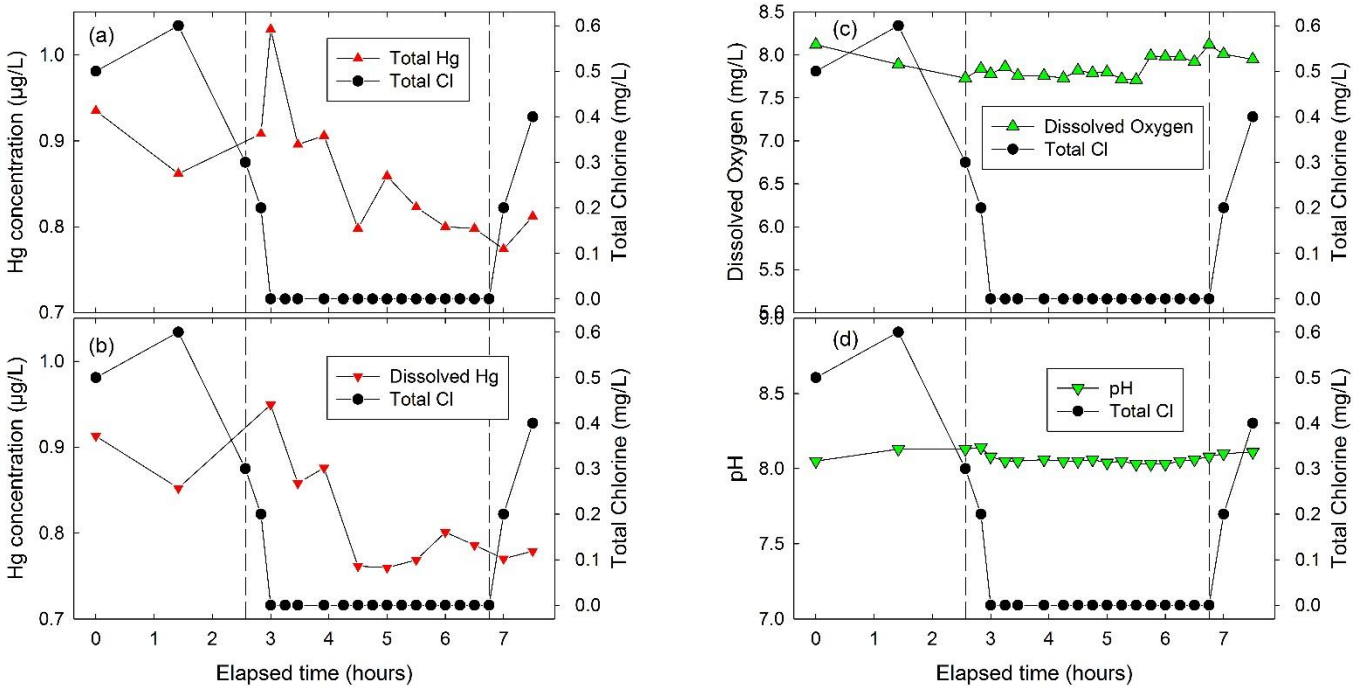

Figure 28. Total (a) and dissolved (b) Hg and total chlorine concentration in water at outfall 200A6 before, during, and after AA addition at several outfalls farther upstream in the storm drain network. No adverse effects were seen in other water quality parameters such as dissolved oxygen (c) or pH (d). Vertical dashed lines in each panel indicate the start and end of the AA additions.

Sediment Characterization

We previously identified several unknowns about EFPC sediments that were of interest from a system assessment and technology development perspective (Peterson et al. 2015). These knowledge gaps included insufficient information on the concentration of Hg in sediments as a function of grain size and along the length of EFPC. We also lacked information regarding how strongly Hg was associated with the sediments—information that contributes to a conceptual understanding of Hg release from sediments to the overlying water column and the efficacy of sorbents applied to sediments for the purpose of immobilizing Hg. To fill these gaps, we conducted an extensive survey of EFPC sediments (Brooks et al. 2017), the results of which are summarized subsequently.

The inventory of Hg in EFPC sediments was estimated to be 337 kg, representing a 67% decrease relative to the previous survey, which was conducted in 1984. The greatest relative improvement in Hg sediment concentration occurred in upstream sections of EFPC, suggestive of downstream transport of contaminated sediments. This overall improvement in Hg inventory likely resulted from several factors including (1) improvements in water quality from Y-12, (2) transport of contaminated sediment out of EFPC, and (3) inputs of cleaner sediment to the creek.

Total Hg in bulk sediments showed low variability along EFPC. The total Hg_T concentration in LEFPC sediments was 16.1 ± 4.9 mg/kg-dw. The decrease in Hg sediment concentrations represents an encouraging trend, but these concentrations remain 8 to 53 times greater than the probable effect concentration (PEC) for freshwater sediments (MacDonald et al. 2000).

Sediment Hg concentration varied with particle size (Figure 29). In the upper reaches of the creek, concentration as a function of grain size followed the expected pattern fine (250 µm > *x* > 125 µm) > medium > coarse (2 mm > *x* > 1 mm) (Figure 29). In the lower reaches of the creek this pattern unexpectedly reversed (coarse = medium > fine) due to unknown causes.

More than 85% of sediment Hg was strongly bound regardless of grain size. This Hg could be removed only with concentrated strong acids. Typically, less than 1% of the Hg_T could be extracted with water or mild acid treatment, suggesting that although the sediments contain a substantial inventory of Hg, that sediment-bound Hg might have limited impact on Hg_D load in the water. Additional testing is required to better understand the relationship between sediment and water-borne Hg.

The similarity of relationships among Hg, organic carbon, and nitrogen between fine sediments and bank soils suggested erosion of bank soils contributing to sediments (see conceptual model of instream sediment relationships in Figure 30). Notably, a localized region of elevated Hg sediment concentration (EFK 20 to EFK 16) coincided with an area in which the HRD has been documented.

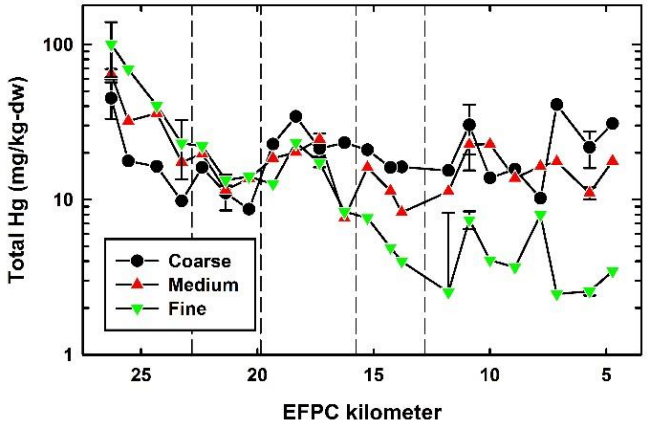

Figure 29. Total Hg in separate sediment size classes along EFPC. Error bars represent the standard deviation of triplicate determinations. Vertical dashed lines indicate creek reach. (Brooks et al. 2017)

Work to date on EFPC sediments has provided a current assessment of Hg concentrations and inventory at high spatial resolution for the first time in more than 30 years. Significant improvement in sediment Hg load was documented, but concentrations remain above ecological indicator concentrations (PEC). To better understand whether sediment-bound Hg is a significant source of Hg to the water column, additional studies are warranted to quantify the rate and extent of Hg release from the sediments to water under representative creek water chemistry conditions. Results of these studies will help inform other technology development and remediation needs such as prioritizing sediments for direct action and the efficacy of sorbents for Hg control and stabilization.

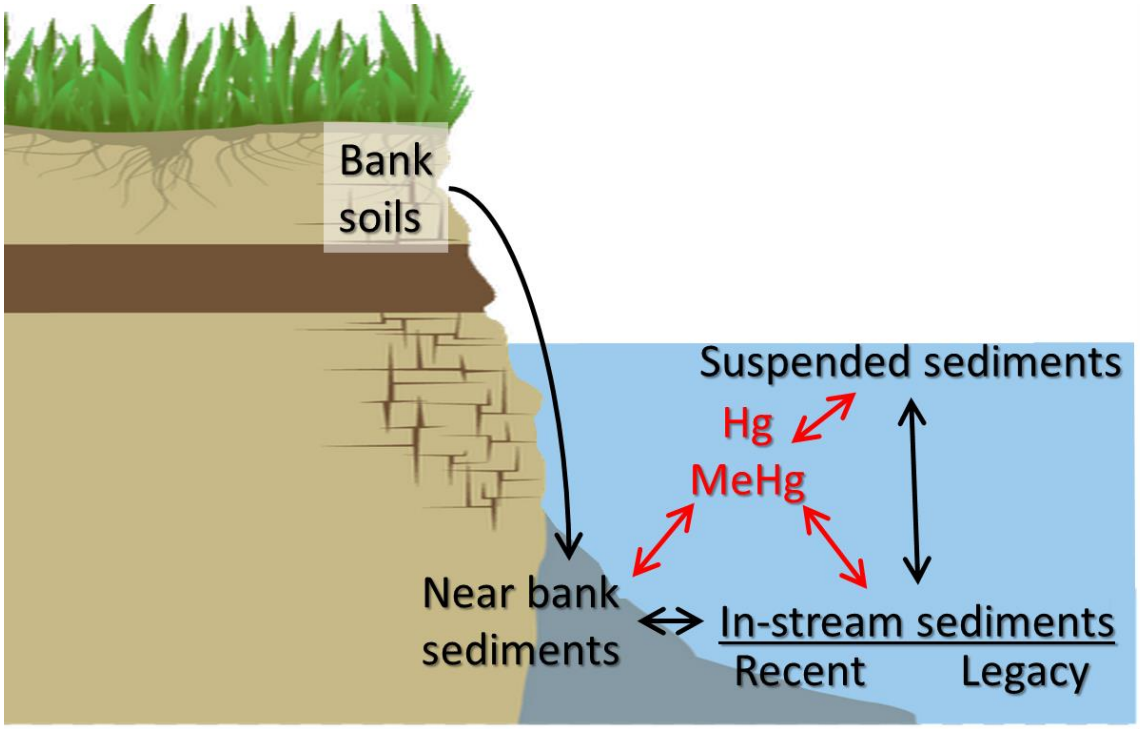

Figure 30. Updated conceptual model of relationships among bank soils, creek sediments, and suspended solids. Erosion of bank soils into EFPC contribute to recent near-bank sediments that are reworked by the creek and eventually are worked into the bulk creek sediments. Near bank, recent, and legacy in-stream sediments are transported downstream as bed load and all contribute to the suspended load. Mercury and MeHg partition onto and off of these sediments, altering their reactivity and availability.

The role of Dissolved Organic Matter on Sorbent Effectiveness

In the case of Hg, the application of sorbents for water treatment operates on several fronts. First, an effective sorbent will remove Hg from the water with attendant improvements in water quality. Second, the conventional wisdom has held that sorbed Hg is not available for methylation. The resulting decrease in MeHg production in the system should then lead to lower MeHg in biota. Lastly, the sorbents might also remove MeHg from solution, improving water quality and potentially decreasing MeHg bioaccumulation by biota (Figure 31).

Despite these potential benefits, most published research on the use of sorbents to address Hg contamination have not been conducted using ubiquitous and naturally occurring DOM, leaving important gaps in our understanding of sorbent applications for treating Hg-contaminated systems. DOM is known to form strong complexes with Hg and MeHg, and these organo-mercury complexes likely have different chemical properties with respect to sorption, desorption, methylation, and uptake. We have been careful to include DOM in our studies of Hg/MeHg-sorbent behavior.

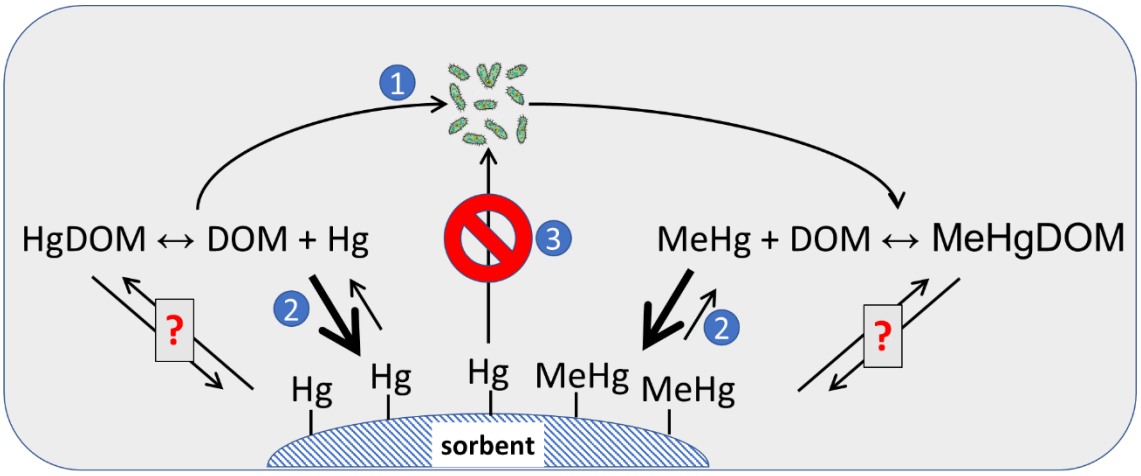

Figure 31. Modes by which sorbents can improve water quality and decrease bioaccumulation. (1) Some microorganisms in the environment can convert inorganic Hg into MeHg; (2) sorbents can remove both Hg and MeHg from the aqueous phase onto the solid phase, improving water quality; (3) conventional wisdom has held that sorbed Hg is not available to be methylated by microorganisms, leading to additional improvements in water quality. It is not known whether sorbed MeHg is taken up by biota. Most experiments have been conducted without ubiquitous naturally occurring DOM, leaving important gaps in our understanding of the effectiveness of sorbents in real settings.

Experiments were completed to assess the effectiveness of four sorbent materials to decrease MeHg production by the known Hg methylator, *Desulfovibrio desulfuricans* ND132 (ND132), and to decrease aqueous (i.e., 0.2 µM filter passing) MeHg concentrations. Biochar, ThiolSAMMS, SediMite, and Organoclay-199 were tested. The sorbents in most cases provided little, if any, inhibition of $MeHg_T$ production (Figure 32) but decreased the percentage of MeHg that passed through a 0.2 µm filter. The $MeHg_T$ produced was substantially greater than the calculated equilibrium aqueous inorganic Hg (Hg_i), based on sorption isotherms, implying that Hg assumed to be sorbed at the start of the assay was bioaccessible over the 24-hour methylation time frame. Additionally, MeHg production increased when Hg_i was introduced as a Hg:DOM complex, as compared with Hg(II). Some of the increased MeHg production might be attributable to lower Hg_i sorption with DOM, but a substantial amount of sorbed Hg must also have been accessible. DOM also increased the filter passing MeHg fraction, stressing the importance of Hg-DOM and MeHg-DOM interactions in experimental investigations. Testing indicated that sulfate concentrations did not affect Hg(II) methylation and could not explain the increased methylation seen with the Hg:DOM complex. Aging of Hg-sorbent mixtures for up to 383 days before the methylation assays did not affect the amount of MeHg produced for Biochar or SediMite treatments but significantly lowered MeHg production for ThiolSAMMS.

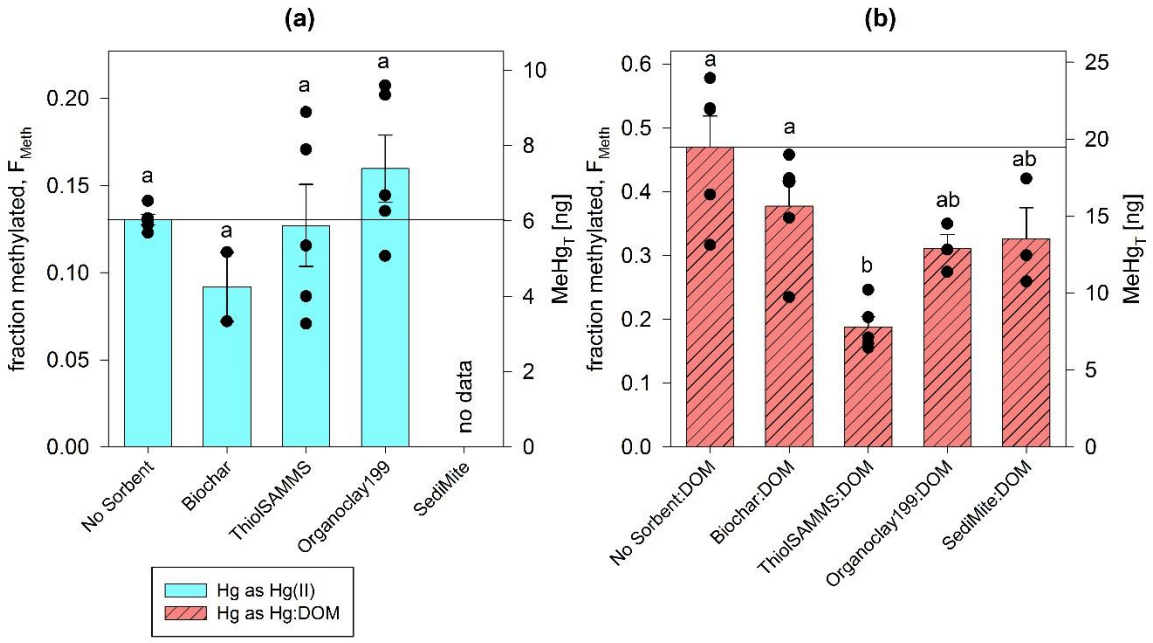

Figure 32. Total MeHg production via ND132 over a 24-hour contact period shown as both fraction methylated, F_{Meth} (i.e., $MeHg_T/Hg_i$) and total mass of MeHg produced, $MeHg_T$, when Hg is added as: (a) Hg(II) and (b) Hg:DOM. Bars indicate the average of the treatment group, with error bars giving the standard error. Dots show the individual replicates within the treatment group. Letters (a–b) indicate the statistical grouping of the treatment. Statistical comparisons were completed for each Hg source separately. A reference line is shown to aid in visual comparison to the baseline control experiment (i.e., no sorbent experiments) (Source: Image courtesy of Muller and Brooks. In review)

Experiments are also under way to evaluate several sorbents (Biochar, ThiolSAMMS, SediMite, and OC-199) for their ability to remove MeHg, both in the presence and absence of DOM. The study is not yet complete, but some general trends have emerged: (1) in the absence of DOM Biochar, ThiolSAMMS and SediMite show comparable MeHg sorption isotherms with estimated sorption capacities decreasing in the order of ThiolSAMMS > Biochar > SediMite, and (2) DOM substantially lowers MeHg sorption onto Biochar and SediMite. For example, in the absence of DOM, Biochar has a MeHg sorption capacity of about 400 µg/kg. When DOM is present, that sorption capacity decreases to 180 µg/kg (Figure 33).

Surface Water and Sediment Future Needs

Within this Task are several areas of continuing and new research that are warranted. Ambient water quality and flow data have supported new information on Hg and MeHg concentration, flux, and possible sources in the LEFPC watershed. Based on mass balance calculations, we have identified the upper reach of the study area as a source of legacy Hg loading to the creek. The dominant source of that Hg likely is the HRD deposits that have been documented. Perhaps equally important and less well understood are the locations, sources, and controls on intermittent Hg loading in the lower study reach. Additionally, at both downstream monitoring points there have been significant trends of increasing Hg and MeHg flux, demonstrating the dynamic changes that occur in the system without direct engineered intervention. Continued monitoring will strengthen the baseline record of flux and concentration against which system responses to natural forcings, directed actions (e.g., MTF construction, bank stabilization), and unintentional actions (e.g., spill and leaks) can be compared.

Studies on Y-12 water have shown that chlorine and dechlorination chemicals have a big impact on Hg loading to UEFPC. Laboratory and field tests indicate that the alternate dechlorination chemical AA can achieve chlorine removal while decreasing Hg loading and without the potential for detrimental side effects on the creek ecosystem. If this work

goes forward, further work is needed to, for example, evaluate longer term effectiveness of AA addition and the effect of inactive ingredients (binding agents, slow release chemicals) on Hg solubility and mobility.

We will complete our study of MeHg removal from solution using sorbents. In addition to providing needed information for possible water treatment approaches, the MeHg-sorbent work provided a basis for understanding another phase of our planned work. Conventional wisdom held that sorbed Hg was not available for methylation. Our results challenged that assumption (Figure 32) but demonstrated that the sorbent significantly lowered the $MeHg_D$ concentration. A critical knowledge gap is whether the sorbed Hg is available for bioaccumulation when ingested by biota at the bottom of the food web. If sorbents can decrease MeHg uptake by biota at the lowest levels of the food web, where the greatest biomagnification values are frequently observed, this benefit should propagate up trophic levels, ultimately resulting in lower MeHg concentrations in fish. We are planning a series of tests using water and sediments from EFPC in which we will test the ability of sorbents to decrease MeHg concentration in benthic invertebrates.

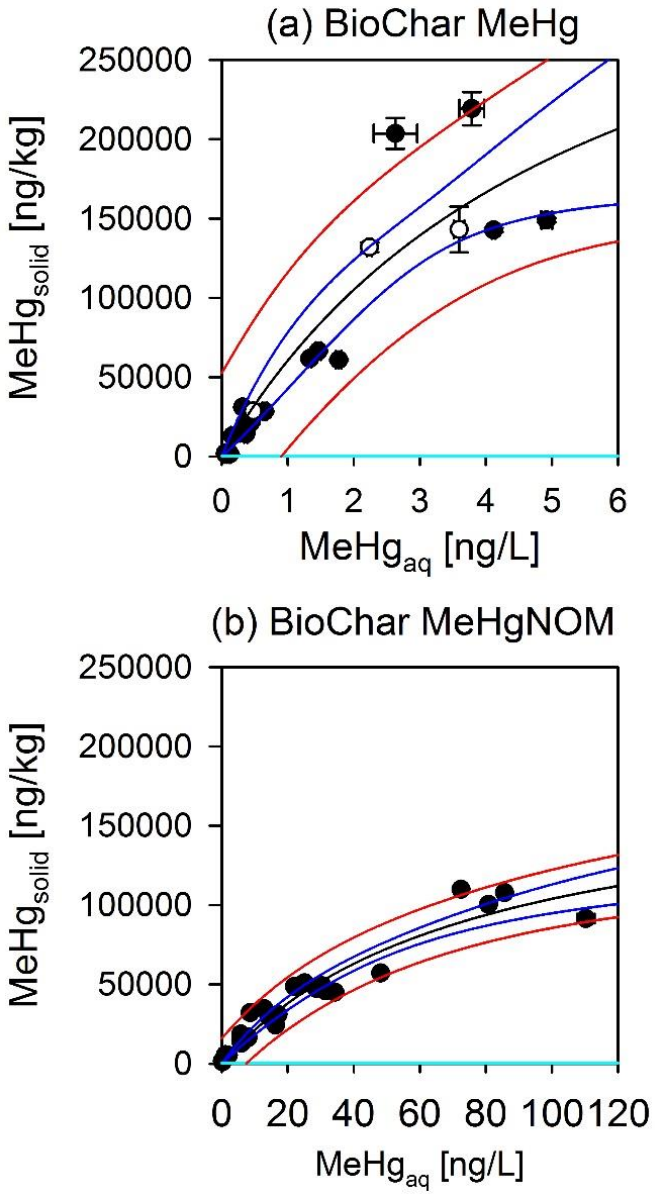

Figure 33. MeHg sorption isotherms onto Biochar in the absence (a) and presence (b) of DOM. Open symbols indicate data points derived by analyzing both the aqueous and the solid phase for MeHg concentration. Black, blue, and red lines represent the Langmuir isotherm fit and the 95% confidence and prediction bands, respectively. The teal line at the bottom represents the ambient MeHg present on the Biochar. Error bars indicate analytical uncertainty propagated through the calculations.

Finally, EFPC has a very high nutrient load and is meso- to eutrophic along its length with respect to both nitrogen and phosphorous because of point and diffuse discharges to the creek. Previous studies of the microbial communities in EFPC suggest lower diversity and richness relative to reference streams. Other measures of EFPC functions suggest the system is stressed. Nutrient uptake velocity is a measure of biotic demand relative to concentration and is related to nutrient retention efficiency. Uptake velocity normalizes for the effects of discharge and stream width, allowing comparison among streams of different size. High uptake velocities are consistent with high biotic demand and nutrient use efficiency, whereas low values are suggestive of low biotic demand and are reflective of ecosystem stress. We calculated nitrate uptake velocity for the upper and lower sections of EFPC where the creek is second order and third order, respectively, and compared those values to other streams, including those that did and those that did not have point source nutrient inputs. EFPC had very low nitrate uptake velocities (~0.1 mm/min) compared with all streams and compared with streams of the same order (ranging from ~1 to 10 mm/min). Additionally, uptake velocities were low with respect to other streams having point source nutrient inputs. We are planning a series of experiments to test the effect of lowering these high nutrient levels on MeHg production in simulated creek environments. These studies rely heavily on the use of the renovated stream mesocosms that will be part of the AEL upgrade.

Ecological Manipulation

Role of Ecology in EFPC

The primary goal of ecological manipulation in EFPC is to examine strategies to reduce Hg bioaccumulation in fish in EFPC through sustainable biological or ecological manipulations. In contrast to virtually all other metals, Hg (especially in its organic form, MeHg) biomagnifies or becomes increasingly concentrated as it is transferred through aquatic food chains to higher trophic levels, namely to fish. Consequently, the consumption of Hg-contaminated fish is the primary exposure route to humans. For this reason, the National Recommended Water Quality Criterion (NRWQC) for Hg is based on a fish tissue concentration rather than an aqueous Hg concentration because the tissue concentration (0.3 mg/kg) is considered to be a more consistent indicator of exposure and risk to humans and aquatic life.

Although most Hg in the environment is Hg_i, a small proportion of Hg_T is microbially transformed to MeHg in the aquatic ecosystem. Anoxic, reducing environments such as wetlands are considered Hg-methylating "hotspots," where large amounts of Hg_i are methylated by sulfate- and iron-reducing bacteria. However, recent research has highlighted freshwater streams as sites of Hg methylation, with favorable conditions for methylation including increased temperatures, the presence of certain filamentous algae, and the presence or absence of certain organic nutrients (Tsui et al. 2010). The methylation of Hg from periphyton- and macrophyte-associated bacteria also has highlighted additional opportunities for Hg methylation within freshwater streams (Acha et al. 2012).

Methylmercury readily crosses cell membranes and binds with proteins, forming complexes that mimic essential amino acids. For this reason, MeHg is highly bioaccumulative, becoming incorporated into protein-rich tissues (e.g., muscle; typically MeHg is >95% of the Hg_T in fish fillets) with long residence times. In aquatic animals, MeHg uptake rates from water and assimilation efficiencies from food are high, while elimination rates are low, leading to a progressively increasing concentration within an organism over time. This also leads to a progressive concentration of Hg within a given food chain as MeHg is transferred from one trophic level to the next.

One of the challenges to effective remediation at Hg-contaminated sites is that while Hg body burdens in fish are often more closely linked to aqueous MeHg than Hg_i concentrations (Tom et al. 2010), MeHg production is not easily predicted or controlled. For example, in systems contaminated by atmospheric deposition with low aqueous Hg_T concentrations (<10 ng/L), there is a correlation between Hg(II) and MeHg concentrations (Kelly et al. 1995). However, in point-source contaminated systems, waterborne Hg_i concentrations can range over several orders of magnitude, while MeHg concentrations in water and biota seldom differ by more than tenfold (Southworth et al. 2004). Decreasing aqueous Hg_i concentrations and loading might often be a more achievable remediation goal than decreasing MeHg concentrations, but this approach has led to mixed results in terms of responses in fish bioaccumulation. A number of source control measures have resulted in rapid responses in lake or reservoir fisheries (Joslin 1994, Turner and Southworth 1999), but examples of similar responses in Hg-contaminated stream ecosystems are less common. Recent work suggests that stream systems might actually be more susceptible than lakes to Hg bioaccumulation, highlighting the need to better understand the ecological drivers of Hg bioaccumulation in stream-dwelling fish (Chasar et al. 2009, Ward et al. 2010a). Although Hg_i concentrations play a part in determining overall Hg concentrations in fish, methylation efficiencies and food web pathways are also important in determining fish tissue concentrations.

Effective Hg remediation in EFPC requires not only an understanding of the nature and magnitude of Hg inputs but also knowledge of the extent to which these inputs must be controlled to achieve the desired reduction of Hg contamination in biota necessary to meet the NRWQC. However, because Hg is accumulated predominantly through the food chain rather than through aqueous exposure, understanding food web structures and transfer pathways for Hg to fish is a key component to successfully implementing strategies to mitigate Hg bioaccumulation. Uptake at the base of the aquatic food chain (algae/periphyton, invertebrates) is the most important concentration step for Hg (with Hg concentrating over 10,000-fold between water and algae). However, although the relationship between Hg concentrations in water and fish has been characterized, the transfer pathways from the base of the food chain remain largely unknown.

Key questions concerning the role of ecological interactions in driving fish tissue Hg concentrations in EFPC included quantifying Hg and MeHg inventories throughout the food webs at various locations throughout EFPC (Peterson et al.

2015). Biological Hg and MeHg inventories serve several purposes for site management and technology development including (1) supporting conceptual model development and site characterization, (2) assessing exposure and risk evaluation, (3) informing site prioritization, (4) remediation selection and design, and (5) providing baseline information for performance, compliance, and long-term monitoring and evaluation. The conceptual model for remediation targets in EFPC assumed that Hg accumulation in fish in EFPC was proportional to waterborne Hg_T. This assumption was the basis for derivation of aqueous Hg target guiding Comprehensive Environmental Response, Compensation, and Liability Act efforts in UEFPC (200 ng/L). Unfortunately, over the past decade aqueous Hg_T concentrations in UEFPC have been fluctuating because of various activities (e.g., Big Spring Treatment System, storm drain clean-outs, cessation of flow augmentation), and fish do not appear to be responding to these changes. Lack of a clear response suggests that the relationship between Hg_i concentration and MeHg production/bioaccumulation observed in UEFPC in the 1990s is not a straightforward, linear relationship.

To address these needs and fill knowledge gaps, we sampled biota throughout the food web at four biological monitoring sites in EFPC (EFK 23.4, EFK 18.2, EFK 13.8, and EFK 6.3). We quantified MeHg and $MeHg_T$ and estimated trophic status using stable isotopes of carbon and nitrogen to assess the relative importance of food web dynamics in determining Hg bioaccumulation in fish. We examined a food web model to identify the most important factors affecting Hg concentrations in fish, and, based on the results, we began laboratory experiments to examine the potential effects of adding native freshwater mussel species to EFPC.

Mercury Inventories

Previous work has shown a nonlinear relationship between aqueous Hg_T and Hg_T in fish fillets in EFPC (Mathews et al. 2013). Although aqueous MeHg concentrations were highlighted as one of the potential reasons for the patterns observed in EFPC, food web processes within the stream were not well understood at the time because routine monitoring captured only aqueous and fish fillet concentrations, ignoring food chain transfer. To establish a baseline understanding of the effect of food web processes on Hg bioaccumulation in EFPC before any potential ecological manipulations, it was critical to characterize the inventory of Hg and MeHg in the biological compartments of the stream. We collected periphyton, invertebrates, forage fish, and upper trophic level fish throughout the stream and analyzed samples for Hg, MeHg, and stable nitrogen isotopes. Stable isotopes of nitrogen are commonly used in food web ecology as a proxy for trophic level because, like MeHg, the heavy nitrogen isotope ^{15}N becomes more and more concentrated as it is transferred up the food chain, leading to isotopic fractionation within the food web. The difference between heavy and light nitrogen isotopes is used to calculate trophic level as follows:

$$\text{Trophic level} = \lambda + (\delta^{15}N_{\text{secondary consumer}} - \delta^{15}N_{\text{base}})/\Delta_n,$$

where l is the trophic position of the organism used to estimate $\delta^{15}N_{base}$ (e.g., l = 1 for primary producers), $\delta^{15}N_{secondary\ consumer}$ is measured directly, and Δ_n is the enrichment in $\delta^{15}N_{secondary}$ per trophic level.

Our results have shown that MeHg concentrations throughout the food webs at upper EFPC sites are lower than those at LEFPC sites, reflecting aqueous exposure at these two sites. However, trophic analysis has shown (Figure 34) that rock bass, the top trophic level fish in this stream, are feeding at a higher trophic level in LEFPC than in UEFPC, suggesting that food web dynamics are playing a role in determining fish tissue concentrations. The trophic level data corroborate historical fish and community survey data, which show more complex communities at downstream sites. A comparison of rock bass at all EFPC sites (Figure 35) shows that within a given species, trophic level generally increases with distance downstream, as does MeHg concentration.

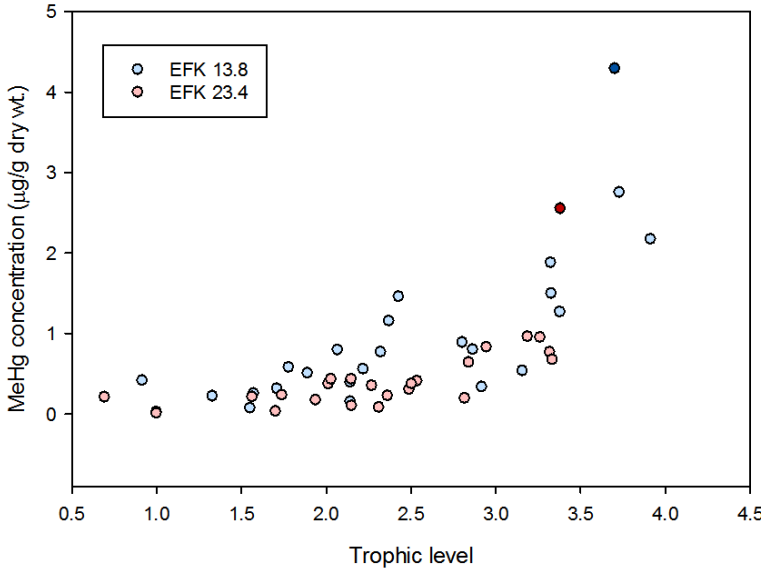

Figure 34. The relationship between MeHg concentrations and trophic level in the food webs of two selected sites in EFPC. Trophic level was calculated using $\delta^{15}N$ values as described in the text. The base of the food chain for trophic level calculations was periphyton. Symbols represent mean values for invertebrates and fish taxa at the two sites. The dark red and dark blue symbols represent rock bass at each sampling location.

The Role of Mussel Filtration on Mercury Dynamics

A statistical examination of the factors influencing Hg concentrations in fish in EFPC showed that unsurprisingly, aqueous MeHg concentrations are significantly and positively correlated with Hg fish tissue concentrations. This examination, which considered 30 years of community structure data in EFPC also showed that the percentage of collector filterers in the community is significantly and negatively correlated to Hg in fish (Figure 36). This finding led to an ongoing investigation of the potential of introducing native freshwater mussels into EFPC to mitigate Hg bioaccumulation in fish.

Freshwater mussels are filter feeders, filtering large volumes of water over their gills to remove algal and detrital particles for nutrition. Because mussels filter particulates from the water column, they have the ability to significantly affect water quality (Figure 37) and, therefore, play a critical role in freshwater ecosystems. These species are of interest in EFPC because they can affect Hg bioaccumulation throughout the food web by exerting effects on periphyton, DOM, methylating bacteria, and aqueous Hg concentrations. ORNL scientists are working closely with the Tennessee Wildlife Resource Agency (TWRA), who has a mission of restoring these native species to Tennessee waters. The reintroduction of native mussels to EFPC could not only mitigate Hg bioaccumulation and risks in this stream but would also provide other ecosystem services including water quality improvement and propagation of sensitive native species.

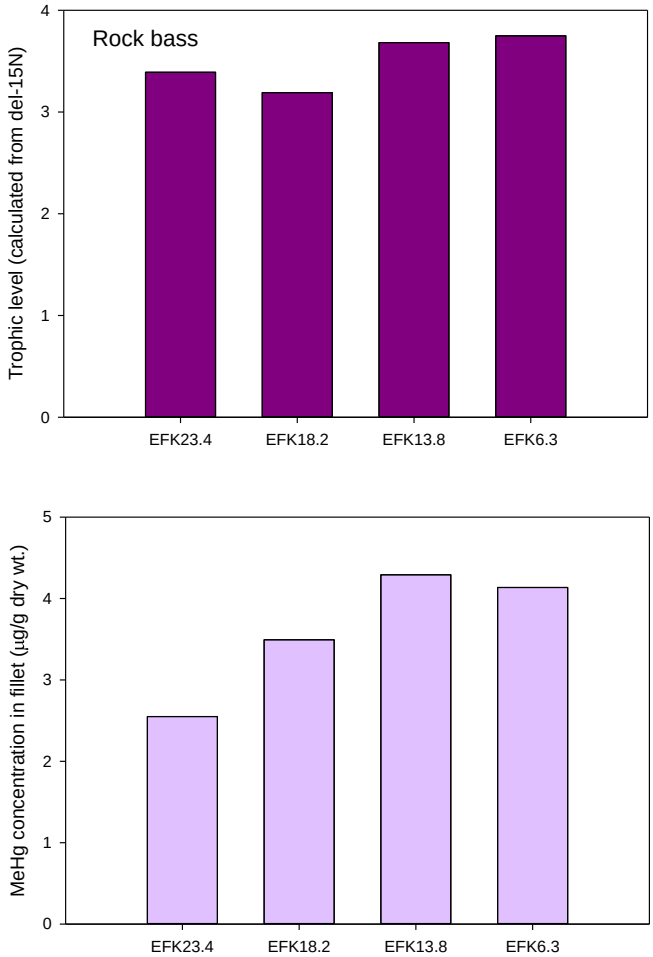

Figure 35. Trophic level of rock bass (top panel) calculated from del ^{15}N signatures, as described in the text, and MeHg concentrations (µg/g dry wt) in rock bass fillets collected at four sites in EFPC.

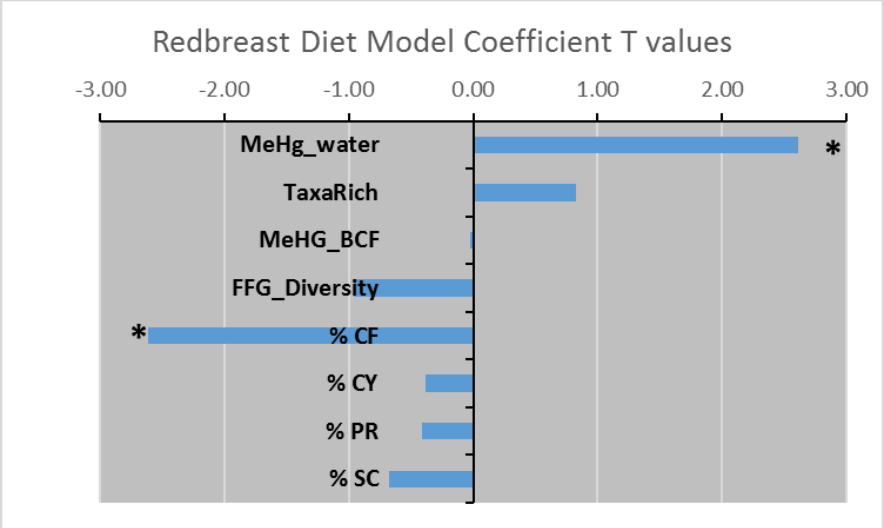

Figure 36. A linear mixed model was developed for redbreast diets under different scenarios, where the predictor variables for MeHg in the diet were: aqueous MeHg, taxa richness, Bioconcentration factors, Functional Feeding Group Diversity, % of collector filterers in invertebrate community, % crayfish, % predators, % scrapers. Values shown are T value coefficients. Asterisks denote significant values.

Figure 37. Demonstration of clam filtration. Both beakers were initially inoculated with the same algal cell concentration. The beaker on right had two clams, while the beaker on left had none. The photo was taken 30 minutes after adding algae.

In order to determine the potential impacts of mussel filtration on Hg dynamics in EFPC, it is necessary to determine (1) filtration or clearance rates of mussels under different environmental conditions, (2) Hg removal rates, and (3) the effects of mussel filtration on Hg methylation rates. Although much of this work to investigate Hg dynamics with mussels will take place with the AEL upgrade, we began field investigations to investigate Hg bioaccumulation rates and laboratory investigations to quantify filtration rates for different species under different environmental conditions.

Our field deployment results show that Hg bioaccumulation rates in Asiatic clams (*Corbicula fluminea*) were much higher in the spring than in the winter (Figure 38). This suggests a positive effect of water temperature on filtration rates. Most biological and metabolic rates are affected by temperature. Microbial activity is also affected by temperature, and Hg methylation rates (which are controlled by microbes) and concentrations are, therefore, also higher in spring in EFPC than in the winter. These results suggest a seasonal component to the efficiency of Hg removal but that filter feeders would be removing Hg at times critical to Hg methylation. Our results also show that unlike fish bioaccumulation patterns, clam bioaccumulation is proportional to aqueous Hg concentrations. There is a strong spatial pattern of higher Hg concentrations upstream where aqueous concentrations are highest and significant decreases with increasing distance downstream.

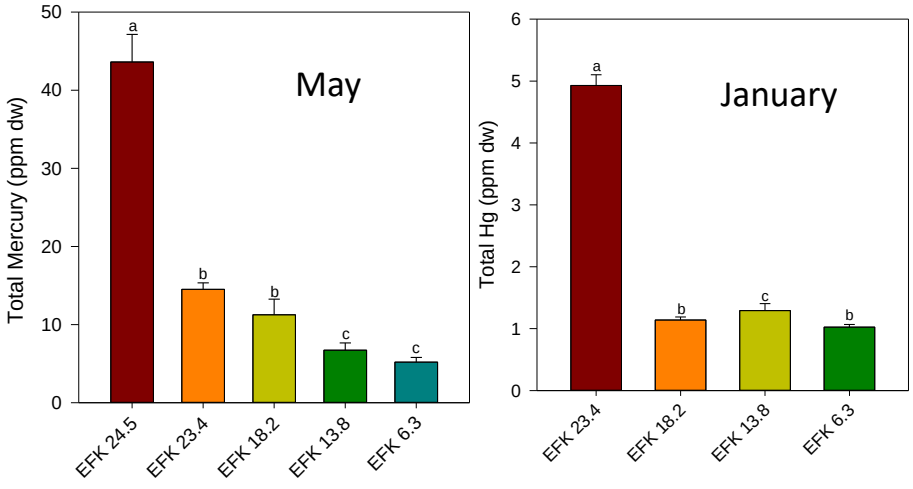

Figure 38. Mean (± 1 SD) Hg$_T$ concentrations in Asiatic clams collected from an uncontaminated stream in Meigs County, Tennessee (Little Sewee Creek), and deployed at 5 sites in EFPC for 4 weeks in May and January. Note different scales on y-axes between graphs.

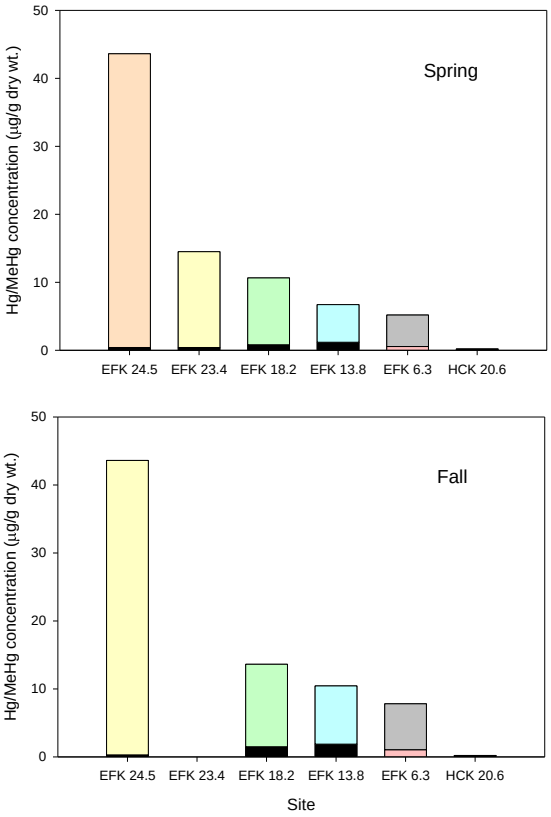

Figure 39. Mean MeHg and $MeHg_T$ concentrations in resident clams collected at 5 sites in EFPC and at the Hinds Creek reference site in spring and fall.

Field collections of resident Corbicula in EFPC show a similar spatial pattern to deployed clams, with the highest Hg_T concentrations at upstream sites within EFPC and decreasing concentrations with distance downstream (Figure 39). Unlike fish tissue where Hg is predominantly found as MeHg, clams accumulate high concentrations of Hg_i, with MeHg making up only a small fraction of Hg_T. There was no difference between concentrations in resident clams collected in spring and fall, likely because once Hg is assimilated, loss rates are slow. The concentrations of total Hg in resident clams in EFPC were comparable to clams that were deployed at these same sites for 4 weeks in the spring, suggesting that rather than being a threshold concentration for these organisms Hg concentrations are coming to an equilibrium between aqueous phase and biological tissue.

The clams collected in EFPC are significantly smaller in size (mean wet wt. ~2 g) than those collected at reference locations (mean wet wt. ~4 g), suggesting either that the age structure of the population in EFPC is significantly different than in reference sites or that the population is stunted. Future work will examine the resident clam population in EFPC to determine the factors affecting Hg accumulation in these organisms, and the potential of EFPC to sustain the addition of other filter feeders. One of the key questions for the project is to determine how many mussels it would take to make a significant difference in aqueous Hg concentrations. The first step to answering this question is to quantify filtration rates of different species under different environmental conditions.

Quantifying Filtration Rates

Asiatic clams (16.59 mm ± 0.36 SE shell length) were collected on May 8 and July 5, 2018, from Sewee Creek in Meigs County, brought to ORNL, and acclimated for 12 days in a flow-through tank of dechlorinated tap water with air diffusers without substrate. Paper Pondshell (*Utterbackia imbecillis*) mussels (mean shell lengths of 59.42 mm ± 2.15 SE) were collected on July 18, 2018, by TWRA personnel from Sumner Sportsman Club Lake in Portland, Tennessee (36.604280, -86.487226), brought to the lab on July 19th, and acclimated for approximately 4 weeks. Bivalves were fed a mixture of live algal cells (*Chlamydomonas reinheirdtii)* and algae from Reed Mariculture: Shellfish diet 1800, TP 1800, and Nanno 3600. Food was dispersed over time through an IV drip.

We calculated filtration rates of bivalves indirectly by taking subsamples of suspended particles in a known volume of water as the bivalve filters over a specified time (Riisgård 2001). Bivalves were placed in small, aerated individual tanks of known volume (100–500 ml water) where they could acclimate to experimental conditions for at least 30 minutes before being fed with a concentrated solution of live algal cells. Control tanks were given the same algal cell concentration but contained no bivalves. One mL subsamples were taken in 5 to 10-minute intervals for 50 to 60 minutes. Each subsample was preserved with 200 µL of 10% formalin until cells could be counted at a later time through flow cytometry (FlowCam). Filtration rate was calculated using the logarithmic equation presented in (Riisgård 2001) as follows: $FR = (V/nt) \ln(C_0/C_t)$, where C_0 and C_t = algal cell concentration at time 0 and time t, V= total volume of experimental system, and n = number of animals. All clearance rates to date have been calculated at 21 ± 1°C, though future experiments will examine the effect of temperature on filtration rates.

Our results show that bivalve filtration rate is positively correlated with mussel size, such that filtration rates were significantly higher in Paper Pond shells than in Asiatic clams on an individual basis but that filtration rates were higher in Asiatic clams on a per gram basis (Figure 40). Since their environments are continuously in a state of flux, understanding abiotic factors influencing unionid mussel filtration rates is essential to understanding the potential for filter feeders to affect Hg dynamics in EFPC. Therefore, we are studying the affects of light, food sources, and temperature on filtration rates.

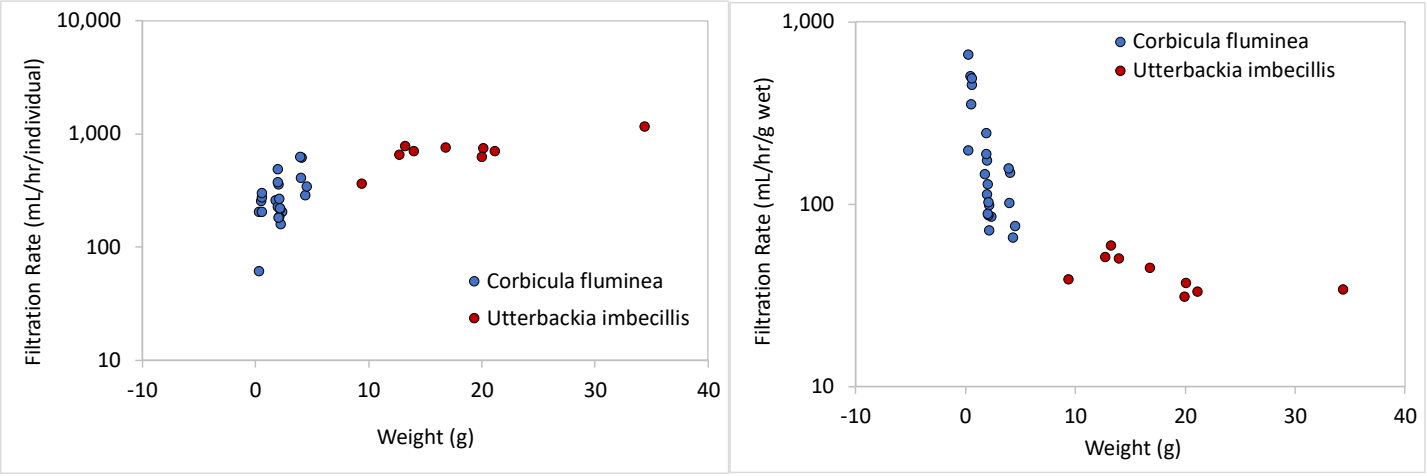

Figure 40. Relationship between bivalve mass (g) and filtration rate.

In particular, it has been noted that there are intraday patterns in which particulate Hg and MeHg increased overnight (Figure 25). These increases coincided with overnight maxima in total suspended solids and turbidity. The extent to which Unionidae mussel filtration rates change within a daily circadian rhythm is studied very little compared with other factors. One of the most commonly studied species is the saltwater mussel *Mytilus edulis*, which has been observed filtering more at night (Nielsen and Stromgren 1985, Robson et al. 2010). Some freshwater mussel species have been reported to detect and respond to light (Haag and Warren 2000, Morton 2008, Robson et al. 2010, Duchini et al. 2015, Kobak and Nowacki 2007), but little is known about how light and/or circadian rhythms affect filtration rates. Preliminary experiments in the laboratory suggest that filtration rates were higher during the day than at night (Figure 41), but it is uncertain whether this is due to light conditions or circadian rhythm. We have performed experiments to examine this question, but data are still pending.

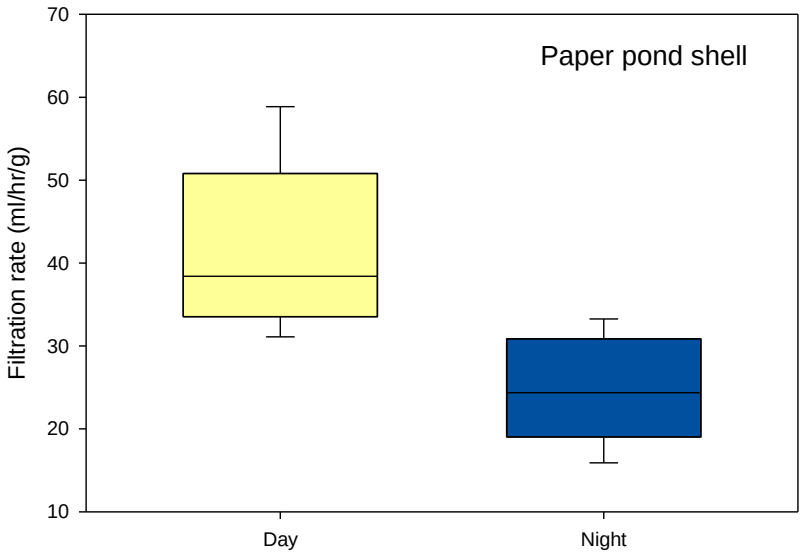

Figure 41. Filtration rates (milliliters/hour/gram) in Paper pond shell mussels measured during the day and at night. Day light 6 µmol/m²/s, Night 0 µmol/m²/s.

We found no preference amongst clams for different algal cell types, as filtration rates were not significantly different between algal cell types. However, not surprisingly, we did find that filtration rates were lower when clams were just fed than when they had been starved for the previous day (Figure 42).

Ongoing experiments are examining the effect of temperature on filtration rate with these two species of bivalves, and new species are expected to arrive in the laboratory in the fall. Future work will examine Hg removal rates, and the effect of mussel filtration on Hg methylation rates.

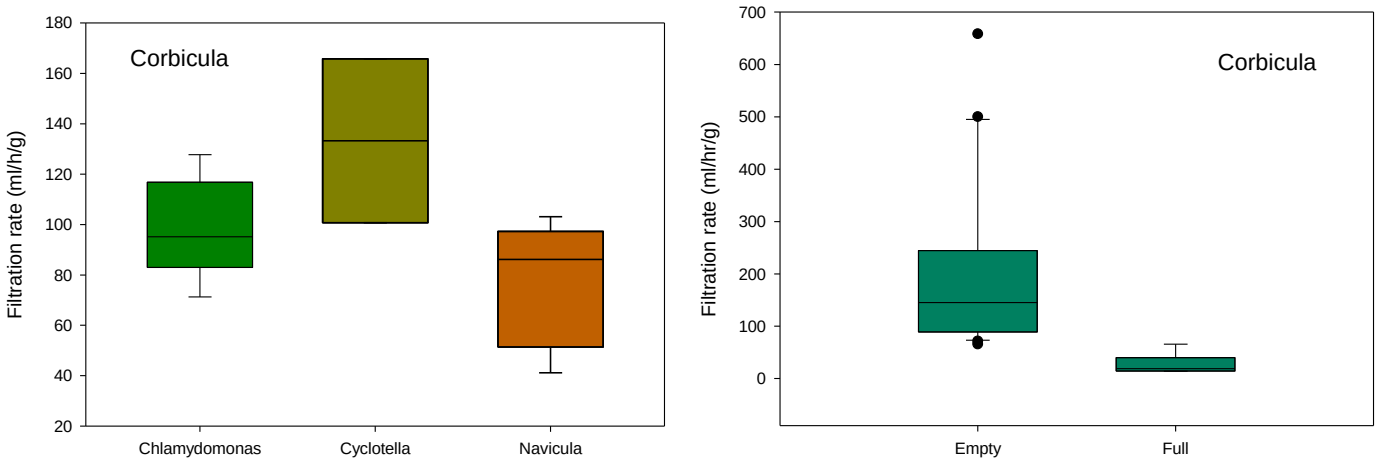

Figure 42. Mean filtration rates in Corbicula fed different algal food types (left panel) and when starved (empty gut) vs. fed (full gut).

Food Chain Modeling

We examined Hg bioaccumulation within EFPC as a function of exposure (aqueous concentrations) but also as a function of biodynamics—biological processes that affect Hg concentrations within organisms (e.g., growth, Hg assimilation, and Hg depuration). We used community data available from Biological Monitoring and Abatement Program (BMAP) studies to examine inventories within the biological compartments of the stream. In particular, we considered somatic growth dilution (SGD) as a way to explain why Hg biomagnification might differ at different sites throughout the creek. The SGD concept is that the concentration of a bioaccumulating contaminant, such as MeHg, becomes more dilute within an organism's body when the organism has a high growth efficiency. Several studies have substantiated the effects of SGD on MeHg concentrations at the individual level, but how SGD affects MeHg concentrations at the population level has not been investigated (Karimi et al. 2007, Ward et al. 2010).

An accurate biodynamic model was constructed for a stoneroller population in a contaminated stream (Peterson et al 2017). Biodynamic models show promise for use as guides to population management. Figure 43 provides site-specific growth rates, which can be used to remove individuals of a given size to minimize MeHg bioaccumulation and trophic transfer. This is analogous to forestry practices, where trees are cut at the point of maximum growth to achieve maximum efficiency. However, though we were able to construct an accurate biodynamic model for stonerollers, we did not see evidence for SGD in stoneroller minnows in EFPC—MeHg concentrations increased with relative growth rates (Figure 44). A reasonable explanation for these results is that MeHg concentrations in periphyton—stonerollers' primary food resource—are driving stoneroller MeHg concentrations (Figure 45). Ultimately, the biodynamics modeling platform allows researchers to examine how varying population size and structure could be used to reduce MeHg standing stock, and eventually fluxes, from biotic compartments. These results point to the importance of understanding periphyton biomass standing stocks and growth rates seasonally and spatially throughout the creek, which will be the focus of future work.

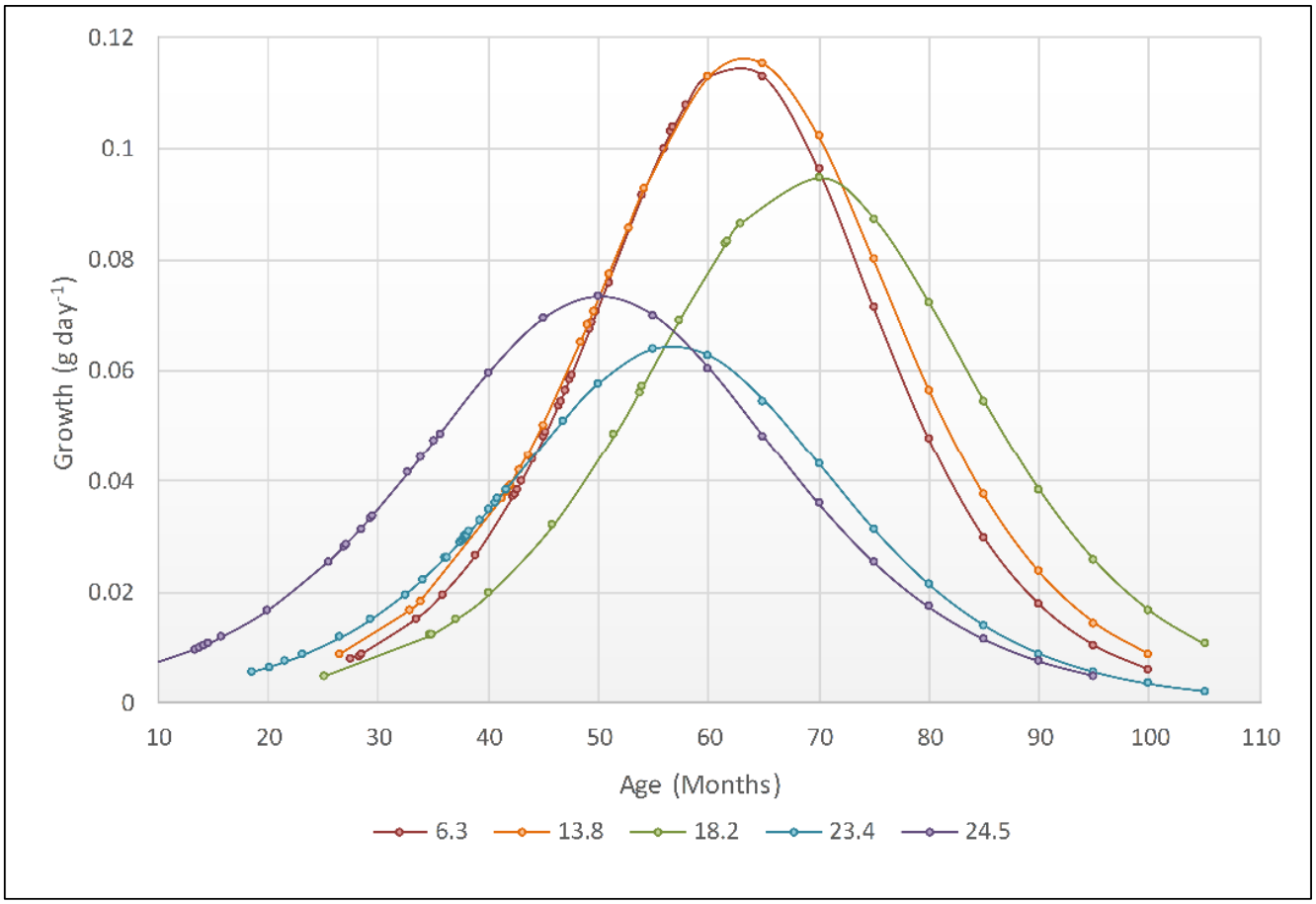

Figure 43. Relationships between stoneroller growth and age at each of the 5 BMAP sites within EFPC.

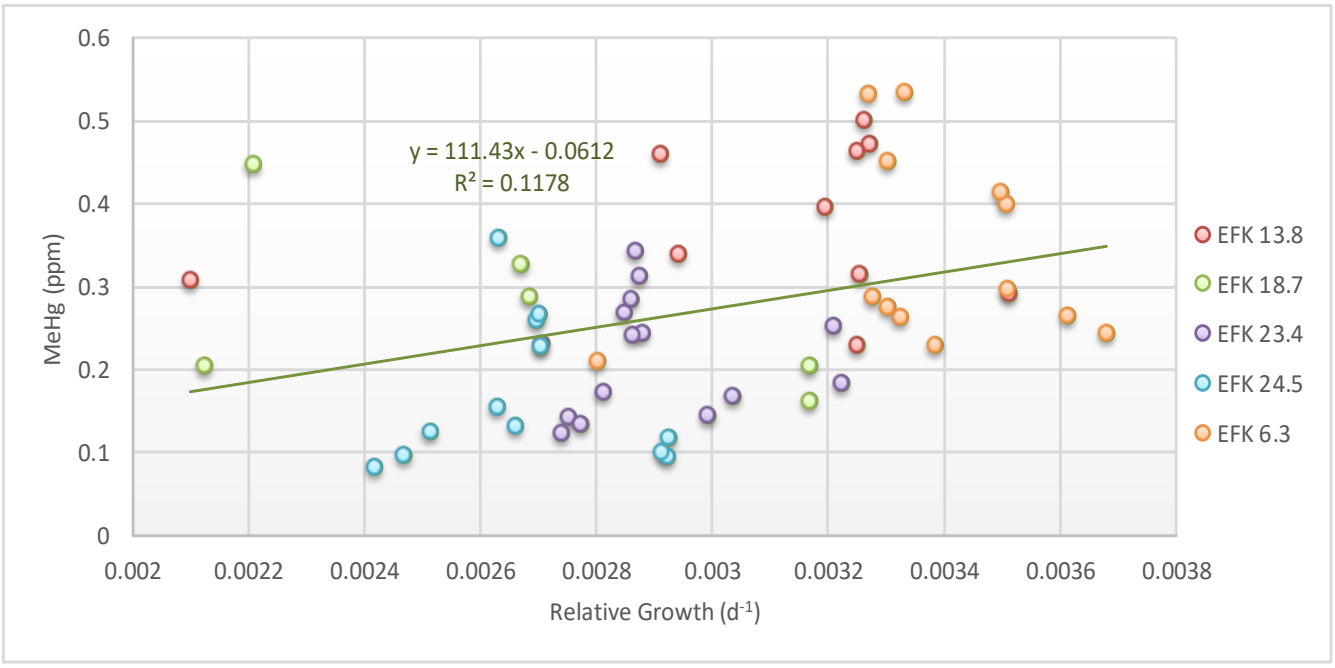

Figure 44. Relationship between relative growth in stoneroller minnows and MeHg concentrations across all EFPC sites.

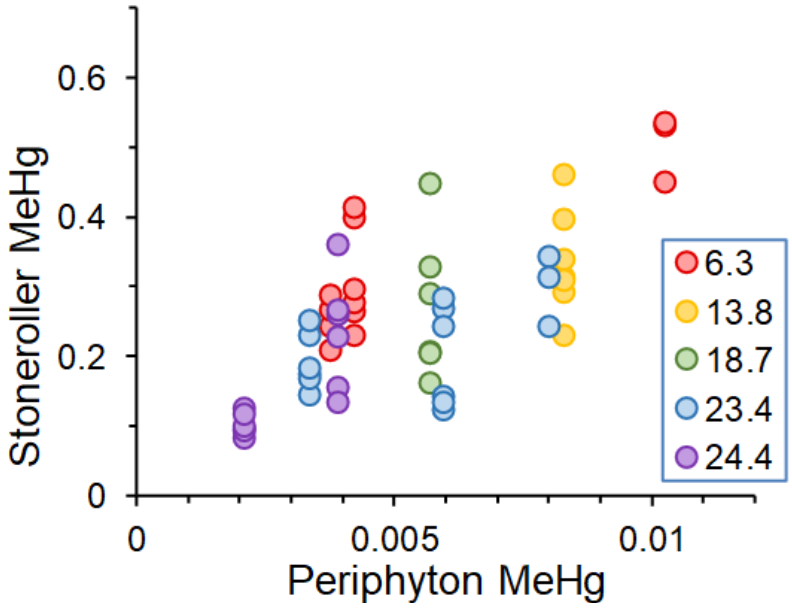

Figure 45. Relationship between stoneroller and periphyton MeHg concentrations.

Ecological Manipulation Future Needs

Within this Task there are several areas of continuing and new research that are warranted. Because periphyton serve as the base of the food chain and are likely a large factor contributing to MeHg production and bioaccumulation in EFPC, understanding periphyton dynamics (e.g., standing stock biomass, growth rate) is critical. We have collected data on Hg inventories in periphyton and are working on methods (potentially using remote sensing) to characterize biomass in the stream.

Further laboratory, field, and modeling work is needed to understand the factors affecting mussel filtration and Hg removal rates and to determine the implications of mussel filtration on Hg methylation. Although experiments to date have focused on filtration rates, upcoming experiments will focus on Hg removal and bioaccumulation rates. Critical to this discussion is a modeling exercise to determine the density of mussels needed to affect Hg removal in the stream and whether the food web in EFPC could support such a density. These studies rely heavily on the use of the renovated stream mesocosms that will be part of the AEL upgrade. Finally, additional food web modeling work is needed to evaluate the potential of fish removals or additions to mitigate Hg trophic transfer in the stream.

Watershed Modeling

Purpose and Status

The purpose of the geospatial integration and watershed modeling effort is to more accurately understand, model, and predict current and future sources of Hg and Hg dynamics in EFPC to inform decisions regarding future remediation strategies and research needs. The ultimate goal is to produce a decision-support tool as a synthesis of models, data organization, geospatial data integration, data mapping, and visualization efforts at high spatial and temporal resolutions as is practically possible to accurately represent current physical and biotic processes and reliably forecast the outcomes of future remediation decisions. The current status of tasks completed and initiated in FY 2018 are provided in Table 5.

Integrated model-based approaches for decision support in environmental remediation has been gaining momentum because of its effectiveness in uniting the different interdependent and interrelated physical, chemical, and biological processes that control the fate of contaminants, specifically Hg, in the environment. As these models are firmly rooted in the systems-based approach, models provide a detailed characterization of the factors and processes that influence the movement and accumulation of Hg. In addition, models are adaptable to different environmental contexts and allow for modification of the critical factors and processes based on site-specific information from the laboratory, as well as field experiments. Therefore, integrated models can connect the laboratory and field-level understanding of the fate of environmental contaminants to a broader spatial scale and expand applicability of experimental information over a larger spatial-scale investigation. Moreover, once the model is calibrated and validated for a specific site and/or context, it can be applied for identifying and prioritizing technological options by *ex ante* evaluation of the efficacy of technology options to reduce contaminants in the environment. Thus, model-based environmental decision making provides a blueprint that assists successful implementation of sustainable environmental remediation.

The specific outcomes of this approach include:

- Spatially relevant models of EFPC ecosystem compartments that are independent but that easily communicate on common spatial and temporal scales.
- Consistent, compatible, accessible, and spatiotemporally comprehensive synthesized data sets that provide the standard for modeling current and future Hg dynamics in EFPC.
- A data organization system for cataloguing field and modeling studies.
- Development of a consistent high-resolution, geo-rectified stream network for EFPC.
- Geospatial integration of watershed-relevant variables summarized in a stream-network fashion.
- Static and dynamic mapping and visualization of geospatial data.

There are multiple benefits of such an approach:

- Explicit efforts to use best available data in modeling and geospatial integration leads to more directed decision-support capabilities.

- Transitioning best available data to operative models increases intimate knowledge of the system and promotes learning of complex behaviors.

- Each iteration of operative model development at higher spatial and temporal resolutions leads to new discoveries (i.e., pattern and process) and understanding.

- Knowledge gaps in modeling efforts (parameters, rates, processes) assist in prioritizing future research efforts.

Table 5. Geospatial integration and watershed modeling subtasks, description of plans, and the status as of FY 2018 (red = not started, yellow = in progress, green = established)

Sub-Task	Plans	Status
Data Organization	Develop file organization system	
	Document types of data for inclusion/exclusion	
	Catalogue system, data owners, data developers, meta-data	
Geospatial Data Integration	LiDAR-derived DEM, landcover, building topographies, stream digitization	
	Geo-rectified stream network and network summarization/accumulation of variables	
	Integrate Kayak habitat mapping datasets	
Mapping & Visualization	LiDAR derived datasets	
	Kayak habitat mapping datasets	
	Hydrology and inundation	
	Floodplain and bank soil Hg content	
Model Efforts		
Surface Hydrology	Calibrated/Validated SWAT model	
	Discharge simulated 1980-2049	
	Future scenario development (OR stormwater retention, MTF)	
Surface Hydraulics	Functional HECRAS model	
	Increase HECRAS accuracy through field calibration/validation	
	Transect calibration	
	Link HECRAS to simulated discharges	
Stream bank erosion & sediment transport	Calibrate and validate BSTEM erosion and flux	
	Simulate erosion with simulated discharges	
Floodplain Groundwater hydrology & recharge	Determine model platform	
	Initiate data integration for calibration	
	Determine approach to link to surface discharge	
Periphyton Production, Hg updake & methylation	Predictor & geospatial variable development (e.g., Forest canopy)	
	Aggregate data and observations on production/methylation	
	Determine model platform	
	Initial model calibration	
Invertebrate & Fish Distribution-Abundance-Production	Assemble predictor variables (depth, habitat layers)	
	Develop SDM abundance models for all fish species and invertebrate groups	
	Extrapolate abundances to stream reach scale	
Invertebrate & Fish Biodynamics	Biodynamic model development for 3 fish and 1 invertebrate	
	Continue biodynamic development/calibration for other biota	
Invertebrate & Fish Functional Roles	Mussel experiments and quantify filtration rates	
	Scale biodynamics to determine roles of grazers in contaminant cycling	
Scenario Development	Standardized and consistent scenarios	
	Stormwater retention scenarios	
	Micro-technologies scenarios	
	Biomanipulation scenarios	

Geospatial Integration

Given the diverse array of tasks associated with the technology development project, the long history of environmental assessment in EFPC, and the recent availability of high-resolution spatial data for the EFPC watershed, a geospatial data integration effort was undertaken to build a foundation for future research and assessment that allows for harnessing new data and integrating historical data.

A summary of this effort to date is as follows:

- Compiled a bare-earth LiDAR digital elevation model (DEM) for the EFPC watershed from the US Geological Survey 3D Elevation program. This LiDAR DEM has a resolution of 2.5 ft, while the best resolution available before the 3DEP program had a resolution of 10 m (Figure 46).

- Geospatially rectified accurate EFPC stream channel geometry:
  - Identified and breached bridges and road crossings in the DEM to allow for proper hydrologic routing.
  - Using the DEM as a background, digitized the centerline of the EFPC stream channel. This was important to do before snapping the kayak data to the LiDAR-derived EFPC main stem to allow for full integration of the kayak survey attributes.
  - Reconditioned the bare-earth DEM to put the EFPC flow line in the center of the stream channel and to route flow through bridges and culverts.
  - Performed a terrain shape analysis on the DEM to map the bank-to-bank EFPC stream channel as an area in addition to the stream flow line.
  - Used the kayak data with the bank-to-bank stream channel data set to assign substrate (e.g., bedrock, small gravel) and hydrologic habitat type (e.g., riffle, pool) for the entire main stem EFPC channel at a resolution of 2.5 ft (Figure 47).

- Developed accurate EFPC watershed stream network topology:
  - Extracted stream network for the EFPC watershed with density similar to the National Hydrography Dataset Plus High Resolution (NHDPlus HR) stream network using the reconditioned LiDAR DEM. This process also produced catchments, and a traceable geometric network was also created from the flow lines.
  - Catchments allow for relating points on the landscape and in the stream-to-stream network and are thus critical to performing stream network analysis of upstream and downstream attributes for stream and landscape characteristics.
  - Traced down the network from the EFPC origin to get the main stem.
  - Snapped the 30,000+ kayak data points to the main stem.

- Determined landscape and watershed characteristics:
  - Analyzed the LiDAR point cloud to map forest canopy at a resolution of 2.5 ft throughout the watershed. Forest canopy allows for assessment of light penetration and shading to the creek (Figure 48).
  - Used LiDAR point cloud data with the US Department of Agriculture (USDA) National Agriculture Imagery Program (NAIP) color-infrared aerial imagery to map high-resolution (2.5 ft) land cover for watershed. Before this analysis, the best available land cover had a resolution of 30 m. Land cover is a widely used landscape characteristic in watershed analyses (Figure 49).

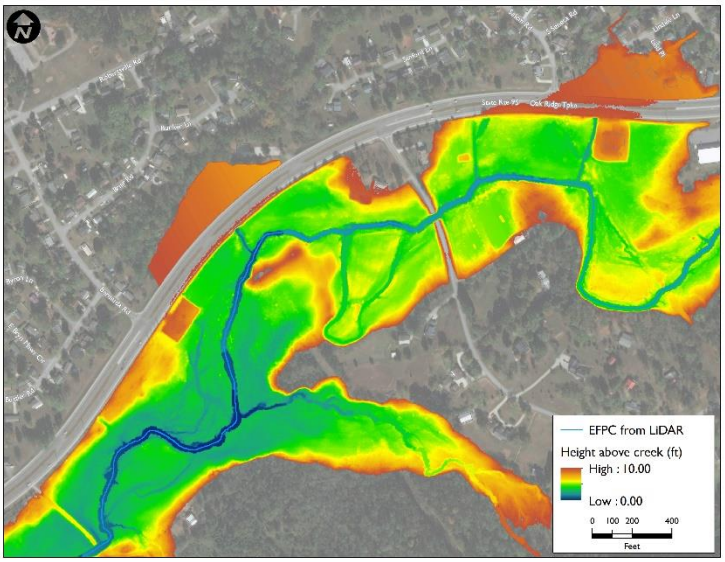

Figure 46 The LiDAR DEM was used to show areas less than 10 ft above the local elevation of EFPC.

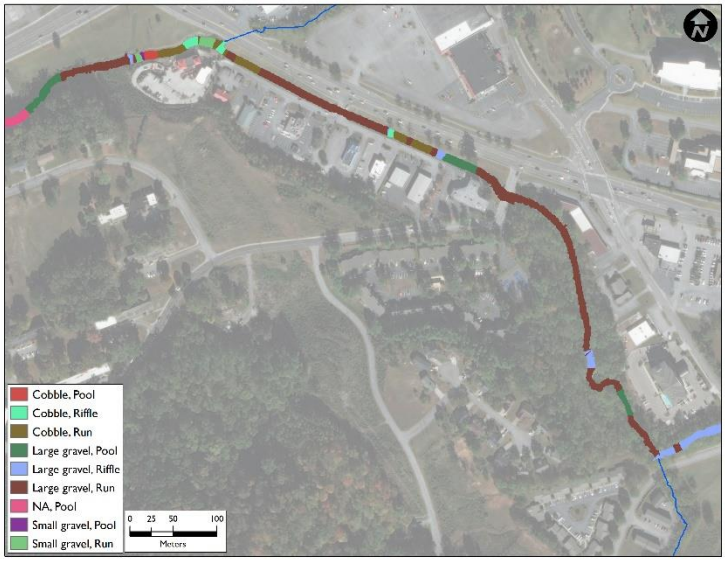

Figure 47. Bank-to-bank habitat map for EFPC main stem showing substrate and hydrology.

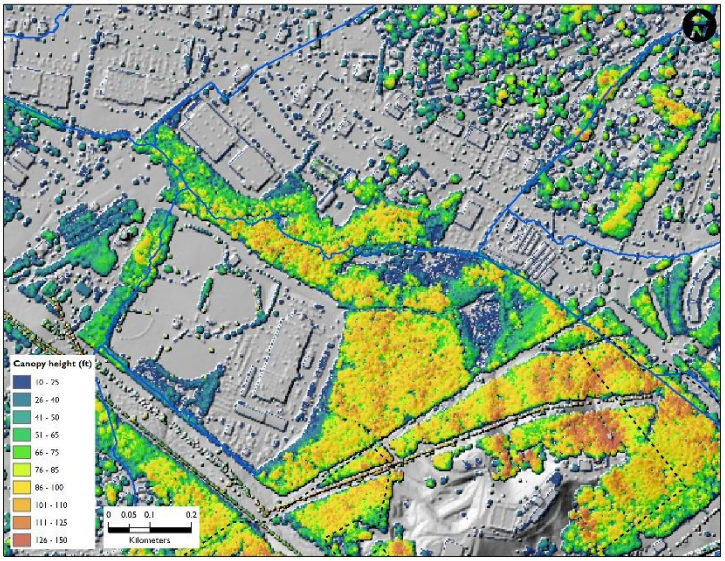

Figure 48. Forest canopy classified by height.

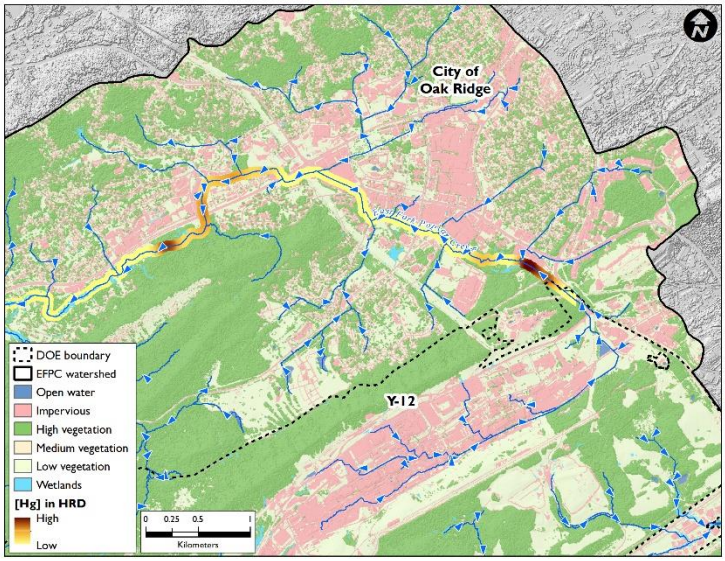

Figure 49. High-resolution land cover and the LiDAR-derived stream network overlaid on the HRD.

Watershed Model Integration

To develop an integrated modeling framework applicable to remediation strategies in EFPC, hydrologic, hydraulic, and ecologic modeling were carefully selected to fully use the information generated from targeted laboratory and field experiments. Once model integration is fully established, it can be used to quantify the impact of changes in landscape, sediment loading, stream bank stability, flow restoration, and ecological manipulation on Hg flux and transportation. The EFPC watershed has never been systematically investigated by sequential coupling of hydrologic, hydraulic, and ecologic models to trace the fate of mercury contamination. The framework adopted here allows for integrated modeling to represent hydrologic, hydraulic, and ecological dynamics of EFPC. The initial results of hydrologic and hydraulic coupling and their simulations are reported.

The integrated modeling framework includes hydrologic, hydraulic, and ecological models that provide: (1) fine spatial- and temporal-scale watershed hydrology simulations; (2) a toolkit for designing alterations to the channel morphology at fine spatial scale; (3) finer scale and spatially explicit hydraulic modeling; and (4) species-specific ecological models for simulating changes in aquatic habitat changes. The modeling effort is divided into three different stages that include selection and coupling of models, calibrations of the model with current conditions, and analysis of scenarios (Figure 50). The first step was to select suitable models that are compactable for coupling. Here, the Soil Water Analysis Tool (SWAT) was used for characterizing the hydrology of the EFPC watershed, and the Hydrologic Engineering Center's River Analysis System (HEC-RAS) model 5.03 was used for hydraulic modeling of streams in the EFPC watershed. In addition, HEC-GeoRAS and GIS-based bathymetry and channel morphology toolboxes were used to derive channel geometry of the watershed. The connections across models were established such that the reach level output on flow and sediment load from SWAT simulations and channel geometry and bathymetry variables from HEC-GeoRAS and the bathymetry toolkit were used as input in the HEC-RAS model. Spatially explicit stream hydrology variables such as flow depth, velocity of flow, sediment load, changes in base of the channel, and channel morphology from HEC-RAS simulation were used as input to ecology models. Thus, the modeling approach can be used to explore the connectivity of Hg flux from the landscape, the concentration of Hg in sediments, and water to bioaccumulation in downstream fish.

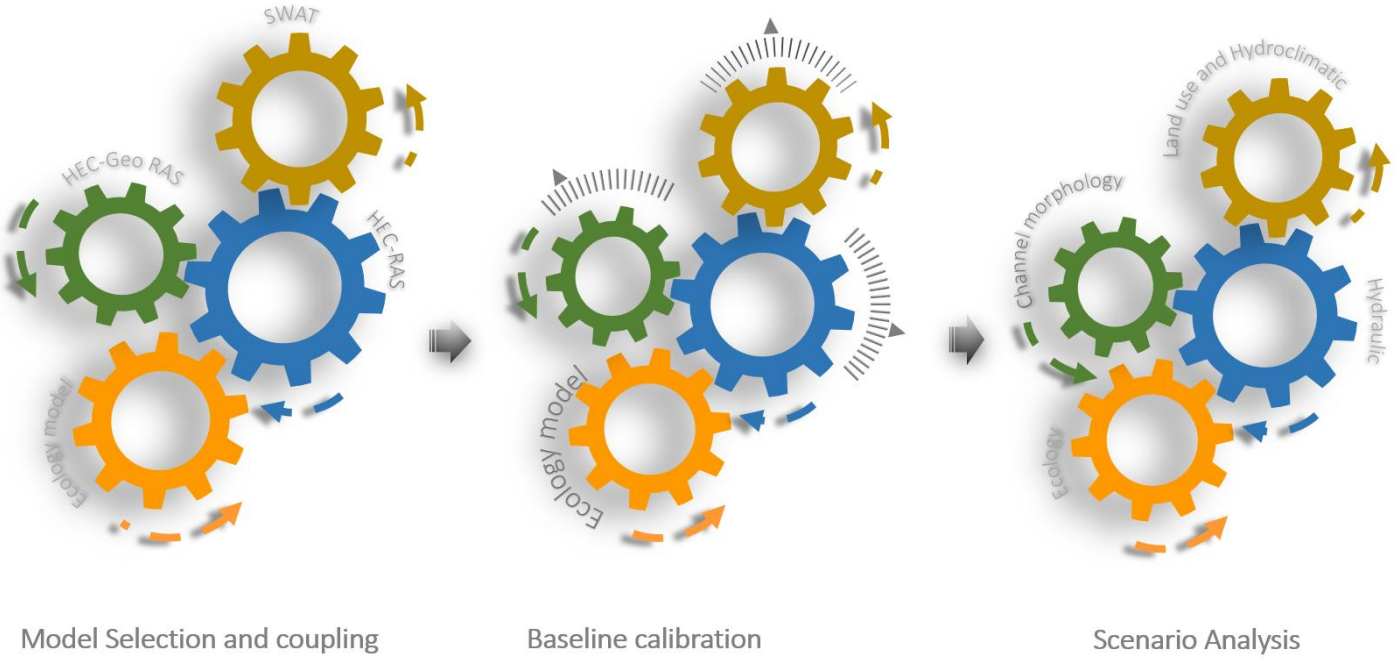

Figure 50. The modeling effort is divided into three different stages (L to R) starting from (1) model selection and coupling to (2) calibration and evaluation of models to create a baseline of the model comparable to current conditions of EFPC to (3) generation and application of scenarios for the critical process in each of the individual models for identifying prioritizing suitable remediation strategies.

SWAT Model of EFPC

SWAT was selected to model the landscape-scale hydrology of the EFPC watershed. The SWAT model is designed to estimate the watershed-scale hydrology and estimate the amount of runoff or streamflow generated by a precipitation event. The model partitions total available water across different components of the water budget of the watershed including evapotranspiration, soil, and stream water. The SWAT model is a physically based, watershed-scale continuous time simulation model operating on a daily time step (Arnold et al. 1998). Major components of the model include hydrology, weather, erosion, soil temperature, growth of vegetation, nutrients, and land management activities. The hydrologic processes include evapotranspiration, infiltration, percolation, channel transmission losses, channel routing, surface and lateral flow, shallow aquifer, deep aquifer, and subsurface drainage discharge. SWAT comprehensively links hydrology, nutrient cycling, and vegetation dynamics, making it ideal to simulate long-term impacts of climate, land use change, and landscape management practices.

High-resolution SWAT modeling used a LiDAR-derived DEM with a resolution of 0.76 m^2 to represent topography together with a high-resolution flow line from the NHD database to represent a stream segment in EFPC. In addition, land cover data for EFPC was obtained from the National Land Cover dataset with a resolution of 30 m^2. The medium resolution (1:250,000 scale) STATSGO soil map (USDA-NRCS 2006) was used to characterize soils in the watershed. The meteorological data needed for SWAT included daily maximum temperature, minimum temperature, precipitation, solar radiation, wind speed, and relative humidity. Most meteorological data on the EFPC watershed were from the Daymet data set during 1980–2016. The watershed was divided into 79 sub-watersheds. The model was calibrated and validated against the flow data from one upstream (Station 17) and one downstream station (New Horizon) in EFPC (Figure 51). Model performance was evaluated using two commonly used error measures, percent bias (PBIAS) and R2. The flow predicted by the model closely matched the measures (PBIAS value of -1% and -4% and R2 values of 0.66 and 0.48). The flow predicted by the calibrated SWAT model for EFPC was used to compute flow rate in streams of the watersheds for two future time periods—2017–2030 and 2031–2049—using projected land use change and climate for the watershed. Outputs from the SWAT model for the different storm events are then used as inputs to the 2D HEC RAS model (HEC RAS 5.03).

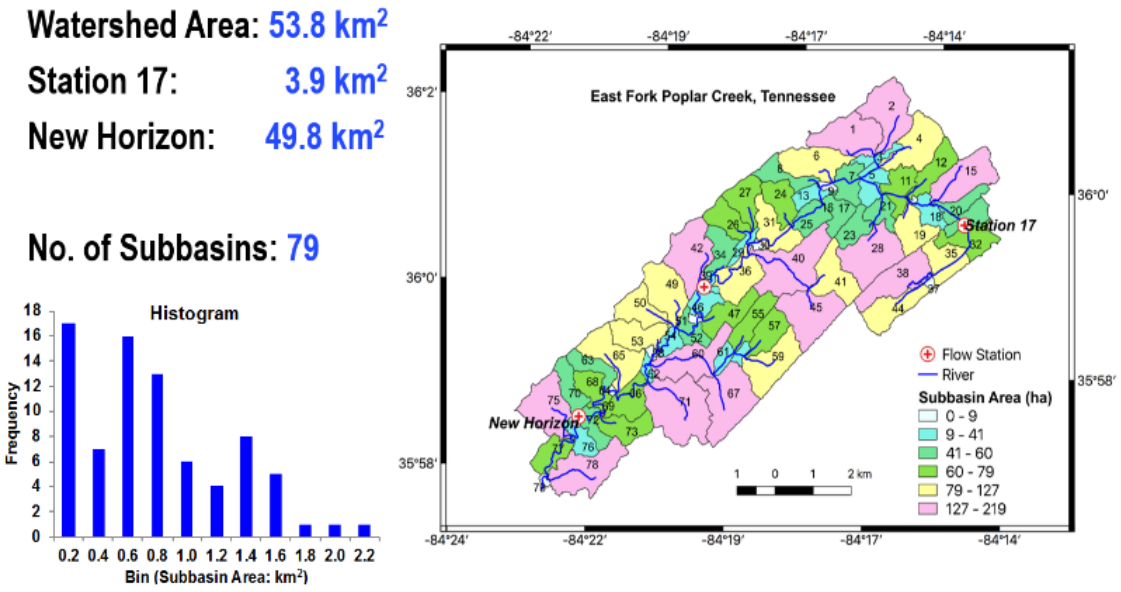

Figure 51. Subbasin areas in the EFPC watershed.

HEC-RAS 2D Model of EFPC

HEC-RAS is an open-channel flow model with flexibility for 1D and 2D hydraulic modeling and is able to account for the effects of obstructions—such as bridges, culverts, and other structures—on the hydraulic properties of open channel flow. The HEC-RAS 2D model, HEC-RAS 5.03, was used for hydraulic modeling of the EFPC watershed. The model provided 1D capability for movable boundary sediment transport and water quality analysis. Two-dimensional analysis is implemented as a mesh/grid-based computation where topography features of area of interest for 2D analysis in a watershed is converted to meshes of similar or different size. Hydraulic calculations are performed at each mesh to compute water surface elevation, critical depth, energy grade elevation, and velocities. The number of mesh is a user-given input, which directly decided the model run time. For the EFPC case, 150,000 meshes were used to represent the stream and extended flood plain (Figure 52). In contrast, HECGeo-RAS can be used to generate channel geometry for HEC-RAS. Sediment simulation in HEC-RAS uses 1D, cross-section–averaged hydraulic properties from 1D computation for sediment transport by raising or lowering cross-section node elevations to simulate erosion or deposition. However, this approach cannot account for bank collapse and toe erosion, which is a dominant source of sediment loading to streams, especially in high flow. Therefore, to account for these processes and feedback between them, the USDA-Agricultural Research Service Bank Stability and Toe Erosion Model has been integrated with the sediment transport methods in HEC-RAS 5.0. HEC-RAS is flexible enough to combine 1D with 2D in a simulation and provide the capability to switch between 1D and 2D across analysis.

A LiDAR-derived DEM with a 0.76 m resolution was used to characterize the topography of the EFPC watershed. As LiDAR sensors are unable to penetrate water, channel geometry estimates from LiDAR-derived DEM are biased, which potentially leads to a reduced flow capacity for a modeled stream in HEC-RAS. This bias in the DEM was corrected using a stream geometry measurement recorded by a kayak-based survey of the main stream in EFPC. The measured values are mosaicked into the original LiDAR DEM to account for the discrepancies in stream geometry calculated by the LiDAR-derived DEM. In addition, HEC-Geo RAS and a bathymetry toolkit were used to calculate stream geometry, which was then compared with the measured channel morphology data from the kayak survey and available measured channel geometry information across the EFPC to make sure channel geometry input for HEC-RAS fairly represents EFPC values. Land cover data from the NLCD was incorporated, and initial Manning's roughness coefficient values were associated with each land cover type. The focus of the modeling exercise is to generate a very high-resolution 2D flow area meshed within 150,000 grids along with further subgrids for the main stream (Figure 53). The flow data input for 15 reaches in HEC-RAS for the EFPC model was taken from corresponding reaches in the SWAT model for EFPC. The normal depth condition based on the slope energy grade line is used as the downstream boundary condition.

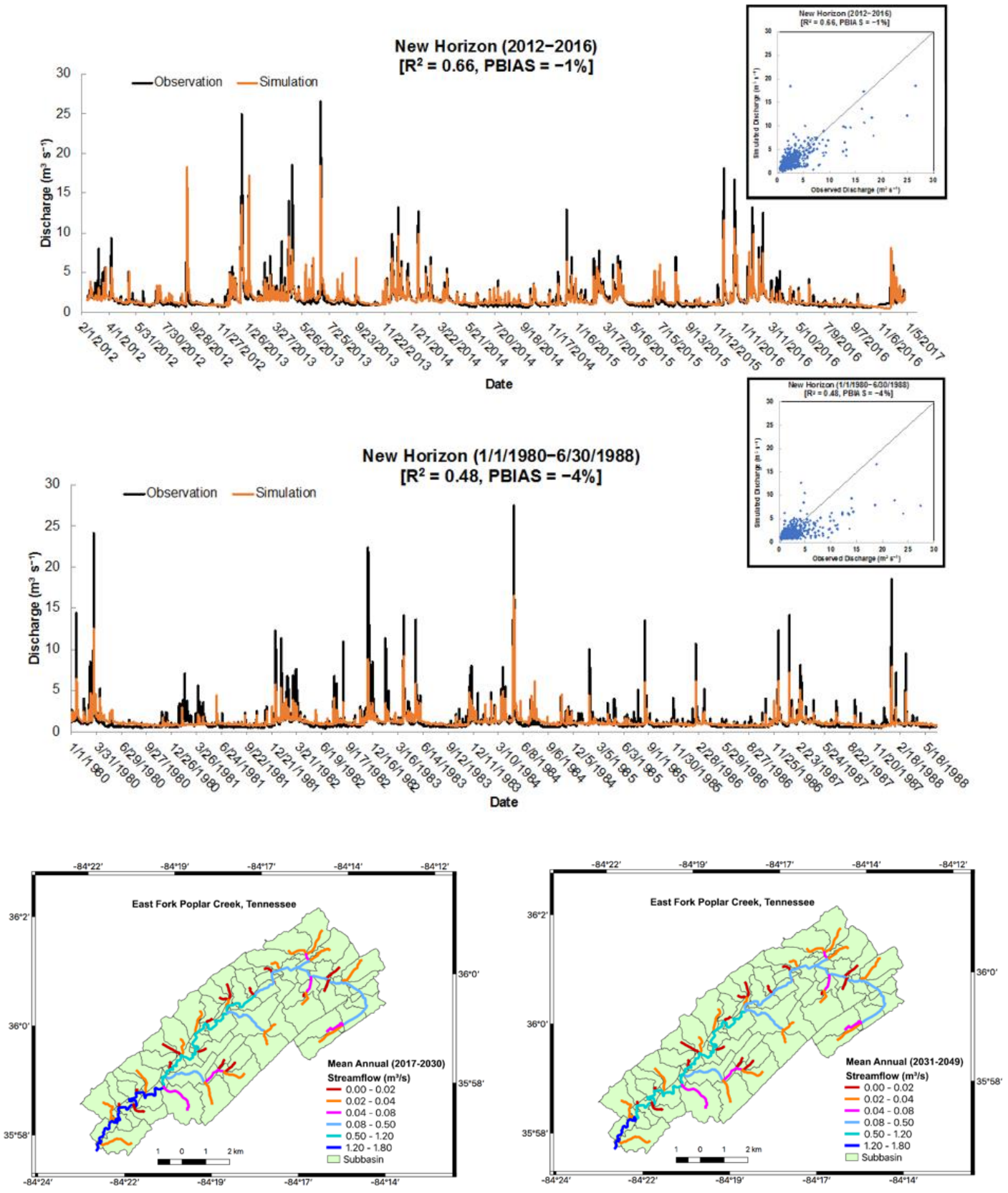

Figure 52. Contrasted stream flow based on observation and simulation (top graphs) and simulated mean annual flow by catchment, 2017–2030 (bottom graphs).

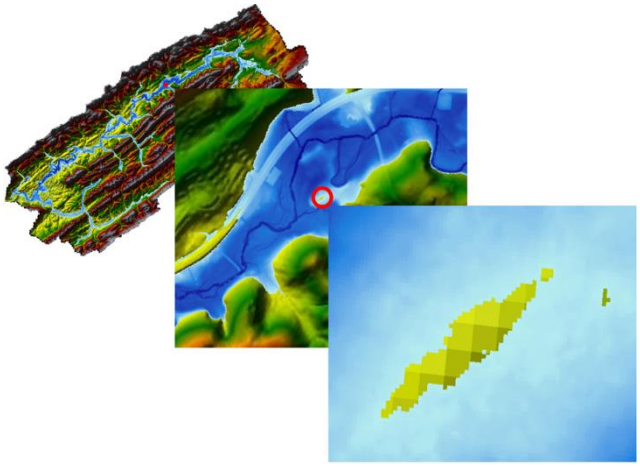

Figure 53. High-resolution modeling of EFPC using HEC-RAS.

All hydraulic models were calibrated to ensure model accuracy. Measured flow rate data from 5.4 and 16.5 were used for calibrating depth and velocity predicted by the model. During these runs, the Manning's roughness coefficient values were adjusted within the range given in the HEC-RAS documents to calibrate the model to distinct flow regimes. The assessment of flow predicted by the model against the measured flow at the stations revealed a good fit overall with an R2 (from a regression of predicted water depth against the observed water depth) value of 0.71, within the expectable limit for model evaluation (Moriasi et al. 2007). A Friedman's Two-way Analysis of Variance by Ranks test revealed that predicted water depth was not significantly different from measured water depth. Figure 54 illustrates the calibrated model's capability to predict water depth over the low-to-high flow event, which reveals that for both low- and high-flow events the model predictions were reasonably good. Modeled flow direction and particle movements are given in Figure 55. The evaluation of predicted sediment loading by the HEC-RAS model explained 32% of the variation in measured sediment loading in the watershed.

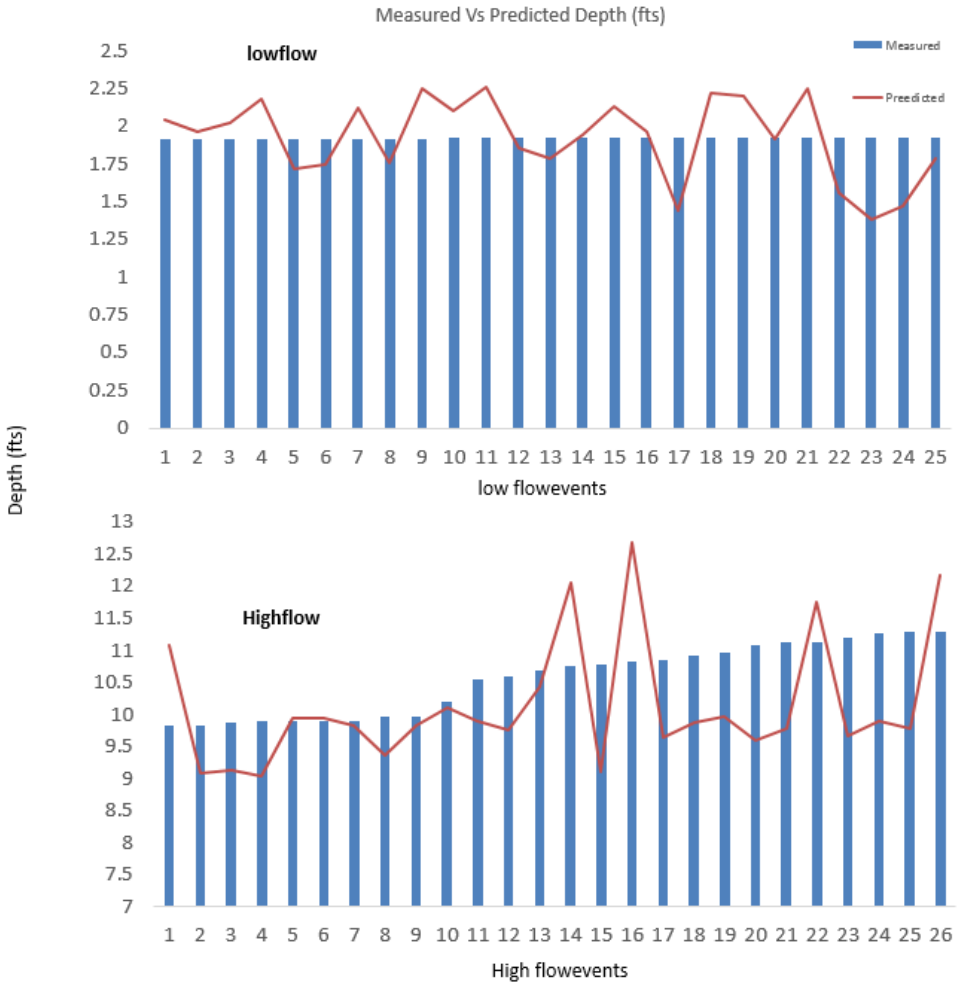

Figure 54. Water depth predicted by calibrated HEC-RAS model for low- and high-flow events.

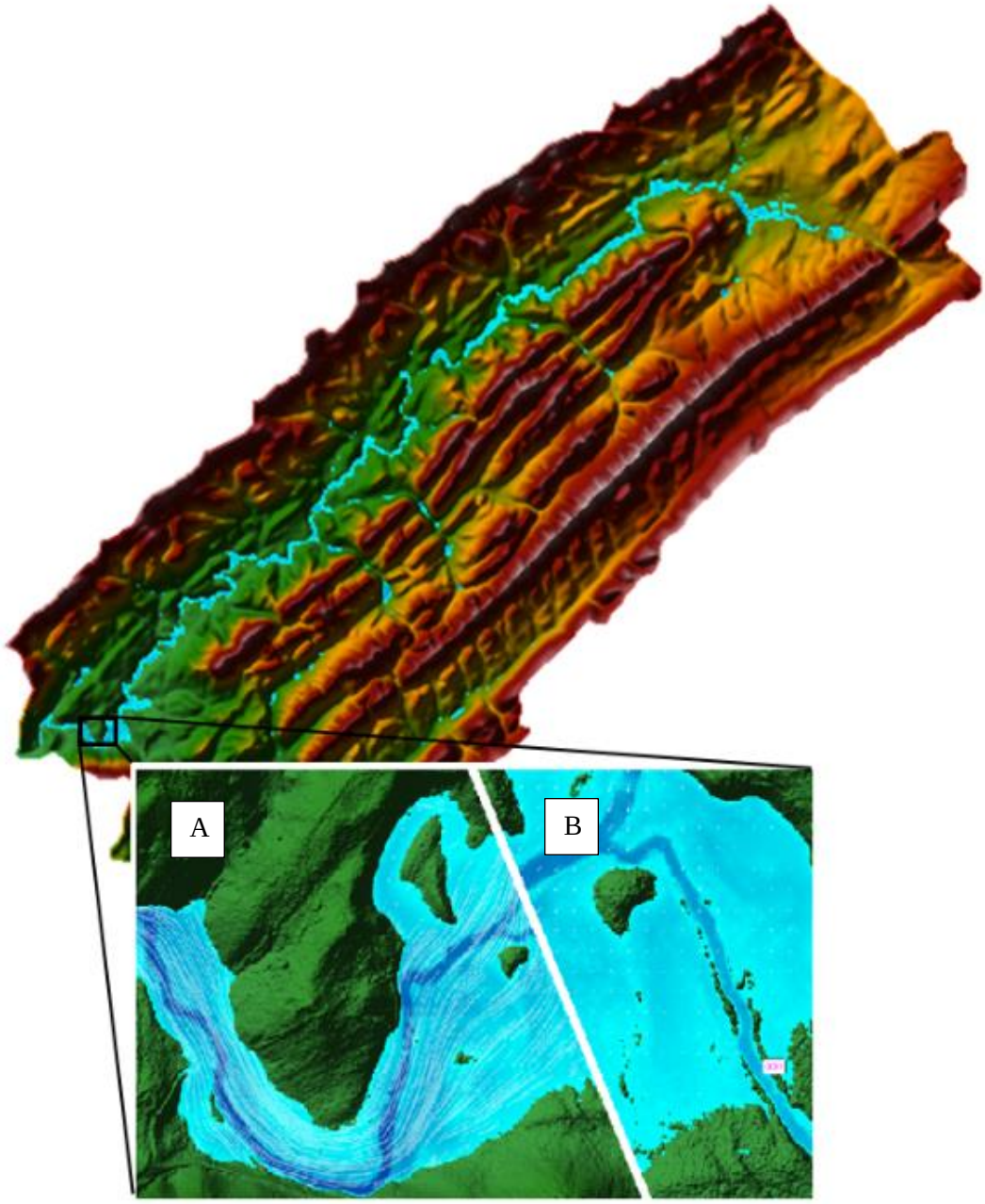

Figure 55. (A) Modeled direction of flow of the precipitation event in EFPC. (B) Particle tracking provision in the HEC-RAS for the same precipitation event.

Conclusions and Future Directions

Significant scientific and technological progress has been made during the 4 years of the Mercury Remediation Technology Development project. A strategy was developed early in the program that is consistent with the adaptive management paradigm and DOE's TRL guidelines. Initially, field studies were prioritized to better understand the Hg sources, transformations, transport, and fate processes in the EFPC system. Systems-level studies have pointed to the importance of stream bank soils—and especially HRDs—in the upstream section of EFPC as a source of Hg to the creek, the relatively small role of groundwater and floodplain sources, the importance of flow and other water chemistry and particle characteristics on the form of Hg, the importance of periphyton on Hg methylation, and the role of MeHg found in prey species on fish receptors. A watershed approach to EFPC remediation is being used because it considers all the contributing factors that affect Hg transformations in the environment. Quantitative modeling was initiated in FY 2018 to simulate remediation and technology development scenarios and better inform future remedial decision-making (Figure 56). Understanding the potential outcomes of environmental change could lead to opportunities for decreasing Hg risks while also managing and restoring the stream for natural resource benefits and/or water quality improvement.

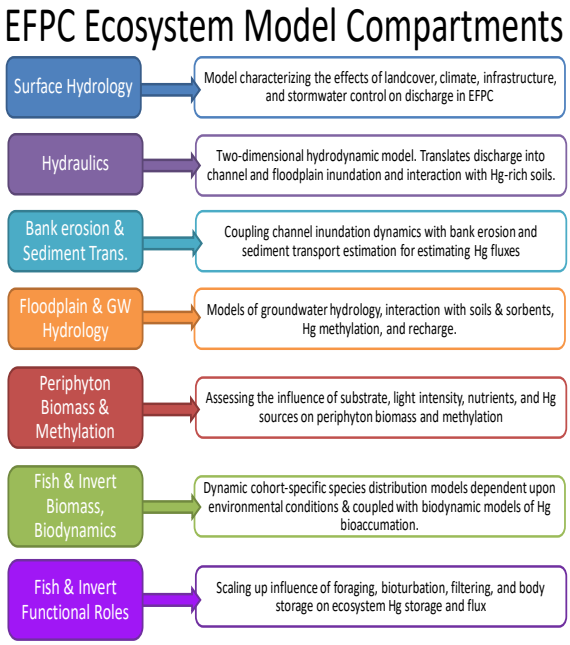

Figure 56. Model compartments informing the understanding of the EFPC watershed ecosystem using HEC-RAS.

With a better spatial and temporal understanding of the watershed system, specific technologies and strategies are being assessed as potential targeted abatement actions. Studies have been conducted to evaluate alternative treatment chemicals on Hg flux, the role of sorbents on Hg and MeHg with dissolved organic matter, and the use of bivalves as a tool for reducing particle-associated Hg in the water column.

Future directions for Hg research and technology development in LEFPC will include (1) targeted field study to inform a key process or research question, (2) enhancement of our watershed-scale understanding through quantitative modeling, (3) a greater emphasis on meso-scale studies of potential technologies in the upgraded AEL (Figure 57), and (4) remediation and technology simulation to inform the LEFPC remedial alternatives evaluation in the mid-2020s. In FY 2019 the design and construction of new experimental capabilities in the AEL at ORNL will provide a unique capability to evaluate Hg remediation technologies in a variety of sources waters. Laboratory studies in the AEL will commence in FY 2020 and will advance the scale of testing beyond field studies and bench-scale testing.

Figure 57. Current Aquatic Ecology Laboratory at ORNL.

Acronyms and Abbreviations

AA	ascorbic acid
AEL	Aquatic Ecology Laboratory
BMAP	Biological Monitoring and Abatement Program
DEM	digital evaluation mode
DOC	dissolved organic carbon
DOE	US Department of Energy
DOM	dissolved organic matter
dw	dry weight
EFK	East Fork Poplar Creek kilometer
EFPC	East Fork Poplar Creek
HEC-RAS	Hydrologic Engineering Center's River Analysis System
Hg	mercury
Hg_D	dissolved mercury
Hg_i	inorganic mercury
Hg_P	particulate mercury
Hg_T	total mercury
HRD	Historical Release Deposit
LEFPC	lower East Fork Poplar Creek
MeHg	methylmercury
MMHg	monomethylmercury
MTF	Mercury Treatment Facility
NAIP	National Agriculture Imagery Program
NHDPlus HR	National Hydrography Dataset Plus High Resolution
NOAA	National Oceanic and Atmospheric Administration
NRWQC	National Recommended Water Quality Criterion
OF200	Outfall 200
OREM	Oak Ridge Office of Environmental Management
ORNL	Oak Ridge National Laboratory
ORWTF	Oak Ridge Wastewater Treatment Facility
PBIAS	percent bias
PEC	probable effect concentration
RSI	Restoration Services, Inc.
SGD	somatic growth dilution
SWAT	Soil Water Analysis Tool
TRL	Technology Readiness Level
TWRA	Tennessee Wildlife Resource Agency
UCOR	URS | CH2M Oak Ridge LLC
UEFPC	upper East Fork Poplar Creek
USDA	US Department of Agriculture
Y-12	Y-12 National Security Complex

References

Acha, D., C. A. Pabon, and H. Hintelmann. 2012. "Mercury methylation and hydrogen sulfide production among unexpected strains isolated from periphyton of two macrophytes of the Amazon." *FEMS Microbiol Ecol* 80(3): 637–645. doi: 10.1111/j.1574-6941.2012.01333.x.

Arnold, J. G., R. Srinivasan, R. S. Muttiah, and J. R. Williams. 1998. "Large Area Hydrologic Modeling and Assessment Part I: Model Development." *Journal of the American Water Resources Association* 34(1): 73–89.

Bloom N. S., E. Preus, J. Katon, and M. Hiltner. 2003. "Selective extractions to assess the biogeochemically relevant fractionation of inorganic mercury in sediments and soils." *Analytica Chimica Acta* 479: 233–248.

Brooks, S., E. Virginia, J. Dickson, J. Earles, K. Lowe, T. Mehlhorn, T. Olsen, C. DeRolph, D. Watson, and M. Peterson. 2017. *Mercury Content of Sediments in East Fork Poplar Creek: Current Assessment and Past Trends*. ORNL/TM-2016/578. Oak Ridge: Oak Ridge National Laboratory. doi: 10.2172/1338545.

Brooks, S. C., K. A. Lowe, T. L. Mehlhorn, T. A. Olsen, X. Yin, A. M. Fortner, and M. J. Peterson. 2018. *Intraday water quality patterns in East Fork Poplar Creek with an emphasis on mercury and monomethylmercury*. ORNL/TM-2018/812. Oak Ridge: Oak Ridge National Laboratory. doi: 10.2172/1437608.

Chasar, L. C., B. C. Scudder, A. R. Stewart, A. H. Bell, and G. A. Aiken. 2009. "Mercury cycling in stream ecosystems. 3. Trophic dynamics and methylmercury bioaccumulation". Environmental science & technology 43, 2733–2739.

Dickson, J. O., M. A. Mayes, S. C. Brooks, T. L. Mehlhorn, K. A. Lowe, J. K. Earles, L. Goñez-Rodriguez, D. B. Watson, and M. J. Peterson. *In review*. "Source relationships between streambank soils and streambed sediments in a mercury-contaminated stream." *J. Soils Sediments*.

DOE. 2017a. *Strategic Plan for Mercury Remediation at the Y-12 National Security Complex, Oak Ridge, Tennessee*. DOE/OR/01-2605&DR/R1. US Department of Energy Oak Ridge Office of Environmental Management.

DOE. 2017b. *Mercury Technology Development Plan for Remediation of the Y-12 National Security Complex and East Fork Poplar Creek, Oak Ridge, Tennessee*. DOE/ORO-2489/Rev. 1. US Department of Energy Oak Ridge Office of Environmental Management.

Duchini, D., D. Boltovskoy, and F. Sylvester. 2015. "Detachment, displacement and reattachment activity in a freshwater byssate mussel (Limnoperna fortunei): the effects of light, temperature and substratum orientation." *Biofouling* 31: 599–611.

DuPont. 2013. "Remediation Proposal South River and a Segment of the South Fork Shenandoah River, Virginia." http://southriverscienceteam.org/news/techdocs/SR_RemediationProposal_2013-10-23_Final.pdf.

Gilmour, C. C. et al. 2013. "Activated Carbon Mitigates Mercury and Methylmercury Bioavailability in Contaminated Sediments." *Environ Sci Technol* 47(22): 13001–13010.

Haag, W. R., and M. L. Warren. 2000. "Effects of light and presence of fish on lure display and larval release behaviors in two species of freshwater mussels." *Animal Behaviour* 60: 879–886.

Hines, M. E., M. Horvat, J. Faganeli, J.-C. J. Bonzongo, T. Barkay, E. B. Major, K. J. Scott, E. A. Bailey, J. J. Warwick, W. B. Lyons. 2000. "Mercury biogeochemistry in the Idrija River, Slovenia, from above the mine into the Gulf of Trieste." *Environ. Res. Sect. A.* 83: 129–139.

Horvat, M., N. Nolde, V. Fajon, V. Jereb, M. Logar, S. Lojen, R. Jacimovic, I., Falnoga, Q. Liya, J. Faganeli, D. Drobne. 2003. "Total mercury, methylmercury and selenium in mercury polluted areas in the province Guizhou, China." *Sci. Tot. Environ.* 304: 231–256.

Joslin, J. D. 1994. "Regional differences in mercury levels in aquatic ecosystems- A discussion of possible causal factors with implications for the Tennessee River System and the Northern Hemisphere." Environmental Management 18: 559–567.

Karimi, R., C. Chen, P. Pickhardt, N. Fisher, and C. Folt. 2007. "Stoichiometric Controls of Mercury Dilution by Growth." *Proceedings of the National Academy of Sciences* 104: 7477–7482.

Kelly, C. A., J. W. M. Rudd, V. L. Louis, and A. Heyes. 1995. "Is total mercury concentration a good predictor of methylmercury concentrations in aquatic systems." *Water Air and Soil Pollution* 80(1–4): 715–724.

Kobak, J., and P. Nowacki. 2007. "Light-related behaviour of the zebra mussel (Dreissena polymorpha, Bivalvia)." *Fundamental and Applied Limnology* 169: 341–352.

Looney, B., et al. 2008. *Recommendations to address technical uncertainties in mitigation and remediation of mercury contamination at the Y-12 Plant, Oak Ridge, Tennessee.* WSRC-STI-2008-00212. US Department of Energy, Office of Environmental Management.

MacDonald, D. D., C. G. Ingersoll, and T. A. Berger. 2000. "Development and evaluation of consensus-based sediment quality guidelines for freshwater ecosystems." *Arch Environ Contam Toxicol* 39: 20–31.

Mathews, T., G. Southworth, M. Peterson, W. K. Roy, R. Ketelle, C. Valentine, and S. Gregory. 2013. "Decreasing aqueous mercury concentrations to achieve safe levels in fish: examining the water-fish relationship in two point-source contaminated streams." *Sci. Total Environ*. 443: 836–843.

Moriasi, D. N., J. G. Arnold, M. W. Van Liew, R. L. Binger, R. D. Harmel, and T. Veith. 2007. "Model Evaluation Guidelines for Systematic Quantification of Accuracy in Watershed Simulations." *Transactions of the American Society of Agricultural and Biological Engineers* 50(3): 885–900.

Morton, B. 2008. "The evolution of eyes in the Bivalvia: New insights." *American Malacological Bulletin* 26: 35–45.

Muller, K. A., and S. C. Brooks. *In review*. "Effectiveness of sorbents to reduce mercury methylation." *Environ. Eng. Sci*.

Nielsen, M. V., and T. Stromgren. 1985. "The Effect of Light on the Shell Length Growth and Defecation Rate of Mytilus-Edulis(L)." *Aquaculture* 47: 205–211.

Olsen, T., K. A. Muller, S. L. Painter, and S. C. Brooks. 2018. "Kinetics of Methylmercury Production Revisited." *Environ. Sci. Technol*. 52(4): 2063–2070. doi: 10.1021/acs.est.7b05152.

Olsen, T. A., C. C. Brandt, and S. C. Brooks. 2016. "Periphyton biofilms influence net methylmercury production in an industrially contaminated system." *Environ. Sci. Technol*. 50(20): 10843–10850. doi: 10.1021/acs.est.6b01538.

Peterson, M. J., S. C. Brooks, T. J. Mathews, M. A. Mayes, A. Johs, D. B. Watson, M. D. Poteat, and E. Pierce. 2015. *Mercury Remediation Technology Development for Lower East Fork Poplar Creek.* ORNL/SPR-2014/645. Oak Ridge: Oak Ridge National Laboratory.

Peterson et al. 2018. *Mercury Remediation Technology Development for Lower East Fork Poplar Creek—2017 Progress Report.* ORNL/TM-2017/480. Oak Ridge: Oak Ridge National Laboratory.

Rhodes, E. L., et al. 2009. "Quantifying bank erosion on the South River from 1937 to 2005, and its importance in assessing mercury contamination." *Applied Geography* 29: 125–134.

Riisgård, H. U. 2001. "On measurement of filtration rates in bivalves—the stony road to reliable data: review and interpretation." *Marine Ecology Progress Series* 211: 275–291.

Riscassi, A. L., C. Miller, and S. C. Brooks. 2016. "Seasonal and flow-driven dynamics of particulate and dissolved mercury and methylmercury in a stream impacted by an industrial mercury source." *Environ. Toxicol. Chem*. 35(6): 1386–1400. doi:10.1002/etc.3310.

Robson, A. A., C. G. de Leaniz, R. P. Wilson, and L. G. Halsey. 2010. "Effect of anthropogenic feeding regimes on activity rhythms of laboratory mussels exposed to natural light." *Hydrobiologia* 655: 197–204.

Ryon, M. G., A. J. Stewart, L. A. Kszos, T. L. Phipps. 2002. "Impacts on streams from the use of sulfur-based compounds for dechlorinating industrial effluents." *Water Air and Soil Pollution* 136: 255–268.

Southworth, G., M. Peterson, and M. Bogle. 2004. "Bioaccumulation factors for mercury in stream fish." *Environ. Pract*. 6: 135–143. https://www.fs.fed.us/eng/pubs/pdf/05231301.pdf.

Southworth, G. R., T. J. Mathews, M. S. Greeley Jr, M. J. Peterson, S. C. Brooks, and R. H. Ketelle. 2013. "Sources of mercury in a contaminated stream-implications for the timescale of recovery." *Environ Toxicol Chem* 32: 764–772.

Stahl Jr., R. G., et al. 2014. "Applying a watershed-level, risk-based approach to addressing legacy contamination in the South River, Virginia: Planning and problem formulation." *Human and Ecological Risk Assessment: An International Journal* 20(2): 316–345.

Tom, K. R., M. C. Newman, and J. Schmerfeld. 2010. "Modeling mercury biomagnification (South River, Virginia, USA) to inform river management decision making." *Environmental Toxicology and Chemistry* 29(4): 1013–1020. doi: 10.1002/etc.117.

Trudel, M., and J. B. Rasmussen. 1997. "Modeling the Elimination of Mercury by Fish." *Environmental Science & Technology* 31: 1716–1722.

Tsui, M. T. K., J. C. Findlay, S. J. Balogh, and Y. H. Nollet. 2010. "In situ production of methylmercury within a stream channel in northern California." *Environ Sci Technol* 44: 6998–7004.

Turner, R. R., and G. R. Southworth. 1999. Mercury Contaminated Sites. R. Ebinghaus, R. R. Turner, L. De Lacerda, O. Vasiliev, and W. Salomons, Eds. Berlin: Springer-Verlag.

Ward, D. M., K. H. Nislow, C. Y. Chen, and C. L. Folt. 2010. "Rapid, Efficient Growth Reduces Mercury Concentrations in Stream-Dwelling Atlantic Salmon." *Transactions of the American Fisheries Society* 139: 1–10.

Watson, D., M. Bevelheimer, C. Brandt, C. DeRolph, S. Brooks, M. Mayes, T. Olsen, J. Dickson, M. Peterson, and D. Ketelle. 2017. *Evaluation of lower East Fork Poplar Creek mercury sources–Model update*. ORNL/SR-2016/503. Oak Ridge: Oak Ridge National Laboratory.

Watson, D., S. Brooks, T. Mathews, M. Bevelheimer, C. DeRolph, C. Brandt, M. Peterson, and D. Ketelle. 2016. *Evaluation of lower East Fork Poplar Creek mercury sources.* ORNL/TM-2016/134. Oak Ridge: Oak Ridge National Laboratory.

USDA-NRCS. 2006. US General Soil Map (STATSGO2). Natural Resources Conservation Service, US Department of Agriculture. http://dx.doi.org/10.15482/USDA.ADC/1242480.